

2-2010

Development and Evaluation of the Midwest Guardrail System Placed Adjacent to a 2:1 Fill Slope

Mitchell J. Wiebelhaus
University of Nebraska-Lincoln, mitchw1@huskers.unl.edu

Ronald K. Faller
University of Nebraska - Lincoln, rfaller1@unl.edu

Robert W. Bielenberg
University of Nebraska - Lincoln, rbielenberg2@unl.edu

John R. Rohde
University of Nebraska - Lincoln, jrohde1@unl.edu

Karla A. Lechtenberg
University of Nebraska - Lincoln, kpolivka2@unl.edu

See next page for additional authors

Follow this and additional works at: <http://digitalcommons.unl.edu/ndor>

 Part of the [Transportation Engineering Commons](#)

Wiebelhaus, Mitchell J.; Faller, Ronald K.; Bielenberg, Robert W.; Rohde, John R.; Lechtenberg, Karla A.; Sicking, Dean L.; Dey, Gopi; and Reid, John D., "Development and Evaluation of the Midwest Guardrail System Placed Adjacent to a 2:1 Fill Slope" (2010). *Nebraska Department of Transportation Research Reports*. 69.
<http://digitalcommons.unl.edu/ndor/69>

This Article is brought to you for free and open access by the Nebraska LTAP at DigitalCommons@University of Nebraska - Lincoln. It has been accepted for inclusion in Nebraska Department of Transportation Research Reports by an authorized administrator of DigitalCommons@University of Nebraska - Lincoln.

Authors

Mitchell J. Wiebelhaus, Ronald K. Faller, Robert W. Bielenberg, John R. Rohde, Karla A. Lechtenberg, Dean L. Sicking, Gopi Dey, and John D. Reid



TESTING CERT # 2937.01

*Midwest States Regional Pooled Fund Research Program
Fiscal Year 2004-2005 (Year 15)
Research Project Number SPR-3(017)
NDOR Sponsoring Agency Code RFPF-05-09*

DEVELOPMENT AND EVALUATION OF THE MIDWEST GUARDRAIL SYSTEM (MGS) PLACED ADJACENT TO A 2:1 FILL SLOPE

Submitted by

Mitch J. Wiebelhaus
Undergraduate Research Assistant

Ronald K. Faller, Ph.D., P.E.
Research Assistant Professor

Robert W. Bielenberg, M.S.M.E., E.I.T.
Research Associate Engineer

John R. Rohde, Ph.D., P.E.
Associate Professor

Karla A. Lechtenberg, M.S.M.E., E.I.T.
Research Associate Engineer

Dean L. Sicking, Ph.D., P.E.
Professor and MwRSF Director

John D. Reid, Ph.D.
Professor

Gopi Dey
Former Undergraduate Research Assistant

MIDWEST ROADSIDE SAFETY FACILITY

University of Nebraska-Lincoln
527 Nebraska Hall
Lincoln, Nebraska 68588-0529
(402) 472-0965

Submitted to

MIDWEST STATES REGIONAL POOLED FUND PROGRAM

Nebraska Department of Roads
1500 Nebraska Highway 2
Lincoln, Nebraska 68502

MwRSF Research Report No. TRP-03-185-10

February 24, 2010

Technical Report Documentation Page

1. Report No. TRP-03-185-10	2.	3. Recipient's Accession No.	
4. Title and Subtitle DEVELOPMENT AND EVALUATION OF THE MIDWEST GUARDRAIL SYSTEM (MGS) PLACED ADJACENT TO A 2:1 FILL SLOPE		5. Report Date February 24, 2010	
		6.	
7. Author(s) Wiebelhaus, M.J., Lechtenberg, K.A., Faller, R.K., Sicking, D.L., Bielenberg, R.W., Reid, J.D., and Rohde, J.R.		8. Performing Organization Report No. TRP-03-185-10	
9. Performing Organization Name and Address Midwest Roadside Safety Facility (MwRSF) University of Nebraska-Lincoln 527 Nebraska Hall Lincoln, Nebraska 68588-0529		10. Project/Task/Work Unit No.	
		11. Contract © or Grant (G) No. SPR-3(017)	
12. Sponsoring Organization Name and Address Midwest States Regional Pooled Fund Program Nebraska Department of Roads 1500 Nebraska Highway 2 Lincoln, Nebraska 68502		13. Type of Report and Period Covered Final Report 2004-2010	
		14. Sponsoring Agency Code RFPF-05-09	
15. Supplementary Notes Prepared in cooperation with U.S. Department of Transportation, Federal Highway Administration			
16. Abstract (Limit: 200 words) <p style="text-indent: 40px;">W-beam guardrail is often used to protect motorists from steep roadside slopes adjacent to high-speed roadways. Although previously designed systems have demonstrated acceptable safety performance, the long posts and half-post spacing have proven to be both costly and introduce maintenance challenges. Furthermore, the improved redirective capacity of the Midwest Guardrail System (MGS) provides the opportunity to eliminate the need for half-post spacing and thereby greatly reduces the cost of placing a barrier at the slope break point.</p> <p style="text-indent: 40px;">A stiffened version of the MGS was developed for use adjacent to steep roadside slopes. The new design incorporates 2,743-mm (9-ft) long posts on a 1,905 mm (75 in.) spacing. With the top of the W-beam mounted at a height of 787 mm (31 in.), this guardrail was successfully crash tested according to the <i>Manual for Assessing Safety Hardware</i> (MASH) safety performance evaluation criteria. Hence, the stiffened MGS guardrail design with full post spacing is acceptable for use on the National Highway System. This new guardrail design will provide a safe and economical alternative for use along highways with steep slopes very close to the travelway.</p>			
17. Document Analysis/Descriptors Highway Safety, Crash Test, Roadside Appurtenance, Compliance Test, MASH, Longitudinal Barrier, Guardrail, Midwest Guardrail System, Roadside Slopes, 2H:1V		18. Availability Statement No restrictions. Document available from: National Technical Information Services, Springfield, Virginia 22161	
19. Security Class (this report) Unclassified	20. Security Class (this page) Unclassified	21. No. of Pages 174	22. Price

DISCLAIMER STATEMENT

This report was funded in part through funding from the Federal Highway Administration, U.S. Department of Transportation. The contents of this report reflect the views and opinions of the authors who are responsible for the facts and the accuracy of the data presented herein. The contents do not necessarily reflect the official views or policies of the state highway departments participating in the Midwest States Regional Pooled Fund Program nor the Federal Highway Administration, U. S. Department of Transportation. This report does not constitute a standard, specification, regulation, product endorsement, or an endorsement of manufacturers.

UNCERTAINTY OF MEASUREMENT STATEMENT

The Midwest Roadside Safety Facility (MwRSF) has determined the uncertainty of measurements for several parameters involved in standard full-scale crash testing and non-standard testing of roadside safety features. Information regarding the uncertainty of measurements for critical parameters is available upon request by the sponsor and the Federal Highway Administration.

The Independent Approving Authority (IAA) for the data contained herein was Mr. Scott K. Rosenbaugh, Research Associate Engineer.

ACKNOWLEDGMENTS

The authors wish to acknowledge several sources that made a contribution to this project: (1) the Midwest States Regional Pooled Fund Program funded by the Connecticut Department of Transportation, Illinois Department of Transportation, Iowa Department of Transportation, Kansas Department of Transportation, Minnesota Department of Transportation, Missouri Department of Transportation, Nebraska Department of Roads, Ohio Department of Transportation, South Dakota Department of Transportation, Wisconsin Department of Transportation, and Wyoming Department of Transportation for sponsoring this project and (2) MwRSF personnel for constructing the barriers and conducting the crash tests.

Acknowledgment is also given to the following individuals who made a contribution to the completion of this research project.

Midwest Roadside Safety Facility

J.C. Holloway, M.S.C.E., E.I.T., Test Site Manager
C.L. Meyer, B.S.M.E., E.I.T., Research Associate Engineer
S.K. Rosenbaugh, M.S.C.E., E.I.T., Research Associate Engineer
A.T. Russell, B.S.B.A., Shop Manager
K.L. Krenk, B.S.M.A, Maintenance Mechanic
A.T. McMaster, Laboratory Mechanic
Undergraduate and Graduate Research Assistants

Connecticut Department of Transportation

Dionysia Oliveira, Transportation Engineer 3

Illinois Department of Transportation

David Piper, P.E., Highway Policy Engineer

Iowa Department of Transportation

David Little, P.E., Assistant District Engineer
Deanna Mayfield, P.E., Methods Engineer
Chris Poole, P.E., Litigation / Roadside Safety Engineer

Kansas Department of Transportation

Ron Seitz, P.E., Bureau Chief
Rod Lacy, P.E., Metro Engineer
Scott King, P.E., Road Design Leader

Minnesota Department of Transportation

Michael Elle, P.E., Design Standard Engineer

Missouri Department of Transportation

Joseph Jones, P.E., Engineering Policy Administrator

Nebraska Department of Roads

Amy Starr P.E., Research Engineer
Phil TenHulzen, P.E., Design Standards Engineer
Jodi Gibson, Research Coordinator

Ohio Department of Transportation

Dean Focke, P.E., Road Safety Engineer (Retired)
Michael Blin, P.E. Standards and Geometrics Engineer

South Dakota Department of Transportation

David Huft, Research Engineer
Bernie Clocksin, Lead Project Engineer

Wisconsin Department of Transportation

John Bridwell, P.E., Standards Development Engineer
Erik Emerson, P.E., Standards Development Engineer

Wyoming Department of Transportation

William Wilson, P.E., Standards Engineer

Federal Highway Administration

John Perry, P.E. Nebraska Division Office
Danny Briggs, Nebraska Division Office

Dunlap Photography

James Dunlap, President and Owner

TABLE OF CONTENTS

	Page
TECHNICAL REPORT DOCUMENTATION PAGE	i
DISCLAIMER STATEMENT	ii
UNCERTAINTY OF MEASUREMENT STATEMENT	ii
ACKNOWLEDGMENTS	iii
TABLE OF CONTENTS	vi
List of Figures	ix
List of Tables	xii
1 INTRODUCTION	1
1.1 Problem Statement	1
1.2 Objective	2
1.3 Scope	2
2 LITERATURE REVIEW	4
2.1 NCHRP 230 Systems	4
2.2 NCHRP 350 Systems	5
3 DEVELOPMENTAL TESTING - DYNAMIC POST TESTING	7
3.1 Dynamic Component Testing	7
4 BARRIER VII COMPUTER SIMULATION MODELING	9
4.1 Background	9
4.2 Computer Model for MGS on a 2:1 Fill Slope	9
4.3 BARRIER VII Simulation Results	16
4.4 Critical Impact Point (CIP) Determination	16
5 TEST REQUIREMENTS AND EVALUATION CRITERIA	21
5.1 Test Requirements	21
5.2 Evaluation Criteria	22
6 TEST CONDITIONS	24
6.1 Test Facility	24
6.2 Vehicle Tow and Guidance System	24
6.3 Test Vehicles	24
6.4 Data Acquisition Systems	32
6.4.1 Accelerometers	32
6.4.2 Rate Transducers	32
6.4.3 Pressure Tape Switches	33

6.4.4 High-Speed Photography	33
7 MGS INSTALLED ADJACENT TO A 2:1 FILL SLOPE (DESIGN NO. 1) DETAILS	36
8 CRASH TEST NO. 1 (706-mm [27¾ in.] MGS)	49
8.1 Test MGS221-1	49
8.2 Weather Conditions	49
8.3 Test Description	50
8.4 Barrier Damage	51
8.5 Vehicle Damage	53
8.6 Occupant Rick Values	54
8.7 Discussion	55
9 MGS INSTALLED ADJACENT TO A 2:1 FILL SLOPE (DESIGN NO. 2) DETAILS	78
10 CRASH TEST NO. 2 (787-mm [31-in.] MGS)	83
10.1 Test MGS221-2	83
10.2 Weather Conditions	83
10.3 Test Description	84
10.4 Barrier Damage	85
10.5 Vehicle Damage	86
10.6 Occupant Rick Values	87
10.7 Discussion	87
11 SUMMARY AND CONCLUSIONS	106
12 RECOMMENDATIONS	108
13 REFERENCES	109
14 APPENDICES	112
APPENDIX A - Barrier VII Finite Element Model CAD Drawing	113
APPENDIX B - Barrier VII Input Deck	116
APPENDIX C - English-Unit System Details - Test No. MGS221-1	121
APPENDIX D - Test Summary Sheets - English Units	130
APPENDIX E - Occupant Compartment Deformation Data, Test No. MGS221-1 ...	133
APPENDIX F - Accelerometer and Rate Transducer Data Analysis, Test No. MGS221-1	137
APPENDIX G - Metric-Unit and English-Unit System Details - Test No. MGS221-2	145
APPENDIX H - Occupant Compartment Deformation, Test No. MGS221-2	162
APPENDIX I - Accelerometer and Rate Transducer Data Analysis, Test No. MGS221-2	166

List of Figures

	Page
Figure 1. Force and Energy vs. Displacement Curves for 2,743-mm (9-ft) Posts	8
Figure 2. Sequential Plots from BARRIER VII Simulation of MGS on 2:1 Slope	12
Figure 3. Sequential Plots from BARRIER VII Simulation of MGS on 2:1 Slope	13
Figure 4. Determination of New Impact Velocity Considering Change in Potential Energy . . .	15
Figure 5. Test Vehicle, Test No. MGS221-1	25
Figure 6. Test Vehicle Dimensions, Test No. MGS221-1	26
Figure 7. Test Vehicle, Test No. MGS221-2	28
Figure 8. Test Vehicle Dimensions, Test No. MGS221-2	29
Figure 9. Vehicle Target Locations, Test No. MGS221-1	30
Figure 10. Vehicle Target Locations, Test No. MGS221-2	31
Figure 11. Location of Cameras, Test No. MGS221-1	34
Figure 12. Location of Cameras, Test No. MGS221-2	35
Figure 13. System Layout Details, Test No. MGS221-1	38
Figure 14. Anchorage Details, Test No. MGS221-1	39
Figure 15. Post Details, Test No. MGS221-1	40
Figure 16. Post Details, Test No. MGS221-1	41
Figure 17. BCT Post and Foundation Tube Details, Test No. MGS221-1	42
Figure 18. Anchor Cable Details, Test No. MGS221-1	43
Figure 19. Ground Strut and Anchor Bracket Details, Test No. MGS221-1	44
Figure 20. Rail Section Details, Test No. MGS221-1	45
Figure 21. MGS Installed Adjacent to a 2:1 Fill Slope, Test No. MGS221-1	46
Figure 22. MGS Installed Adjacent to a 2:1 Fill Slope, Test No. MGS221-1	47
Figure 23. MGS Installed Adjacent to a 2:1 Fill Slope, Test No. MGS221-1	48
Figure 24. Summary of Test Results and Sequential Photographs, Test No. MGS221-1	56
Figure 25. Additional Sequential Photographs, Test No. MGS221-1	57
Figure 26. Additional Sequential Photographs, Test No. MGS221-1	58
Figure 27. Additional Sequential Photographs, Test No. MGS221-1	59
Figure 28. Additional Sequential Photographs, Test No. MGS221-1	60
Figure 29. Documentary Photographs, Test No. MGS221-1	61
Figure 30. Documentary Photographs, Test No. MGS221-1	62
Figure 31. Impact Location, Test No. MGS221-1	63
Figure 32. Vehicle Final Position and Trajectory Marks, Test No. MGS221-1	64
Figure 33. System Damage, Test No. MGS221-1	65
Figure 34. Post Nos. 3 through 6 Damage, Test No. MGS221-1	66
Figure 35. Post Nos. 7 through 10 Damage, Test No. MGS221-1	67
Figure 36. Post Nos. 11 through 14 Damage, Test No. MGS221-1	68
Figure 37. Post Nos. 15 through 17 Damage, Test No. MGS221-1	69
Figure 38. Post Nos. 20, and 22 through 24 Damage, Test No. MGS221-1	70
Figure 39. Post Nos. 25 through 27 Damage, Test No. MGS221-1	71
Figure 40. Upstream Anchorage Damage, Test No. MGS221-1	72
Figure 41. Downstream Anchorage Damage, Test No. MGS221-1	73
Figure 42. Vehicle Damage, Test No. MGS221-1	74

Figure 43. Vehicle Damage, Test No. MGS221-1	75
Figure 44. Undercarriage Damage, Test No. MGS221-1	76
Figure 45. Occupant Compartment Damage, Test No. MGS221-1	77
Figure 46. MGS Installed Adjacent to a 2:1 Fill Slope System Modifications, Test No. MGS221-2	79
Figure 47. MGS Installed Adjacent to a 2:1 Fill Slope System Modifications, Test No. MGS221-2	80
Figure 48. MGS Installed Adjacent to a 2:1 Fill Slope, Test No. MGS221-2	81
Figure 49. MGS Installed Adjacent to a 2:1 Fill Slope, Test No. MGS221-2	82
Figure 50. Summary of Test Results and Sequential Photographs, Test No. MGS221-2	89
Figure 51. Additional Sequential Photographs, Test No. MGS221-2	90
Figure 52. Additional Sequential Photographs, Test No. MGS221-2	91
Figure 53. Additional Sequential Photographs, Test No. MGS221-2	92
Figure 54. Additional Sequential Photographs, Test No. MGS221-2	93
Figure 55. Documentary Photographs, Test No. MGS221-2	94
Figure 56. Impact Location, Test No. MGS221-2	95
Figure 57. Vehicle Final Position and Trajectory Marks, Test No. MGS221-2	96
Figure 58. System Damage, Test No. MGS221-2	97
Figure 59. System Damage, Test No. MGS221-2	98
Figure 60. Post Nos. 9 through 12 Damage, Test No. MGS221-2	99
Figure 61. Post Nos. 13 through 15 Damage, Test No. MGS221-2	100
Figure 62. Post Nos. 16 through 18 Damage, Test No. MGS221-2	101
Figure 63. Upstream Anchorage Damage, Test No. MGS221-2	102
Figure 64. Downstream Anchorage Damage, Test No. MGS221-2	103
Figure 65. Vehicle Damage, Test No. MGS221-2	104
Figure 66. Vehicle Damage, Test No. MGS221-2	105
Figure A-1. Barrier VII Finite Element Model CAD Drawing	114
Figure A-2. Barrier VII Finite Element Model CAD Drawing	115
Figure C-1. System Layout Details, Test No. MGS221-1 (English)	122
Figure C-2. Rail Detail, Test No. MGS221-1 (English)	123
Figure C-3. Post Details, Test No. MGS221-1 (English)	124
Figure C-4. Post Details, Test No. MGS221-1 (English)	125
Figure C-5. Post and Foundation Tube Details, Test No. MGS221-1 (English)	126
Figure C-6. Anchor Cable Details, Test No. MGS221-1 (English)	127
Figure C-7. Ground Strut and Anchor Bracket Details, Test No. MGS221-1 (English)	128
Figure C-8. Rail Details, Test No. MGS221-1 (English)	129
Figure D-1. Summary of Test Results and Sequential Photographs (English), Test No. MGS221-1	131
Figure D-2. Summary of Test Results and Sequential Photographs (English), Test No. MGS221-2	132
Figure E-1. Occupant Compartment Deformation Data - Set 1, Test MGS221-1	134
Figure E-2. Occupant Compartment Deformation Data - Set 2, Test MGS221-1	135
Figure E-3. Occupant Compartment Deformation Index (OCDI), Test MGS221-1	136
Figure F-1. Graph of Longitudinal Deceleration, Test MGS221-1	138

Figure F-2. Graph of Longitudinal Occupant Impact Velocity, Test MGS221-1	139
Figure F-3. Graph of Longitudinal Occupant Displacement, Test MGS221-1	140
Figure F-4. Graph of Lateral Deceleration, Test MGS221-1	141
Figure F-5. Graph of Lateral Occupant Impact Velocity, Test MGS221-1	142
Figure F-6. Graph of Lateral Occupant Displacement, Test MGS221-1	143
Figure F-7. Graph of Roll, Pitch, and Yaw Angular Displacement, Test No. MGS221-1	144
Figure G-1. System Layout Details, Test No. MGS221-2 (Metric)	146
Figure G-2. Rail Detail, Test No. MGS221-2 (Metric)	147
Figure G-3. Post Details, Test No. MGS221-2 (Metric)	148
Figure G-4. Post Details, Test No. MGS221-2 (Metric)	149
Figure G-5. Post and Foundation Tube Details, Test No. MGS221-2 (Metric)	150
Figure G-6. Anchor Cable Details, Test No. MGS221-2 (Metric)	151
Figure G-7. Ground Strut and Anchor Bracket Details, Test No. MGS221-2 (Metric)	152
Figure G-8. Rail Details, Test No. MGS221-2 (Metric)	153
Figure G-9. System Layout Details, Test No. MGS221-2 (English)	154
Figure G-10. Rail Detail, Test No. MGS221-2 (English)	155
Figure G-11. Post Details, Test No. MGS221-2 (English)	156
Figure G-12. Post Details, Test No. MGS221-2 (English)	157
Figure G-13. Post and Foundation Tube Details, Test No. MGS221-2 (English)	158
Figure G-14. Anchor Cable Details, Test No. MGS221-2 (English)	159
Figure G-15. Ground Strut and Anchor Bracket Details, Test No. MGS221-2 (English)	160
Figure G-16. Rail Details, Test No. MGS221-2 (English)	161
Figure H-1. Occupant Compartment Deformation Data - Set 1, Test MGS221-2	163
Figure H-2. Occupant Compartment Deformation Data - Set 2, Test MGS221-2	164
Figure H-3. Occupant Compartment Deformation Index (OCDI), Test MGS221-2	165
Figure I-1. Graph of Longitudinal Deceleration, Test MGS221-2	167
Figure I-2. Graph of Longitudinal Occupant Impact Velocity, Test MGS221-2	168
Figure I-3. Graph of Longitudinal Occupant Displacement, Test MGS221-2	169
Figure I-4. Graph of Lateral Deceleration, Test MGS221-2	170
Figure I-5. Graph of Lateral Occupant Impact Velocity, Test MGS221-2	171
Figure I-6. Graph of Lateral Occupant Displacement, Test MGS221-2	172
Figure I-7. Graph of Yaw Angular Displacement, Test MGS221-2	173

List of Tables

	Page
Table 1. BARRIER VII Simulation Parameters for 2,743-mm (9-ft) Posts on a 2:1 Fill Slope .	14
Table 2. Summary of BARRIER VII Simulation Results for 10 Percent Moment Reduction . .	17
Table 3. Summary of BARRIER VII Simulation Results for 20 Percent Moment Reduction . .	18
Table 4. CIP Analysis Results	19
Table 5. MASH Test Level 3 Crash Test Conditions	22
Table 6. MASH Evaluation Criteria for Crash Tests	23
Table 7. Weather Conditions, Test No. MGS221-1	49
Table 8. Summary of OIV, ORA, THIV, and PHD Values, Test No. MGS221-1	54
Table 9. Weather Conditions, Test No. MGS221-2	83
Table 10. Summary of OIV, ORA, THIV, and PHD Values, Test No. MGS221-2	88
Table 11. Summary of Safety Performance Evaluation Results	107

1 INTRODUCTION

1.1 Problem Statement

W-beam guardrail is often used to protect motorists from steep roadside slopes adjacent to high-speed roadways. A roadside slope placed immediately behind a guardrail system greatly reduces the soil resistance associated with lateral deflection of the barrier. This reduction in the post-soil forces greatly reduces a system's energy-absorption capability and significantly increases dynamic rail deflections and can produce rail rupture or vehicle override. Further, when the guardrail extends over the embankment, the gap between the bottom of the rail and the ground will be greatly magnified and thereby increase the risk of severe wheel snag.

Full-scale crash testing has shown that for standard W-beam guardrails, the back side of the post must be placed approximately 610 mm (2 ft) from the slope break point in order to assure acceptable safety performance (1). This same study also showed that lengthening the guardrail posts to 2.1 m (7 ft) can allow the back of standard guardrail posts to be placed only 305 mm (1 ft) from the slope break point. Unfortunately, many constricted roadsides have insufficient space to allow the posts to be placed even 305 mm (1 ft) from the slope break point.

One stiffened W-beam guardrail has been developed that has been proven to be crashworthy when installed with the center of the guardrail posts at the slope break point on slopes as steep as 2:1 (2-3). This system utilized half-post spacing and 2,134-mm (7-ft) long, W152x13.4 (W6x9) guardrail posts. The dynamic deflection of this system was 821 mm (32.3 in.) when impacted with the ¾-ton pickup truck. Although this system has demonstrated acceptable safety performance, the long posts and half-post spacing have proven to be both costly and introduce maintenance

challenges. However, utilizing longer posts is more economical to the users than having a system with posts installed at half post spacing.

The Midwest Guardrail System (MGS) has proven to more than double the redirective capacity of the standard W-beam guardrail (4-5). The MGS utilizes mid-span guardrail splices, an increased top rail mounting height of 787 mm (31 in.), an increased blockout depth of 305 mm (12 in.), and a reduced post embedment of 1,016 mm (40 in.). The improved redirective capacity of the MGS provides the opportunity to eliminate the need for half-post spacing and thereby greatly reduces the cost of placing a barrier at the slope break point. In recognition of the potential for reducing barrier costs for constricted sites with steep roadside slopes, the Midwest States Pooled Fund Program elected to fund the research study described herein.

1.2 Objective

The objective of this research was to develop a MGS guardrail system that was capable of being installed at the slope break point of a 2:1 foreslope by utilizing the benefits of the recently developed MGS guardrail. The MGS on a 2:1 fill slope system was designed to meet the Test Level 3 (TL-3) safety performance criteria set forth in the *Manual for Assessing Safety Hardware* (MASH) (6). This study was performed by the Midwest Roadside Safety Facility (MwRSF) in cooperation with the Midwest States Regional Pooled Fund Program.

1.3 Scope

The research objective was achieved through the completion of several tasks. First a literature review was undertaken to review previous evaluations of W-beam guardrail systems placed adjacent to slopes. Next, dynamic bogie testing was performed on steel posts placed at the slope break point of 2:1 foreslope in order to evaluate the post-soil behavior for various embedment

depths. Following this phase, computer simulation modeling was undertaken to determine the optimum design for the guardrail system. After the final design was completed, the guardrail system was fabricated and constructed at the MwRSF's outdoor test site. After fabrication of the test installation, two full-scale vehicle crash tests were performed utilizing 1/2-ton Quad Cab pickup trucks, weighing approximately 2,268 kg (5,000 lb). The targeted impact conditions for these tests were an impact speed of 100 km/h (62 mph) and an impact angle of 25 degrees. Next, the test results were analyzed, evaluated, and documented. Finally, conclusions and recommendations were made that pertain to the safety performance of the MGS system installed adjacent to a 2:1 foreslope.

2 LITERATURE REVIEW

2.1 NCHRP 230 Systems

Previous testing on W-beam guardrail systems installed adjacent to a slope was conducted by ENSCO, Inc. and was met with mixed results (1). The research study consisted of several static and dynamic pendulum tests on guardrail posts in soil as well as four full-scale vehicle crash tests on W-beam barriers. The crash tests of the W-beam guardrail systems placed adjacent to a slope were evaluated according to the criteria provided in National Cooperative Highway Research Program (NCHRP) Report No. 230 (2).

The first impact consisted of a full-scale vehicle crash test on a standard G4(1S) guardrail system with the back-side flanges of 2.1-m (7-ft) long steel posts installed at the break point of a 2:1 foreslope. The 2,044-kg (4,506-lb) passenger-size sedan, used in test no. 1717-1-88, impacted the rail and penetrated behind the system due to the failure of the upstream end anchor cable system.

Following the failure of test no. 1717-1-88, the guardrail system was modified by changing the upstream end anchor system to an eccentric loader BCT. The modified guardrail system was still configured with the back-side flanges of 2.1-m (7-ft) long steel posts installed at the break point of a 2:1 foreslope. The 1,973-kg (4,350-lb) passenger-size sedan, used in test no. 1717-2-88, impacted the rail and began to redirect. Subsequently, the end anchor released slightly and allowed the rail height to drop, thus causing the vehicle to vault over the rail. The vehicle then rolled onto its side before coming to a rest.

After review of the second test, it was found the eccentric loader BCT had been installed wrong, so a retest of test no. 1717-2-88 was then performed due to the upstream end anchor failure. The 1,970-kg (4,343-lb) passenger-size sedan, used in test no. 1717-3-88, impacted the rail and was

redirected safely. However, it is noted that the vehicle's speed change was 11.2 m/s (36.7 ft/s), which was greater than the 6.7 m/s (22.0 ft/s) velocity change allowed by NCHRP Report No. 230.

The final full-scale vehicle crash test was performed on a standard G4(1S) guardrail system with the back-side flanges of 1.8-m (6-ft) long steel posts installed at the break point of a 2:1 foreslope. The 1,978-kg (4,361-lb) passenger-size sedan, used in test no. 1717-4-88, impacted the rail and was redirected. During the test, significant vehicle penetration into the rail system was observed. A high change in vehicle speed was also observed in this test, similar to that found in test no. 1717-3-88. Finally, the vehicle showed no tendency to fall down the slope as it remained quite stable with little vehicle roll.

Following the completion of the study, ENSCO researchers concluded that a standard G4(1S) guardrail system with the back-side flanges of either 1,829-mm (6-ft) or 2,134-mm (7-ft) long steel posts installed at the break point of a 2:1 fill slope will redirect a large sedan (NCHRP 230 – test designation 10). However, it was noted that the dynamic rail deflection for the 1,829-mm (6-ft) long post length was approximately 1,219 mm (48 in.). Therefore, the recommended post length for guardrails placed on the break point of a 2:1 fill slope was 2,134 mm (7 ft).

2.2 NCHRP 350 Systems

In 2000, MwRSF conducted a full-scale vehicle crash test on a W-beam guardrail installed adjacent to a 2:1 foreslope (2-3). This W-beam system was evaluated according to the criteria provided in NCHRP Report 350 (8). The test installation consisted of W-beam guardrail supported by 2,134-mm (7-ft) long, W152x13.4 (W6x9) steel guardrail posts spaced 953 mm (37 ½ in.) on center and installed with the center of the posts at the slope break point. For the full-scale test, test no. MOSW-1, a 2,024-kg (4,462-lb) 3/4-ton pickup truck impacted the system 238 mm (9 3/8 in.)

downstream from the centerline of post no. 17, located within the half-post spacing region, at a speed of 100.7 km/h (62.6 mph) and at an angle of 28.5 degrees. The vehicle was safely redirected, and the test was determined to be acceptable according to the TL-3 safety performance criteria presented in NCHRP Report 350 (8).

3 DEVELOPMENTAL TESTING - DYNAMIC POST TESTING

3.1 Dynamic Component Testing

Dynamic impact testing of W152x13.4 (W6x9) steel posts placed at the break point of a 2:1 fill slope was performed to evaluate the post-soil behavior for various embedment depths as well as to select a steel post alternative for use in the BARRIER VII (9) numerical analyses. Additional details related to the dynamic post testing are provided in the referenced MwRSF research report (10).

A total of seventeen bogie crash tests were performed with post lengths varying from 1,829 mm (6 ft) through 2,743 mm (9 ft) and with embedment depths ranging between 1,016 mm (40 in.) and 1,930 mm (76 in.). For each bogie test, raw acceleration data was acquired and filtered, and then force-displacement and energy-displacement graphs were plotted. From the energy-displacement graphs, the average post-soil forces were calculated for a 381-mm (15-in.) displacement at the center rail height. Average post-soil forces were then compared to the baseline average post capacity of 28 kN (6 kips), which is representative of steel posts found in the MGS placed on a level terrain (10-14). From these comparisons, a recommended post length was selected for the 1,905-mm (75-in.) standard post spacing. A 2,743-mm (9-ft) long post with a 1,930-mm (76-in.) embedment depth was found to best meet the post requirements, while providing an average force of 28.43 kN (6.39 kips), determined from the two tests shown in Figure 1. As such, this post configuration was recommended for evaluation using computer simulation modeling.

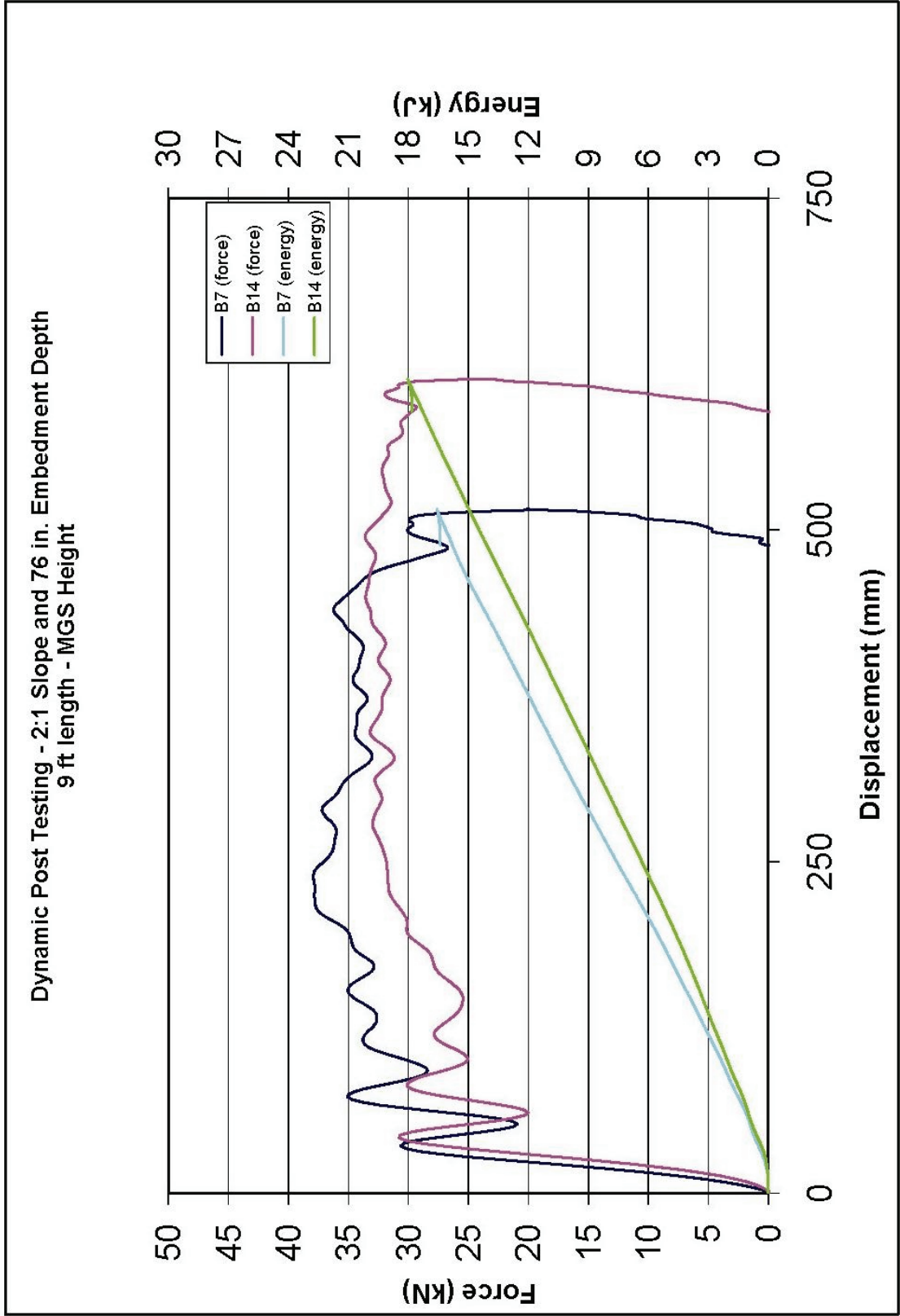


Figure 1. Force and Energy vs. Displacement Curves for 2,743-mm (9-ft) Posts (10)

4 BARRIER VII COMPUTER SIMULATION MODELING

4.1 Background

The safety performance of longitudinal traffic barriers has traditionally been evaluated through the use of full-scale vehicle crash testing. For these crash tests, vehicles are not propelled into the barrier systems at arbitrary locations nor at randomly-selected impact conditions. Historically, crash tests have been performed at an impact location that maximizes the potential for test failure, thus representing the worst-case impact condition. This impact location is commonly referred to as the Critical Impact Point (CIP). BARRIER VII (9), a two-dimensional, non-linear, finite element computer program, has been widely used to analyze vehicle-to-barrier collisions and to predict the dynamic performance of longitudinal barrier systems. In addition, BARRIER VII can be used to determine the CIP for a given barrier system. Although other computer programs exist to study vehicular impacts with longitudinal barriers, BARRIER VII is the most validated program for the prediction of barrier deflections, wheel snag, and vehicle pocketing.

For this research project, multiple BARRIER VII computer simulations were performed in order to evaluate barrier alternatives for the MGS installed on a 2:1 fill slope and to determine the CIP for the proposed crash test planned for the final as-built barrier configuration.

4.2 Computer Model for MGS on a 2:1 Fill Slope

A calibrated and validated BARRIER VII computer model of the MGS system placed on a 2:1 fill slope was needed to evaluate the longitudinal barrier system. As such, the validated finite element analysis (FEA) model from test no. NPG-4 was first used to obtain baseline input parameters for the BARRIER VII simulations (10-14). Test no. NPG-4 consisted of a ¾-ton pickup truck (2000P vehicle) impacting at the TL-3 impact conditions of NCHRP Report 350. MASH

requires a heavier, ½-ton, four-door, Quad Cab pickup truck, weighing 2,268 kg (5,000 lb), and impacting at a speed of 100 km/h (62.1 mph) and at an angle of 25 degrees (6). Because the MGS placed on a 2:1 fill slope was to be developed to meet impact conditions provided in MASH, another validated FEA model was used to obtain additional BARRIER VII input parameters which consisted of the vehicle properties which represent the new 2270P pickup truck. Following test no. 2214MG-2 conducted under NCHRP Project 22-14(2), which was performed on the MGS placed on level terrain and according to the TL-3 impact conditions found in MASH (15-16), MwRSF researchers constructed a BARRIER VII model for a CIP study undertaken during the NCHRP project. It should be noted that the reader may refer to the project documentation of NCHRP 22-14(2) for further information. The BARRIER VII model representing test no. 2214MG-2 used the same input parameters, posts, and barrier elements as those found in the model for test no. NPG-4. However, the vehicle parameters were modified to represent the mass, inertia, and crush stiffness of the 2270P vehicle. Thus, the additional vehicle parameters for BARRIER VII were obtained.

The final barrier model had a total of 173 nodes, 201 members (172 beam members and 29 post members), 4 different beam types, and 3 different post types and a total length of 53.3 m (175 ft). The four different types of beam members correlated to four different lengths, dependent upon their location along the rail. However, the other properties of the beam members remained the same. Typical beam member length in the impact region was 238 mm (9.375 in.). The rail was attached to the posts through a common node every 1,905 mm (75 in.).

For the MGS on a 2:1 fill slope, the modeled posts consisted of 2,743-mm (9-ft) long sections as compared to the 1,829-mm (6-ft) long posts used in the simulations of test nos. NPG-4 and 2214MG-2. The yield moment for the 2,743-mm (9-ft) long posts was calculated based upon

the force-deflection data obtained from the head-on collisions between the bogie and the embedded posts.

However, the vehicle does not always impact the post in a central manner during an actual vehicle crash test, thus resulting in an eccentric load condition imparted to the post. The rail element is typically blocked out and away from the front face of the guardrail post in order to reduce wheel snag on the posts and to help maintain adequate guardrail height. The rail offset, in combination with axial loading imparted to the rail, produces an additional torsional load condition that can further reduce the lateral post capacity observed in central bogie post tests. To account for the effect of this combined loading in real world applications, the post moment capacity about the A-axis (strong-axis bending) should be reduced in the BARRIER VII computer simulation modeling.

Based on experience from prior research studies involving the FEA analysis of longitudinal barrier systems, the actual post moment capacity of 17,917 kN-mm (158.58 kip-in.) was reduced by 10 to 20 percent to account for combined loading on the post (2-3,12-13). BARRIER VII input parameters for the 787-mm (31-in.) tall MGS with a 10 percent moment reduction and a 20 percent moment reduction are given in Table 1. The BARRIER VII finite element model and sample input deck for the MGS-2:1 fill slope system are provided in Appendices A and B, respectively.

After the implementation of these modifications, the FEA model was deemed an appropriate barrier system for representing the actual MGS installed on a 2:1 fill slope. A graphical comparison of the actual barrier displacements for test no. 2214MG-2 and the simulated barrier displacements for the MGS on a 2:1 fill slope are provided in Figures 2 and 3. It should be noted that the MGS on a 2:1 fill slope model was initially calibrated without taking into consideration the slope.

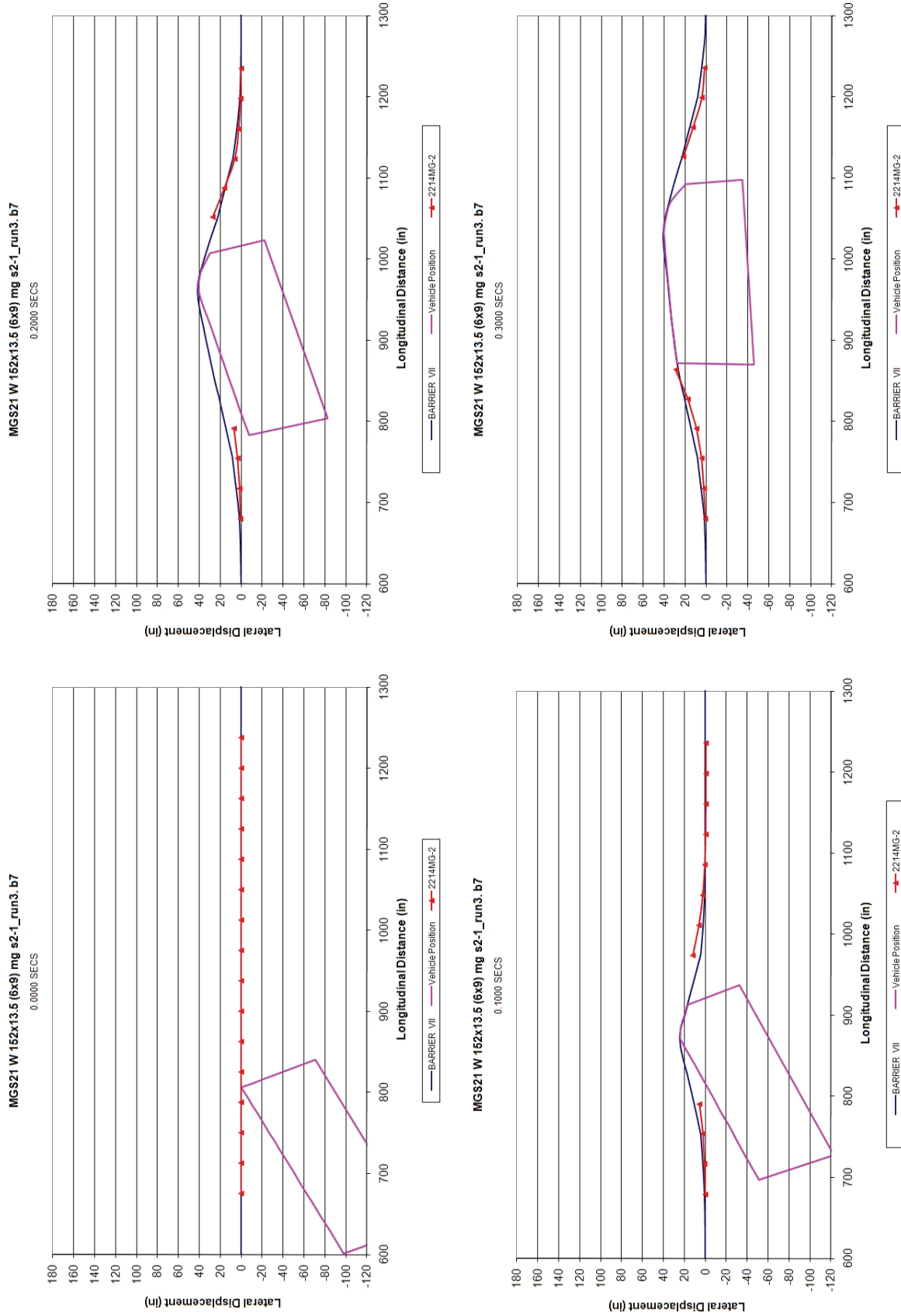


Figure 2. Sequential Plots from BARRIER VII Simulation of MGS on 2:1 Slope

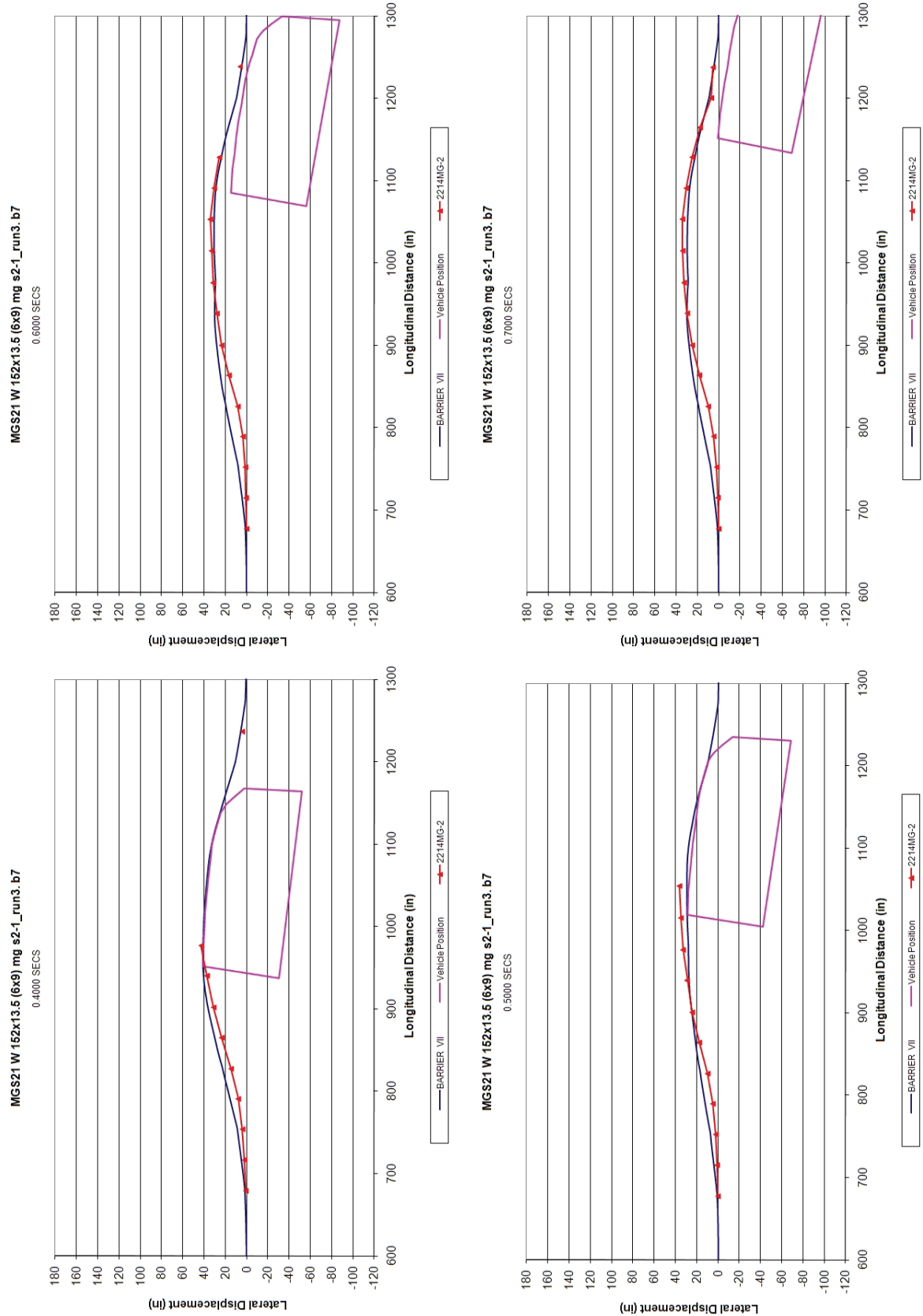


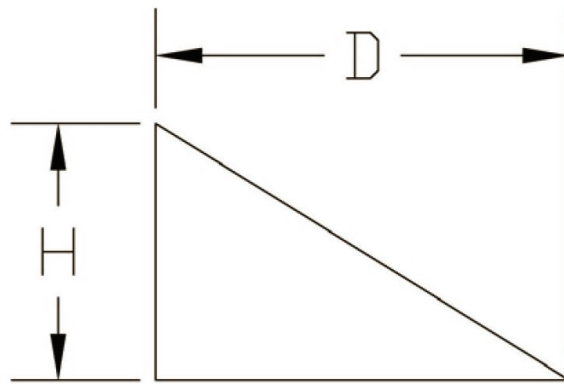
Figure 3. Sequential Plots from BARRIER VII Simulation of MGS on 2:1 Slope

Table 1. BARRIER VII Simulation Parameters for 2,743-mm (9-ft) Posts on a 2:1 Fill Slope

BARRIER VII Parameters		Input Values		
		No Moment Reduction	10 Percent Moment Reduction	20 Percent Moment Reduction
K_B – Strong Axis Post Stiffness	kN/mm (kip/in.)	0.912 (5.21)	0.912 (5.21)	0.912 (5.21)
K_A – Weak Axis Post Stiffness	kN/mm (kip/in.)	0.701 (4.00)	0.701 (4.00)	0.701 (4.00)
M_A – Strong Axis Bending Moment	kN-mm (kip-in.)	17917 (158.58)	16125 (142.72)	14333 (126.86)
M_B – Weak Axis Bending Moment	kN-mm (kip-in.)	10494 (92.88)	10494 (92.88)	10494 (92.88)
δ_{FB} – Strong Axis Failure Displacement	mm (in.)	381 (15)	381 (15)	381 (15)
μ_K – Kinetic Friction Coefficient	Vehicle to Barrier	0.35	0.35	0.35
I_{Mz} – 2270P Mass Moment of Inertia - Yaw	N-m-sec ² (lb-ft-sec ²)	4971 (44000)	4971 (44000)	4971 (44000)

According to the guidelines provided in MASH, longitudinal barrier systems should be evaluated using the minimum acceptable guardrail height when subjected to pickup truck impacts. For the MGS installed on flat terrain, this minimum height has been understood to be 706 mm (27³/₄ in.). As such, BARRIER VII computer modeling was used to analyze and evaluate the MGS placed on a 2:1 fill slope when installed at both the 787-mm (31-in.) and 706-mm (27³/₄-in.) top mounting heights. For the lower height tolerance, the moment arm would decrease by 83 mm (3¹/₄ in.); thus, the moment about the A-axis (strong-axis bending), M_A , for the 10 and 20 percent moment reduction values was 17,533 kN-mm (155.19 kip-in.) and 15,598 kN-mm (138.06 kip-in.), respectively.

As the vehicle impacts the barrier and travels down the slope, its velocity can actually increase due to gravity. However, since BARRIER VII does not account for changes in elevation, additional velocity must be added to the vehicle's initial velocity in order to compensate for the vehicle movement down the slope. For this study, this additional velocity was calculated using conservation of energy based upon the maximum rail deflection and initial impact velocity. For each rail height and moment reduction system, the maximum rail deflection was determined for an impact at the nominal velocity of 100 km/h (62.1 mph). Using conservation of energy, Figure 4, and the maximum rail deflections, a new impact velocity was calculated, for use in BARRIER VII, that considered the change in potential energy for each rail height and moment reduction configuration.



$$\frac{1}{2}MV_h^2 = \frac{1}{2}MV_s^2 + MgH$$

where

D = maximum lateral rail deflection

H = c.g. height drop = $D/2$

M = vehicle mass

V_s = velocity on road surface

V_h = velocity at a depth H below road surface

Figure 4. Determination of New Impact Velocity Considering Change in Potential Energy

4.3 BARRIER VII Simulation Results

A total of eight sets of simulations were performed in order to determine the CIP. For each set, ten simulations were performed at ten closely spaced impact nodes between two posts, post nos. 12 and 13. In addition, a splice was located at the midspan between these two posts. For the MGS, a satisfactory safety performance had been shown for top mounting heights ranging between 706 mm (27¾ in.) and 813 mm (32 in.), with a nominal top mounting height of 787 mm (31 in.). Therefore, simulations were performed at two heights, one at 706 mm (27¾ in.) and the other at 787 mm (31 in.). The first four simulations were performed at a 10 percent moment reduction, two at a 706-mm (27¾-in.) top mounting height and two at a 787-mm (31-in.) top mounting height. At each height, simulations were performed at two vehicle speeds, the normal speed of 100 km/h (62.14 mph) and at an increased speed due to movement down the slope. The other four simulations were performed in a similar manner, but with a 20 percent moment reduction. The summary of the simulation results are shown in Tables 2 and 3.

4.4 Critical Impact Point (CIP) Determination

Determining the CIP of a system can be quite difficult since there are not set criteria for BARRIER VII that clearly defines failure of a system. Traditionally, the CIP determination has been based upon the impact condition which produced a worst practical condition and potential guardrail failure while considering: (1) wheel-assembly snagging on guardrail posts; (2) vehicle pocketing into the guardrail system; (3) dynamic lateral deflection of the guardrail system; and (4) axial force in the W-beam guardrail. Additional discussion on the determination of the CIP can be found in a research paper by Reid, et al ([17](#)).

Table 2. Summary of BARRIER VII Simulation Results for 10 Percent Moment Reduction

10% moment reduction, V=100 km/h, Top Mounting Height = 787 mm (31 in.)					
Impact Node	Max. Deflection (in.)	Max. Rail Force (kips)	Max. Snag (in.)	Max. Slope 3 node	
60	43.25	65.16	0.86	0.2246	
61	41.74	67.07	0.00	0.2299	
62	42.12	65.83	0.00	0.2415	
63	42.62	67.33	0.32	0.2412	
64	43.31	67.60	2.28	0.2422	
65	43.43	67.61	3.35	0.2294	
66	43.27	67.22	3.57	0.2131	
67	43.05	66.22	2.42	0.2212	
68	40.80	68.44	4.88	0.2278	
69	41.20	66.98	0.00	0.2365	

10% moment reduction, V=100 km/h + potential energy, Top Mounting Height = 706 mm (27 3/4 in.)					
Impact Node	Max. Deflection (in.)	Max. Rail Force (kips)	Max. Snag (in.)	Max. Slope 3 node	
60	36.53	72.70	1.59	0.2424	
61	36.77	71.64	0.22	0.2541	
62	37.40	71.91	2.57	0.2529	
63	37.76	71.47	4.33	0.2474	
64	38.29	71.85	5.51	0.2360	
65	38.73	72.08	6.71	0.2242	
66	35.13	72.19	5.12	0.2548	
67	35.72	72.93	6.42	0.2442	
68	36.41	73.73	1.53	0.2415	
69	36.53	74.28	0.27	0.2470	

10% moment reduction, V=100 km/h + potential energy, Top Mounting Height = 787 mm (31 in.)					
Impact Node	Max. Deflection (in.)	Max. Rail Force (kips)	Max. Snag (in.)	Max. Slope 3 node	
60	43.11	65.27	1.04	0.2299	
61	41.53	66.48	0.00	0.2357	
62	42.09	65.66	0.00	0.2415	
63	42.92	67.35	0.68	0.2456	
64	43.41	67.89	2.73	0.2410	
65	43.49	67.65	3.80	0.2294	
66	43.40	67.50	5.24	0.2137	
67	42.92	65.67	2.73	0.2302	
68	40.88	68.14	5.18	0.2274	
69	41.48	67.43	0.00	0.2365	

10% moment reduction, V=100 km/h + potential energy, Top Mounting Height = 706 mm (27 3/4 in.)					
Impact Node	Max. Deflection (in.)	Max. Rail Force (kips)	Max. Snag (in.)	Max. Slope 3 node	
60	36.74	71.99	1.56	0.2422	
61	37.00	72.10	0.28	0.2527	
62	37.59	71.82	2.87	0.2527	
63	38.02	71.73	4.52	0.2474	
64	38.51	72.37	5.83	0.2360	
65	39.00	72.70	4.82	0.2242	
66	35.01	71.50	5.59	0.2542	
67	35.77	73.03	6.82	0.2442	
68	36.61	73.85	1.66	0.2427	
69	36.77	74.23	0.33	0.2470	

Table 3. Summary of BARRIER VII Simulation Results for 20 Percent Moment Reduction

20% moment reduction, V=100 km/h, Top Mounting Height = 787 mm (31 in.)						
Impact Node	Max. Deflection (in.)	Max. Rail Force (kips)	Max. Snag (in.)	Max. Slope 3 node		
60	47.22	64.20	2.91	0.2185		
61	47.62	64.47	3.07	0.2185		
62	46.91	64.84	3.63	0.2240		
63	44.68	66.81	3.57	0.2363		
64	45.08	66.01	0.00	0.2349		
65	45.20	66.19	0.00	0.2242		
66	45.30	66.89	3.46	0.2123		
67	45.68	65.85	2.23	0.2210		
68	46.68	65.00	3.01	0.2210		
69	46.04	65.74	2.96	0.2129		

20% moment reduction, V=100 km/h + potential energy, Top Mounting Height = 706 mm (27 3/4 in.)						
Impact Node	Max. Deflection (in.)	Max. Rail Force (kips)	Max. Snag (in.)	Max. Slope 3 node		
60	38.79	72.76	1.45	0.2362		
61	38.66	70.88	3.27	0.2419		
62	39.15	70.95	4.63	0.2451		
63	39.73	72.69	5.66	0.2419		
64	40.09	73.07	0.00	0.2311		
65	40.60	71.64	4.73	0.2246		
66	39.86	70.27	4.14	0.2283		
67	37.67	71.97	2.84	0.2422		
68	38.13	72.23	1.42	0.2415		
69	38.22	72.40	3.29	0.2409		

20% moment reduction, V=100 km/h + potential energy, Top Mounting Height = 787 mm (31 in.)						
Impact Node	Max. Deflection (in.)	Max. Rail Force (kips)	Max. Snag (in.)	Max. Slope 3 node		
60	47.61	64.12	3.14	0.2185		
61	47.84	64.41	3.61	0.2185		
62	45.30	66.72	2.87	0.2298		
63	44.86	67.05	4.03	0.2404		
64	45.23	65.93	0.00	0.2356		
65	45.48	66.37	0.00	0.2242		
66	45.50	66.70	3.78	0.2123		
67	45.62	65.16	2.53	0.2210		
68	46.63	64.30	3.35	0.2191		
69	47.17	66.28	3.55	0.2120		

20% moment reduction, V=100 km/h + potential energy, Top Mounting Height = 706 mm (27 3/4 in.)						
Impact Node	Max. Deflection (in.)	Max. Rail Force (kips)	Max. Snag (in.)	Max. Slope 3 node		
60	38.29	71.53	2.15	0.2417		
61	38.84	70.52	3.48	0.2419		
62	39.27	71.13	4.88	0.2467		
63	39.76	72.09	5.93	0.2419		
64	40.31	72.98	0.00	0.2312		
65	40.83	71.97	4.82	0.2242		
66	40.59	71.21	3.76	0.2201		
67	37.70	72.25	2.89	0.2407		
68	38.17	72.37	1.41	0.2431		
69	38.45	72.37	3.59	0.2362		

The maximum deflections found during the CIP analysis of the MGS on a 2:1 fill slope were similar to those observed during actual full-scale crash testing of the standard MGS on level terrain (12-16). The range of maximum rail axial forces during the CIP analysis was small; and the MGS has proven to more than double the redirective capacity of the standard W-beam guardrail(4-5). Similarly, the range of pocketing angles for all CIP simulations was small and ranged from 12 to 14 degrees, which is about half of the critical pocketing angle of 23 degrees established during the development of the MGS transition (18-19). Therefore, maximum dynamic deflection, maximum axial force, and maximum pocketing angle were not deemed critical factors for the MGS on a 2:1 fill slope CIP determination. However, wheel snagging was deemed to be a significant contributing factor for the CIP determination of the MGS on a 2:1 fill slope. The CIP analysis of the eight sets of simulation results is shown in Table 4.

Table 4. CIP Analysis Results

Moment Reduction	Top Mounting Height	Velocity	CIP	
			Node Number	Location (from centerline of post no. 13)
Percent	mm (in.)			mm (in.)
10	787 (31)	nominal	68	119 (4 ¹¹ / ₁₆) upstream
10	787 (31)	increased	66	476 (18 ³ / ₄) upstream
10	706 (27 ³ / ₄)	nominal	65	714 (28 ¹ / ₈) upstream
10	706 (27 ³ / ₄)	increased	67	238 (9 ³ / ₈) upstream
20	787 (31)	nominal	62	1,429 (56 ¹ / ₄) upstream
20	787 (31)	increased	63	1,141 (46 ⁷ / ₈) upstream
20	706 (27 ³ / ₄)	nominal	63	1,141 (46 ⁷ / ₈) upstream
20	706 (27 ³ / ₄)	increased	63	1,141 (46 ⁷ / ₈) upstream

*The highlighted simulation was the selected CIP for full-scale testing.

From the eight design variations that were evaluated and shown in Tables 2 and 3, it was determined that the most valid model was the MGS with the minimum 706-mm (27³/₄-in.) top mounting height on a 2:1 fill slope. This was based on the fact that the maximum wheel snag occurred with the design variation utilizing a 10 percent reduction in the strong-axis bending moment as discussed previously. This also verified that it was appropriate to include the slope effects, i.e., the associated minor increase in impact velocity.

From the BARRIER VII simulations, the CIP was selected to occur at node 67 or 238 mm (9³/₈ in.) upstream from the centerline of post no. 13 (node 69) or 595 mm (23⁷/₁₆ in.) downstream from the centerline of the splice between post nos. 12 and 13. For the selected CIP, the simulation revealed a maximum dynamic rail deflection of 909 mm (35.77 in.) at post no. 15 (node 87), while the maximum wheel snag was observed at post no. 16 (node 96) in the amount of 173 mm (6.82 in.). Finally, the maximum rail tension for this system was 325 kN (73.03 kips) at 476 mm (18³/₄ in.) downstream from the centerline of post no. 14 (node 80) or 476 mm (18³/₄ in.) upstream from the centerline of the splice between post nos. 14 and 15.

5 TEST REQUIREMENTS AND EVALUATION CRITERIA

5.1 Test Requirements

Longitudinal barriers, such as W-Beam guardrail systems, must satisfy impact safety standards in order to be accepted by the Federal Highway Administration (FHWA) for use on National Highway System (NHS) new construction projects or as a replacement for existing designs not meeting current safety standards. In recent years, these safety standards have consisted of the guidelines and procedures published in NCHRP Report 350 (2). However, NCHRP Project 22-14(2) generated revised testing procedures and guidelines for used in the evaluation of roadside safety appurtenances and are provided in MASH (6). According to TL-3 of MASH, the longitudinal barrier system must be subjected to two full-scale vehicle crash tests. The two full-scale crash tests are as follows:

1. Test Designation 3-10. A 1,100-kg (2,425-lb) small car impacting the W-beam system at a nominal speed and angle of 100 km/h (62 mph) and 25 degrees, respectively.
2. Test Designation 3-11. A 2,268-kg (5,000-lb) pickup truck impacting the W-beam system at a nominal speed and angle of 100 km/h (62 mph) and 25 degrees, respectively.

However, W-beam barriers struck by small cars have been shown to meet safety performance standards with little lateral deflections (12-15,20-22) and with no significant potential for occupant risk problems. In addition, the MGS with maximum height tolerance was successfully impacted by a small car weighing 1,174 kg (2,588 lb) at 97.8 km/h (60.8 mph) and 25.4 degrees according to the TL-3 safety performance criteria set forth in MASH (23). Thus, the 1,100-kg (2,425-lb) passenger car crash test was deemed unnecessary for this project. The test conditions for TL-3 longitudinal

barriers are summarized in Table 5. Test Designation 3-11 was conducted for the MGS system described herein.

Table 5. MASH Test Level 3 Crash Test Conditions

Test Article	Test Designation	Test Vehicle	Impact Conditions			Evaluation Criteria ¹
			Speed		Angle (degrees)	
			(km/h)	(mph)		
Longitudinal Barriers	3-10	1100C	100	62	25	A,D,F,H,I
	3-11	2270P	100	62	25	A,D,F,H,I

¹ Evaluation criteria explained in Table 6.

5.2 Evaluation Criteria

According to MASH, the evaluation criteria for full-scale vehicle crash testing are based on three appraisal areas: (1) structural adequacy; (2) occupant risk; and (3) vehicle trajectory after collision. Criteria for structural adequacy are intended to evaluate the ability of the barrier to contain, redirect, or allow controlled vehicle penetration in a predictable manner. Occupant risk evaluates the degree of hazard to occupants in the impacting vehicle. Vehicle trajectory after collision is a measure of the potential for the post-impact trajectory of the vehicle to become involved in secondary collisions with other vehicles or fixed objects, thereby increasing the risk of injury to the occupant of the impacting vehicle and to other vehicles. This criterion also indicates the potential safety hazard for the occupants of other vehicles or the occupants of the impacting vehicle when subjected to secondary collisions with other fixed objects. These three evaluation criteria are summarized in Table 6 and defined in greater detail in MASH (6). The full-scale vehicle crash tests were conducted and reported in accordance with the procedures provided in MASH.

Table 6. MASH Evaluation Criteria for Crash Tests

Evaluation Factors	Evaluation Criteria		
Structural Adequacy	A. Test article should contain and redirect the vehicle or bring the vehicle to a controlled stop; the vehicle should not penetrate, underride, or override the installation although controlled lateral deflection of the test article is acceptable		
Occupant Risk	D. Detached elements, fragments or other debris from the test article should not penetrate or show potential for penetrating the occupant compartment, or present undue hazard to other traffic, pedestrians, or personnel in a work zone. Deformations of, or intrusions into, the occupant compartment should not exceed limits set forth in Section 5.3 and Appendix E of MASH.		
	F. The vehicle should remain upright during and after collision. The maximum roll and pitch angles are not to exceed 75 degrees.		
	H. Occupant Impact Velocities (OIV) (see Appendix A, Section A5.3 for calculation procedure) should satisfy the following limits:		
	Occupant Impact Velocity Limits, ft/s (m/s)		
	Component	Preferred	Maximum
	Longitudinal and Lateral	30 ft/s (9.1 m/s)	40 ft/s (12.2 m/s)
I. The Occupant Ridedown Acceleration (see Appendix A, Section A5.3 for calculation procedure) should satisfy the following limits:			
Occupant Ridedown Acceleration Limits (g's)			
Component	Preferred	Maximum	
Longitudinal and Lateral	15.0 g's	20.49 g's	

6 TEST CONDITIONS

6.1 Test Facility

The testing facility is located at the Lincoln Air Park on the northwest (NW) side of the Lincoln Municipal Airport and is approximately 8.0 km (5 mi.) NW of the University of Nebraska-Lincoln.

6.2 Vehicle Tow and Guidance System

A reverse cable tow system with a 1:2 mechanical advantage was used to propel the test vehicle. The distance traveled and the speed of the tow vehicle were one-half that of the test vehicle. The test vehicle was released from the tow cable before impact with the barrier system. A digital speedometer on the tow vehicle increases the accuracy of the test vehicle impact speed.

A vehicle guidance system developed by Hinch ([24](#)) was used to steer the test vehicle. A guide-flag, attached to the left-front wheel and the guide cable, was sheared off before impact with the barrier system. The 9.5-mm (3/8-in.) diameter guide cable was tensioned to approximately 15.6 kN (3,500 lb), and supported laterally and vertically every 30.5 m (100 ft) by hinged stanchions. The hinged stanchions stood upright while holding up the guide cable, but as the vehicle was towed down the line, the guide-flag struck and knocked each stanchion to the ground. For test nos. MGS221-1 and MGS221-2, the guidance systems were 331 m (1,087 ft) long.

6.3 Test Vehicles

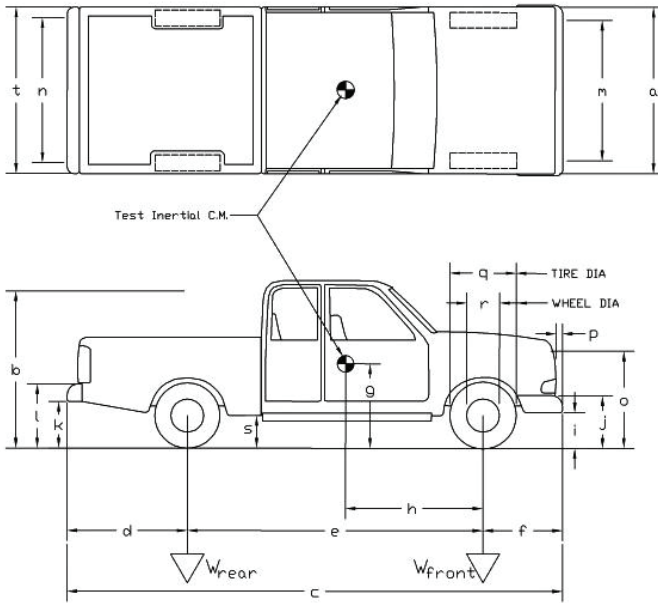
For test no. MGS221-1, a 2003 Dodge Ram 1500 Quad Cab pickup truck was used as the test vehicle. The test inertial and gross static weights were 2,268 kg (5,000 lb). The test vehicle is shown in Figure 5, and vehicle dimensions are shown in Figure 6.



Figure 5. Test Vehicle, Test No. MGS221-1

Date: 8/25/2006 Test Number: MGS221-1 Model: Ram 1500 Q.C.
 Make: Dodge Vehicle I.D.#: 1D7HA18Z735106906
 Tire Size: P265/70 R17 Year: 2003 Odometer: 95152

*(All Measurements Refer to Impacting Side)



Vehicle Geometry -- mm (in.)

a	1955.8 (77.0)	b	1905 (75.0)
c	5791.2 (228.0)	d	1035.1 (40.75)
e	3562.4 (140.25)	f	1193.8 (47.0)
g	717.55 (28.25)	h	1565.3 (61.625)
i	400.05 (15.75)	j	654.05 (25.75)
k	546.1 (21.5)	l	755.65 (29.75)
m	1720.9 (67.75)	n	1714.5 (67.5)
o	1117.6 (44.0)	p	88.9 (3.5)
q	806.45 (31.75)	r	489.9 (18.5)
s	419.1 (16.5)	t	1911.4 (75.25)
Wheel Center Height Front	364.18 (15.125)		
Wheel Center Height Rear	387.35 (15.25)		
Wheel Well Clearance (FR)	914.4 (36.0)		
Wheel Well Clearance (RR)	984.25 (38.75)		
Frame Height (FR)	457.2 (18.0)		
Frame Height (RR)	730.25 (28.75)		
Engine Type	8 CYL. GAS		
Engine Size	5.9L		

Transmission Type:

Automatic

Weights kg (lbs)	Curb	Test Inertial	Gross Static
W-front	1314.5 (2898)	1279.1 (2820)	1279.1 (2820)
W-rear	1001.1 (2207)	988.83 (2180)	988.83 (2180)
W-total	2315.6 (5105)	2268 (5000)	2268 (5000)

	RWD
Front GVWR	3650
Rear GVWR	3900
Total GVWR	6650

Note any damage prior to test: None

Figure 6. Test Vehicle Dimensions, Test No. MGS221-1

For test no. MGS221-2, a 2004 Dodge Ram 1500 Quad Cab pickup truck was used as the test vehicle. The test inertial and gross static weights were 2,274 kg (5,013 lb). The test vehicle is shown in Figure 7, and vehicle dimensions are shown in Figure 8.

The Suspension Method (25) was used to determine the vertical component of the center of gravity (c.g.) for the pickup trucks. This method is based on the principle that the c.g. of any freely suspended body is in the vertical plane through the point of suspension. The vehicle was suspended successively in three positions, and the respective planes containing the c.g. were established. The intersection of these planes pinpointed the location of the center of gravity. The longitudinal component of the c.g. was determined using the measured axle weights. The location of the final centers of gravity are shown in Figures 6 and 8 through 10.

Square black and white-checked targets were placed on the vehicles to aid in the analysis of the high-speed videos, as shown in Figures 9 and 10. Checkered targets were placed at the c.g. on the left-side door, the right-side door, and the roof of the vehicle. The remaining targets were located for reference so that they could be viewed from the high-speed cameras for video analysis.

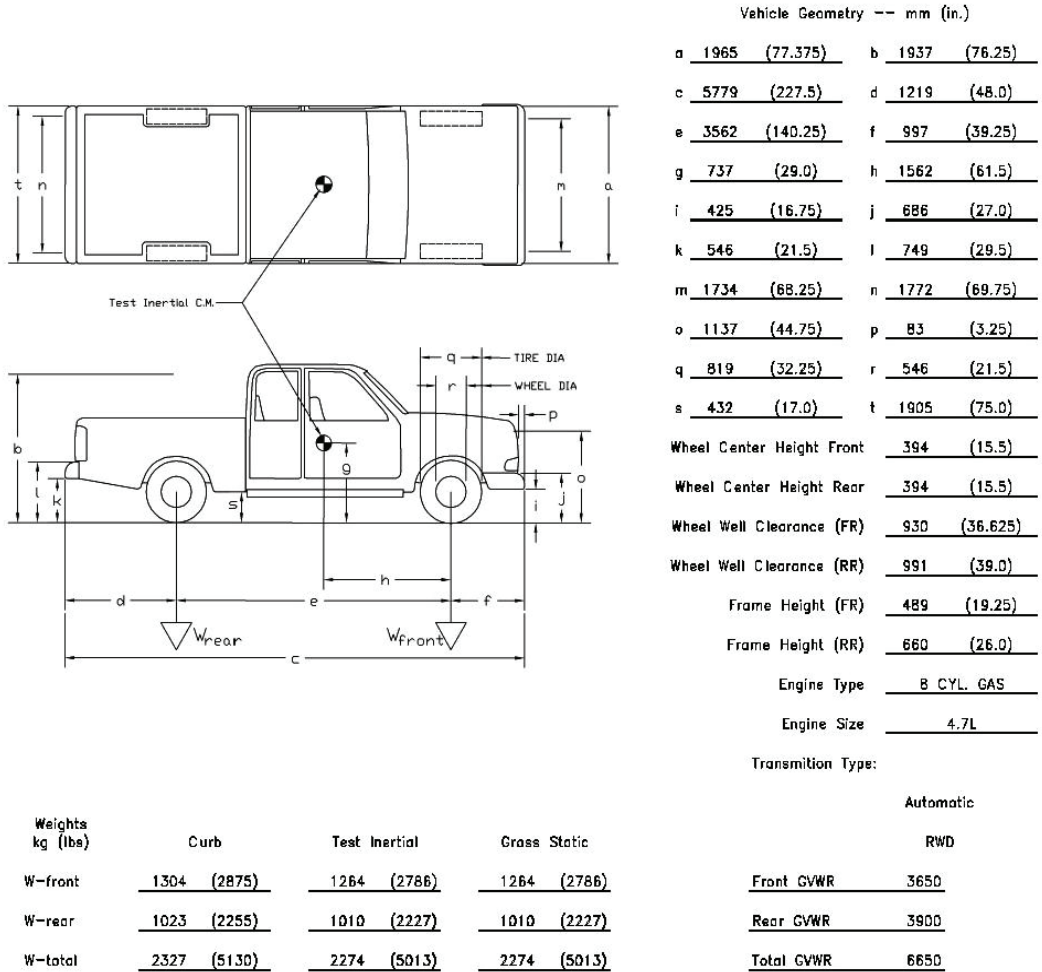
The front wheels of the test vehicles were aligned for camber, caster, and toe-in values of zero so that the vehicles would track properly along the guide cable. A 5B flash bulb was mounted on the left quarter point of the vehicle's dash to pinpoint the time of impact with the test article on the high-speed video footage. The flash bulb was fired by a pressure tape switch mounted at the impact corner of the bumper. A remote-controlled brake system was installed in the test vehicle so the vehicle could be brought safely to a stop after the tests.



Figure 7. Test Vehicle, Test No. MGS221-2

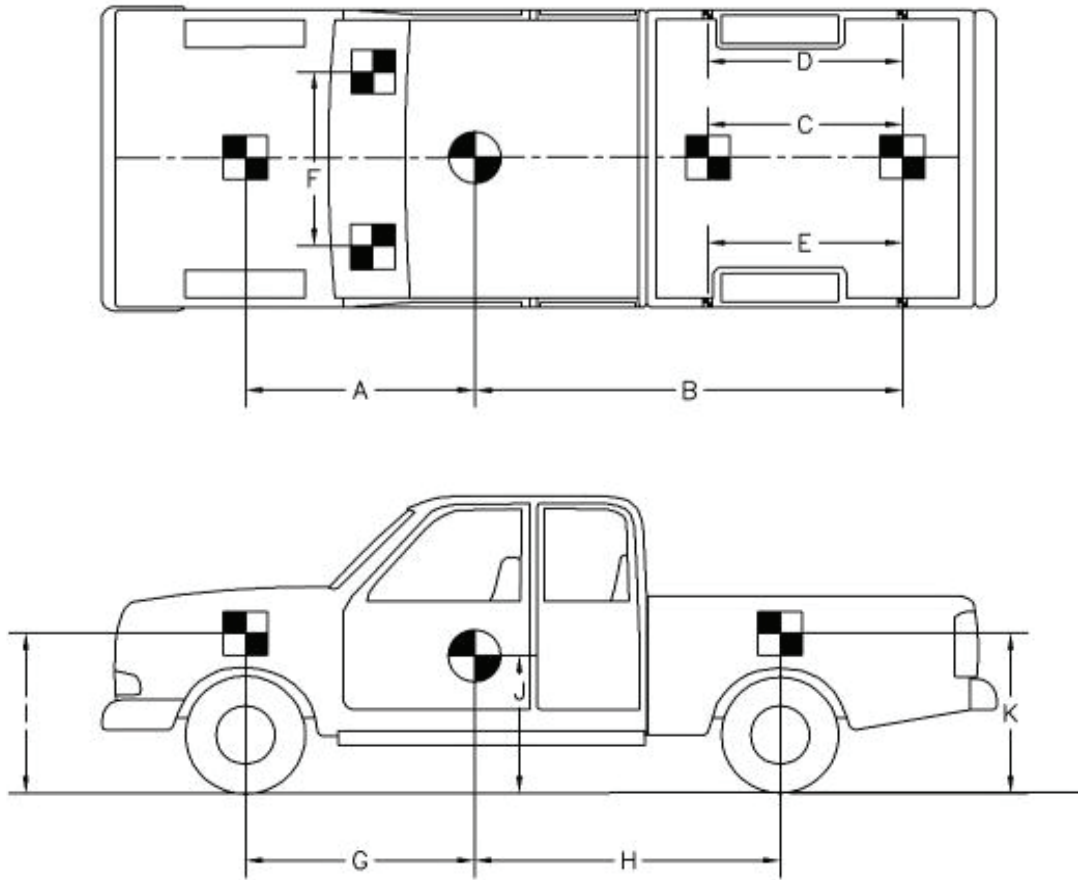
Date: 12/15/2006 Test Number: MGS221-2 Model: Ram 1500 Q.C.
Make: Dodge Vehicle I.D.#: 1D7HA1BN44S599703
Tire Size: 275/60 R20 Year: 2004 Odometer: NA

*(All Measurements Refer to Impacting Side)



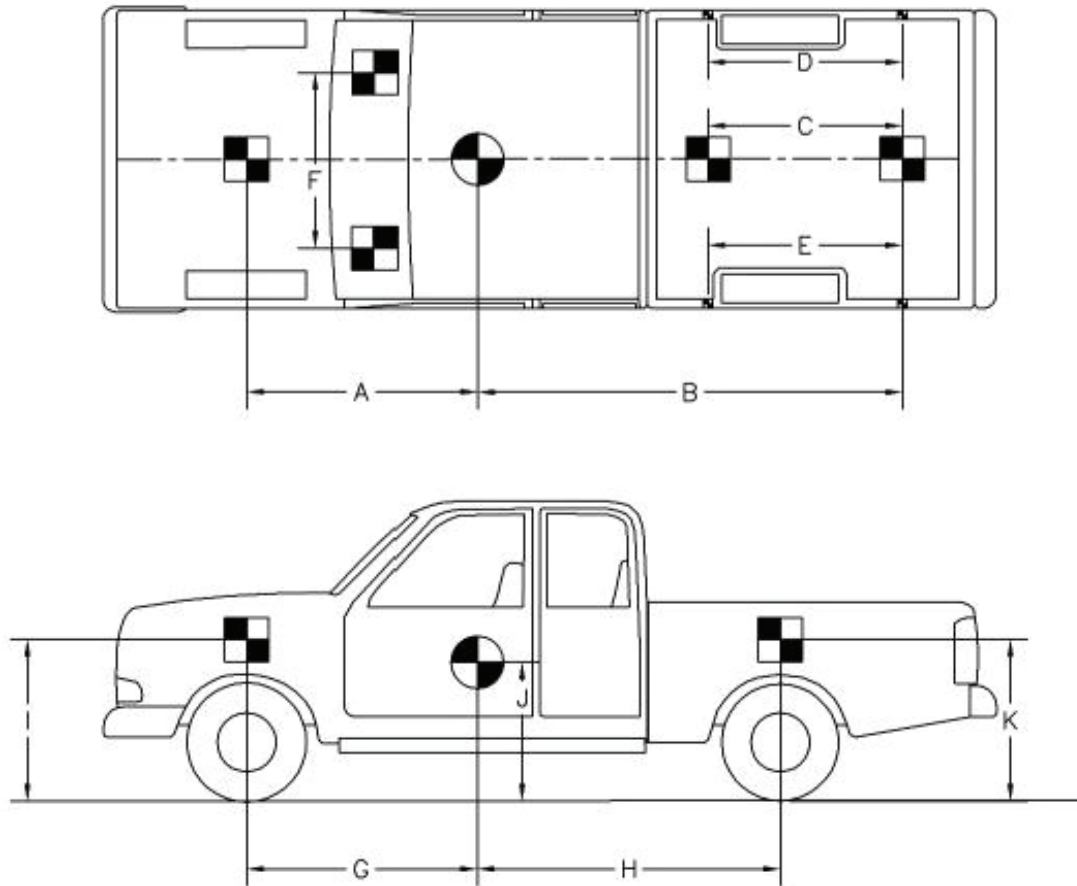
Note any damage prior to test: Katrina Flood Damaged

Figure 8. Test Vehicle Dimensions, Test No. MGS221-2



TEST #: <u>MGS221-1</u>					
TARGET GEOMETRY-- mm (in.)					
A	<u>1880</u>	(74.0)	E	<u>1626</u>	(64.0)
B	<u>2645</u>	(104.125)	F	<u>927</u>	(36.5)
C	<u>1121</u>	(44.125)	G	<u>1565</u>	(61.625)
D	<u>1626</u>	(64.0)	H	<u>1997</u>	(78.625)
I	<u>1019</u>	(40.125)	J	<u>718</u>	(28.25)
K	<u>1089</u>	(42.875)			

Figure 9. Vehicle Target Locations, Test No. MGS221-1



TEST #: MGS221-2					
TARGET GEOMETRY-- mm (in.)					
A	1861	(73.25)	E	1622	(63.875)
B	2648	(104.25)	F	895	(35.25)
C	1130	(44.5)	G	1562	(61.5)
D	1626	(64.0)	H	2000	(78.75)
			I	1035	(40.75)
			J	737	(29.0)
			K	1105	(43.5)

Figure 10. Vehicle Target Locations, Test No. MGS221-2

6.4 Data Acquisition Systems

6.4.1 Accelerometers

Two environmental shock and vibration sensor/recorder systems were used to measure the accelerations in the longitudinal, lateral, and vertical directions. All of the accelerometers were mounted near the center of gravity of the test vehicles.

One triaxial piezoresistive accelerometer system, Model EDR-4 6DOF-500/1200, was developed by Instrumented Sensor Technology (IST) of Okemos, Michigan and includes three differential channels as well as three single-ended channels. The EDR-4 6DOF-500/1200 was configured with 24 MB of RAM memory, a range of ± 500 g's, a sample rate of 10,000 Hz, and a 1,677 Hz anti-aliasing filter. "EDR4COM" and "DynaMap Suite" computer software programs and a customized Microsoft Excel worksheet were used to analyze and plot the accelerometer data.

Another system, Model EDR-3, was a triaxial piezoresistive accelerometer system developed by Instrumented Sensor Technology (IST) of Okemos, Michigan. The EDR-3 was configured with 256 kB of RAM memory, a range of ± 200 g's, a sample rate of 3,200 Hz, and a 1,120 Hz lowpass filter. The computer software program "DynaMax 1 (DM-1)" and a customized Microsoft Excel worksheet were used to analyze and plot the accelerometer data.

6.4.2 Rate Transducers

An Analog Systems 3-axis rate transducer with a range of 1,200 degree/sec in each of the three directions (pitch, roll, and yaw) was used to measure the rates of motion of the test vehicles. The rate transducer was mounted inside the body of the EDR-4M6 and recorded data at 10,000 Hz to a second data acquisition board inside the EDR-4M6 housing. The raw data measurements were then downloaded, converted to the appropriate Euler angles for analysis, and plotted. "DynaMax 1

(DM-1)” and DADiSP computer software programs were used to analyze and plot the rate transducer data.

6.4.3 Pressure Tape Switches

For both tests, five pressure-activated tape switches, spaced at 2-m (6.6-ft) intervals, were used to determine the speed of the vehicle before impact. Each tape switch fired a strobe light which sent an electronic timing signal to the data acquisition system as the left-front tire of the test vehicle passed over it. Test vehicle speed was determined from electronic timing mark data recorded using TestPoint software. Strobe lights and high-speed video analysis are used only as a backup in the event that vehicle speed cannot be determined from the electronic data.

6.4.4 High-Speed Photography

For test MGS221-1, four high-speed AOS VITcam video cameras, with operating speeds of 500 frames/sec, were used to film the crash test. Five Canon and two JVC digital video cameras, all with a standard operating speed of 29.97 frames/sec, were also used to film the crash test. Camera details and a schematic of all eleven camera locations for test MGS221-1 are shown in Figure 11.

For test MGS221-2, four high-speed AOS VITcam video cameras, with operating speeds of 500 frames/sec, were used to film the crash test. Four Canon and two JVC digital video cameras, all with a standard operating speed of 29.97 frames/sec, were also used to film the crash test. Camera details and a schematic of all ten camera locations for test MGS221-2 are shown in Figure 12.

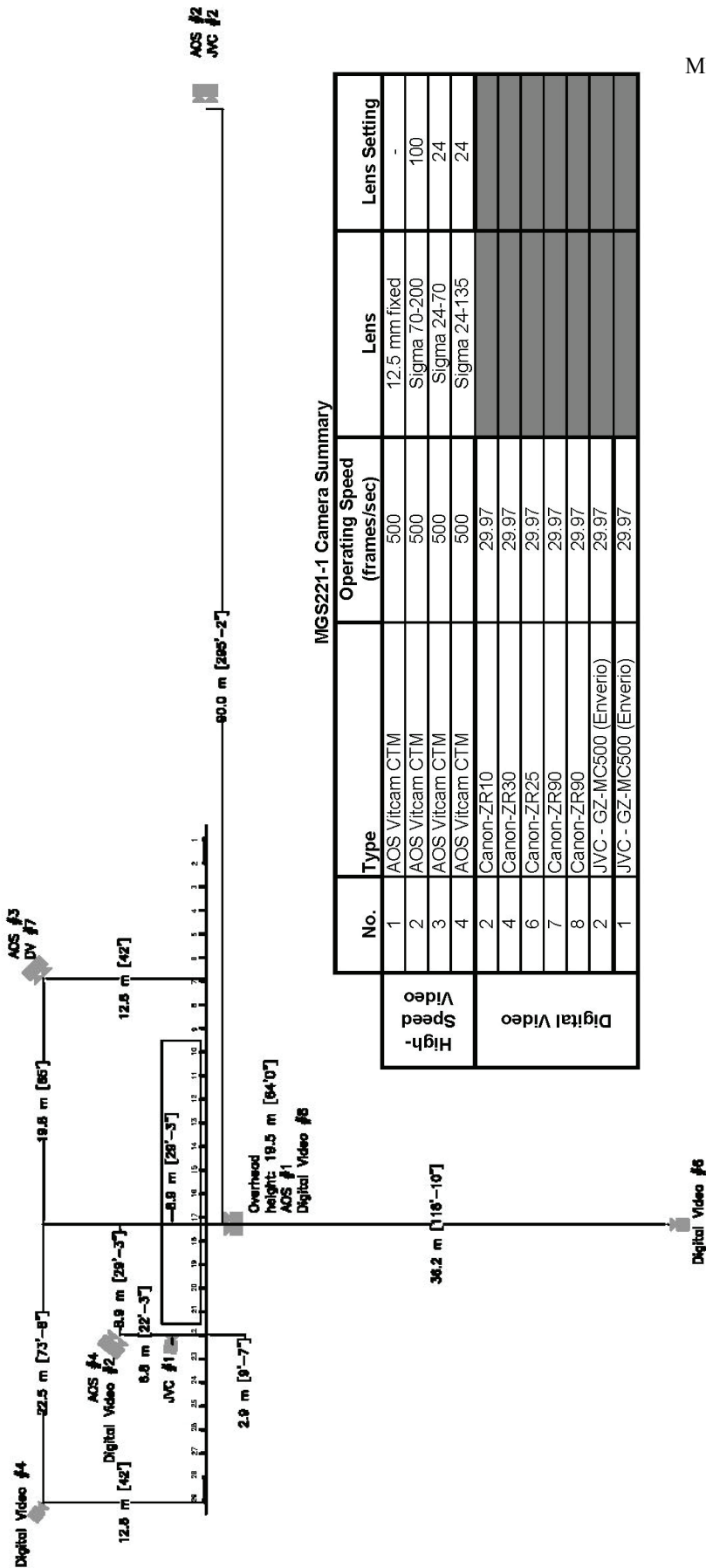
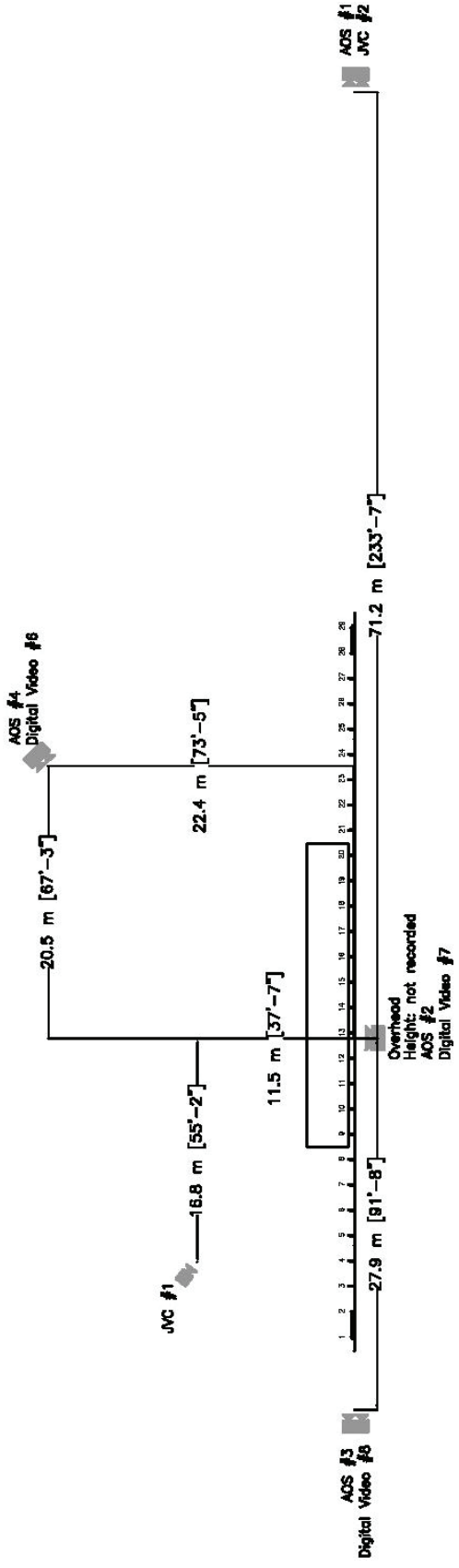


Figure 11. Location of Cameras, Test No. MGS221-1



MG221-2 Camera Summary

No.	Type	Operating Speed (frames/sec)	Lens	Lens Setting
1	AOS Vitcam CTM	500	Sigma 70-200	135
2	AOS Vitcam CTM	500	Fixed 12.5mm	-
3	AOS Vitcam CTM	500	Sigma 24-70	70
4	AOS Vitcam CTM	500	Fixed 50mm	-
2	Canon-ZR10	29.97		
6	Canon-ZR25	29.97		
7	Canon-ZR90	29.97	wide angle	
8	Canon-ZR90	29.97		
1	JVC - GZ-MC500 (Everio)	29.97		
2	JVC - GZ-MC40u (Everio)	29.97		

Video	Speed	High-Speed
1	500	
2	500	
3	500	
4	500	
2	29.97	
6	29.97	
7	29.97	
8	29.97	
1	29.97	
2	29.97	

Digital Video #2

Figure 12. Location of Cameras, Test No. MGS221-2

7 MGS INSTALLED ADJACENT TO A 2:1 FILL SLOPE (DESIGN NO. 1) DETAILS

The test installation consisted of 53.3 m (175 ft) of standard 2.66-mm thick (12-gauge) W-beam guardrail supported by steel posts. Anchorage systems similar to those used on tangent guardrail terminals were utilized on both the upstream and downstream ends of the guardrail system. Design details are shown in Figures 13 through 20. The corresponding English-unit drawings are shown in Appendix C. Photographs of the test installation are shown in Figures 21 through 23.

The entire system was constructed with twenty-nine guardrail posts. Post nos. 3 through 8 and 21 through 27 were galvanized ASTM A36 steel W152x13.4 (W6x9) sections measuring 1,829 mm (6 ft) long. Post nos. 9 through 20 were also ASTM A36 steel W152x13.4 (W6x9) sections, but measured 2,743-mm (9-ft) long. Post no. 1, 2, 28, and 29 were timber posts measuring 140-mm wide x 190-mm deep x 1,080-mm long (5½-in. x 7½-in. x 42½-in.) and were placed in 1,829-mm (6-ft) long steel foundation tubes, as shown in Figure 17. The timber posts and foundation tubes were part of anchor systems designed to replicate the capacity of a tangent guardrail terminal.

Post nos. 1 through 29 were spaced 1,905 mm (75 in.) on center. For posts nos. 3 through 8 and 21 through 27, the soil embedment depth was 1,099 mm (43¼ in.), as shown in Figure 16. For post nos. 9 through 20, the soil embedment depth was 2,013 mm (79¼ in.) at the center of the post, as shown in Figure 15. For post nos. 3 through 27, 152-mm wide x 305-mm deep x 362-mm long (6-in. x 12-in. x 14¼-in.) wood spacer blockouts were used to block the rail away from the front face of the steel posts.

Standard 2.66-mm thick (12-gauge) W-beam rails with additional post bolt slots at half-post spacing intervals were placed between post nos. 1 and 29, as shown in Figures 14 and 20. The W-beam's top rail height was 706 mm (27¾ in.) with a 550-mm (21⅝ in.) center mounting height. The

ail splices have been moved to the center of the span location, as shown in Figures 14 and 20. All lap-splice connections between the rail sections were configured to reduce vehicle snag at the splice during the crash test.

A 2:1 foreslope pit was excavated behind post nos. 9 through 20, as shown in Figures 13 and 21. The maximum pit dimensions were 3.0 m (10 ft) wide and 1.5 m (5 ft) deep. The length of the pit was 22.9 m (75 ft), spanning from the mid-span between post nos. 8 and 9 to the mid-span between post nos. 20 and 21.

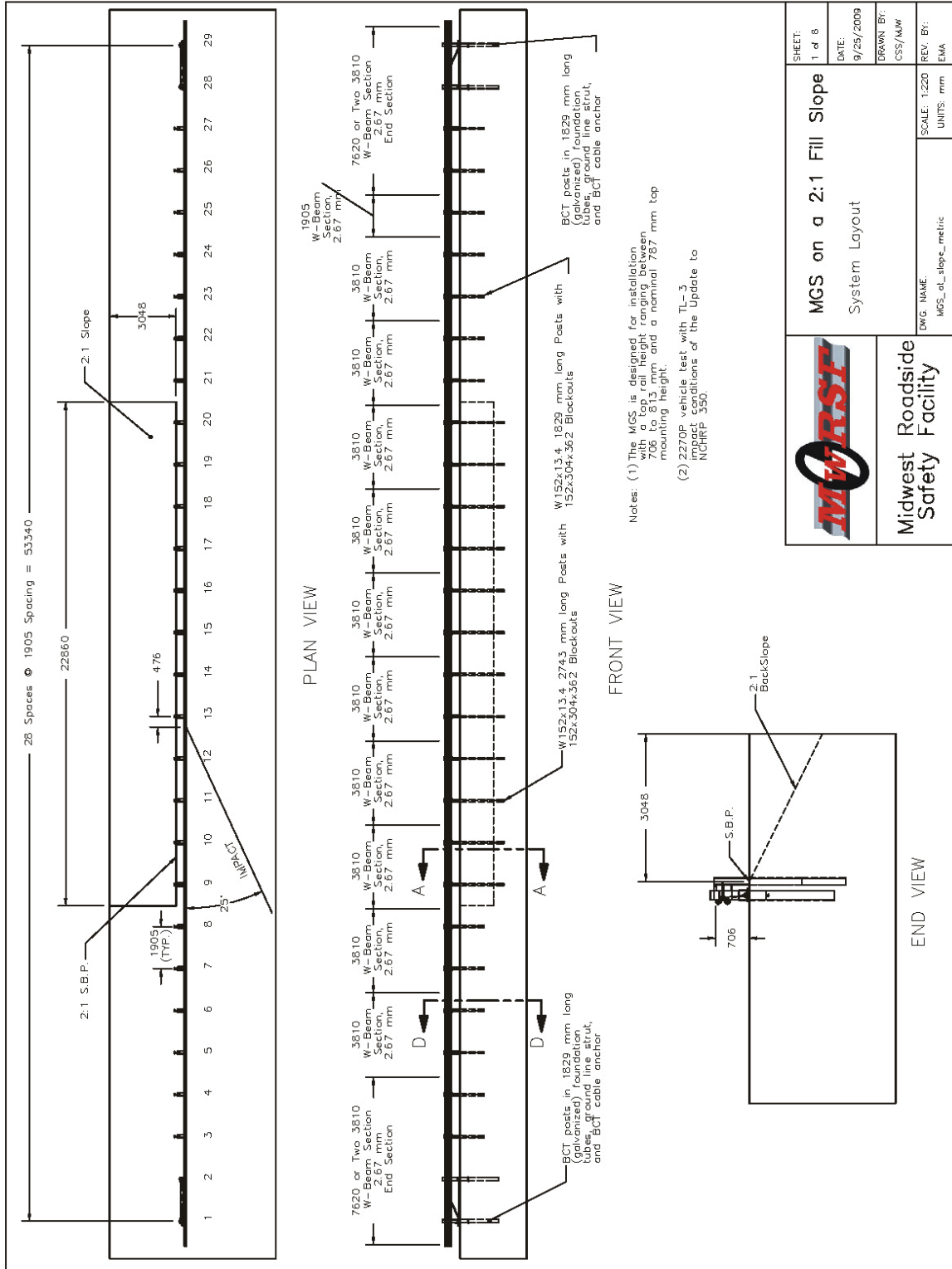


Figure 13. System Layout Details, Test No. MGS221-1

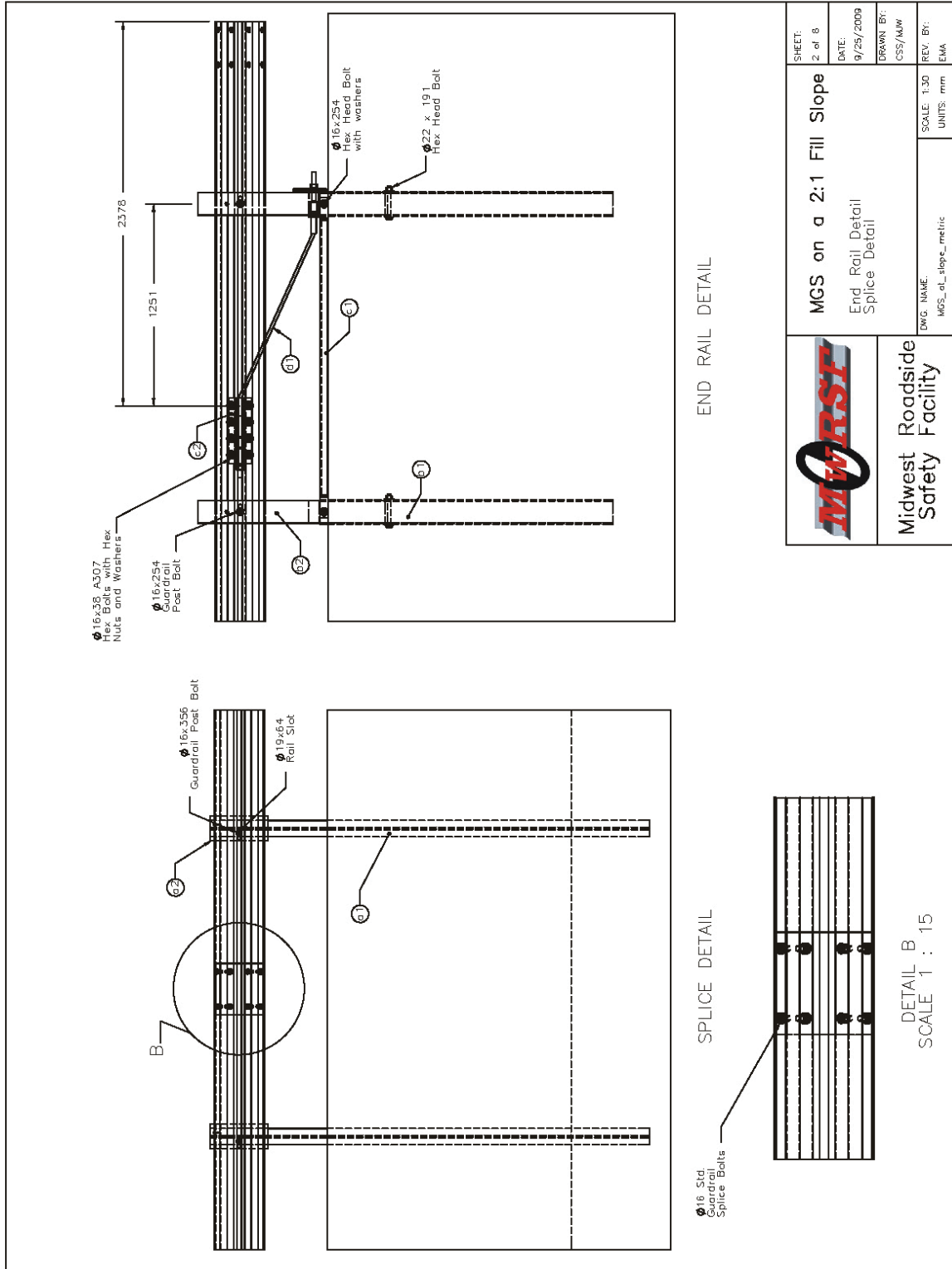


Figure 14. Anchorage Details, Test No. MGS221-1

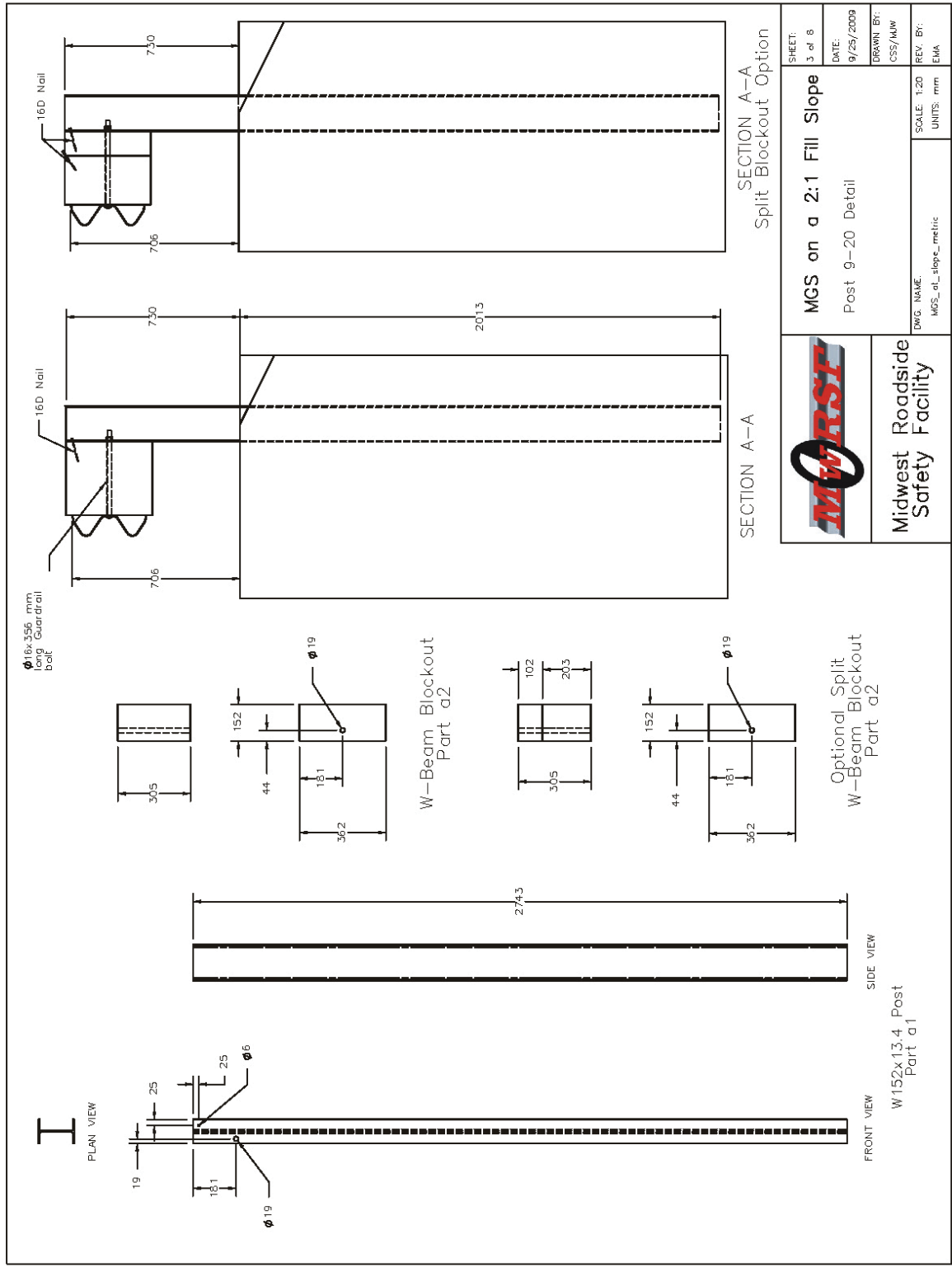
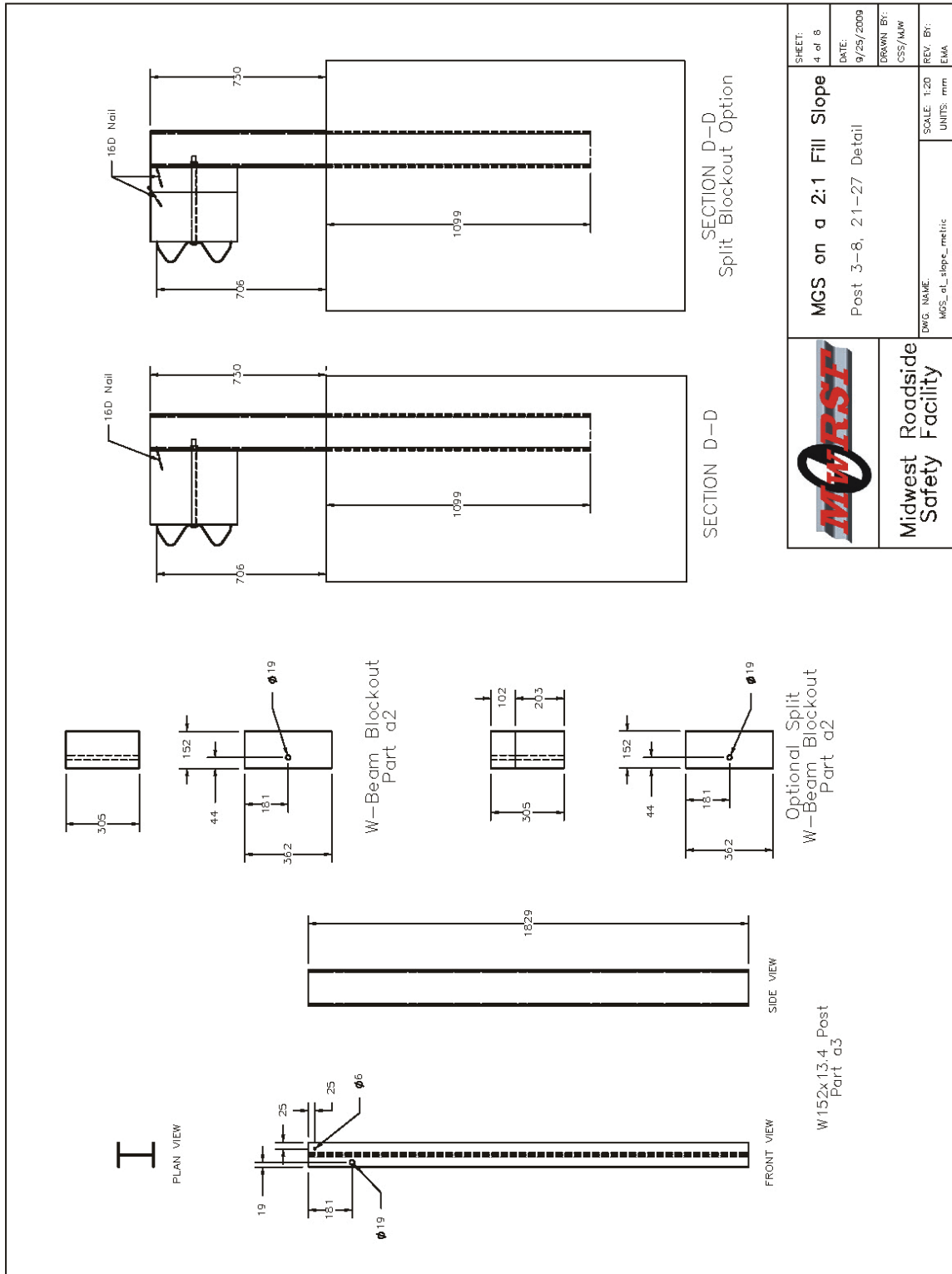


Figure 15. Post Details, Test No. MGS221-1




 Midwest Roadside Safety Facility	MGs on a 2:1 Fill Slope Post 3-8, 21-27 Detail	SHEET: 4 of 8 DATE: 9/25/2009 DRAWN BY: CSS/AMW REV. BY: EMA
	DWG. NAME: MG5_sl_slope_metric SCALE: 1:20 UNITS: mm	

Figure 16. Post Details, Test No. MGS221-1

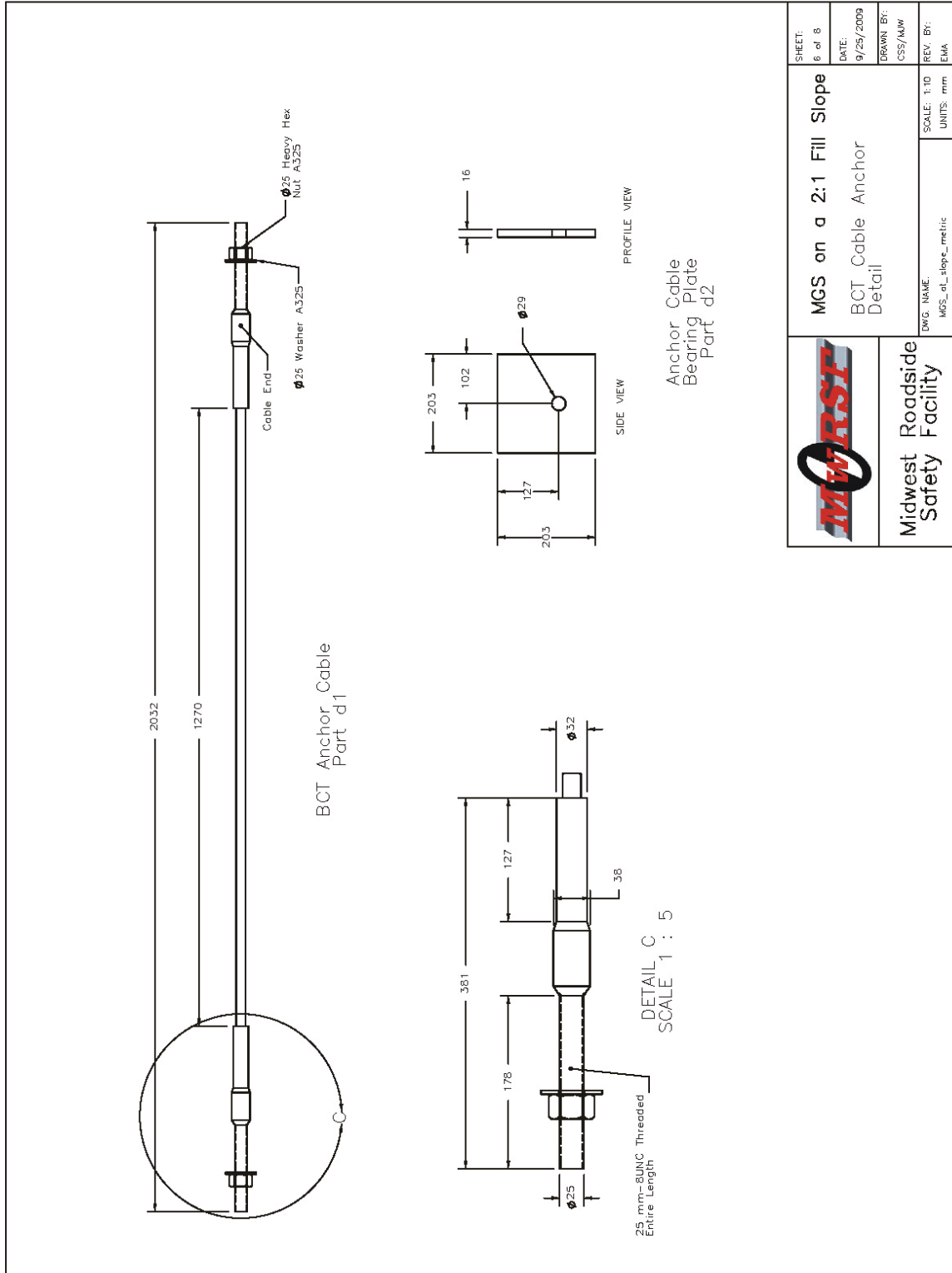
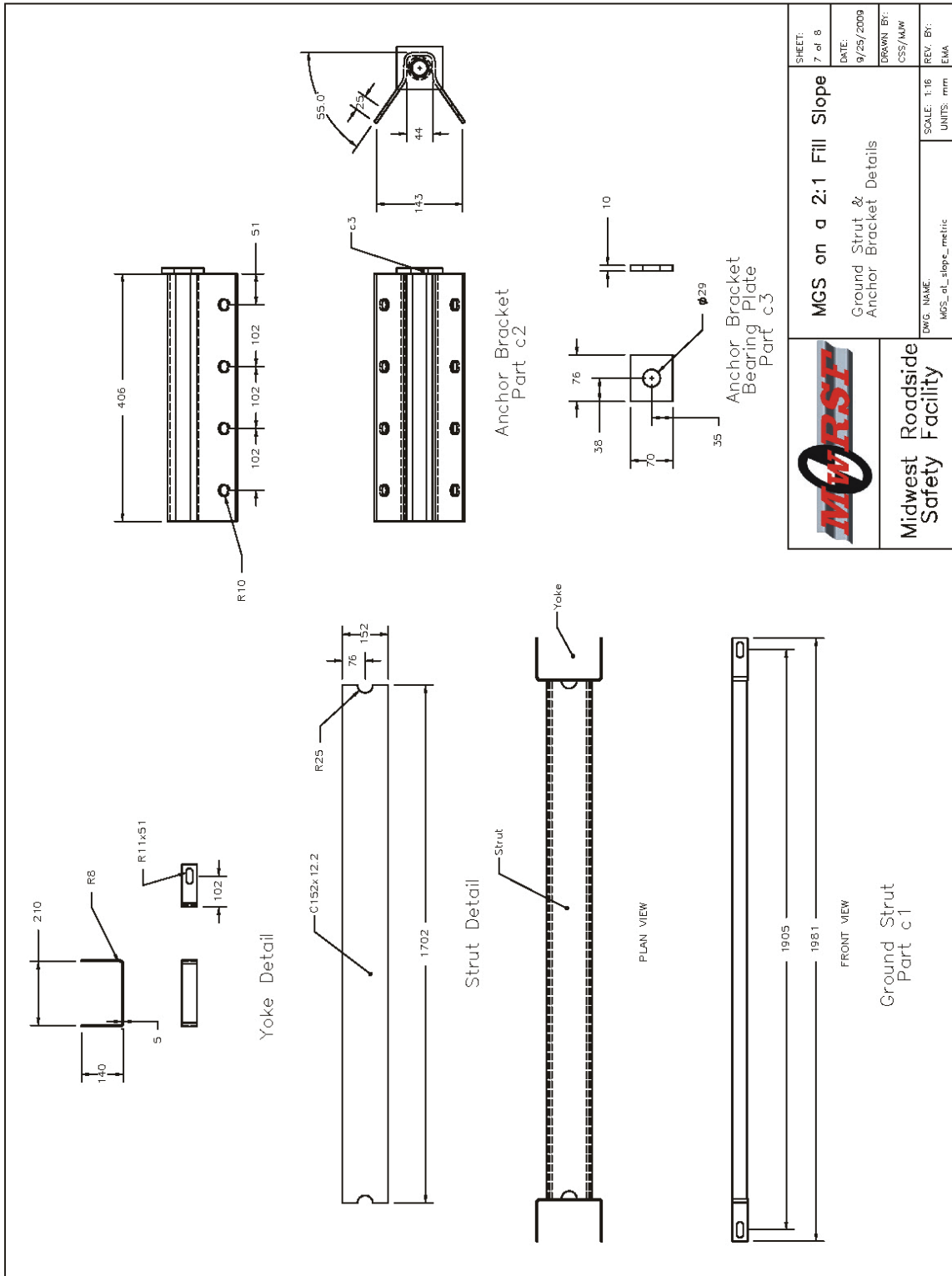


Figure 18. Anchor Cable Details, Test No. MGS221-1




 Midwest Roadside Safety Facility	MG5 on a 2:1 Fill Slope Ground Strut & Anchor Bracket Details	SHEET: 7 of 8 DATE: 9/25/2009 DRAWN BY: CSS/AMW
	DWG. NAME: MG5_sl_slope_metric SCALE: 1:16 UNITS: mm REV. BY: EMA	

Figure 19. Ground Strut and Anchor Bracket Details, Test No. MGS221-1

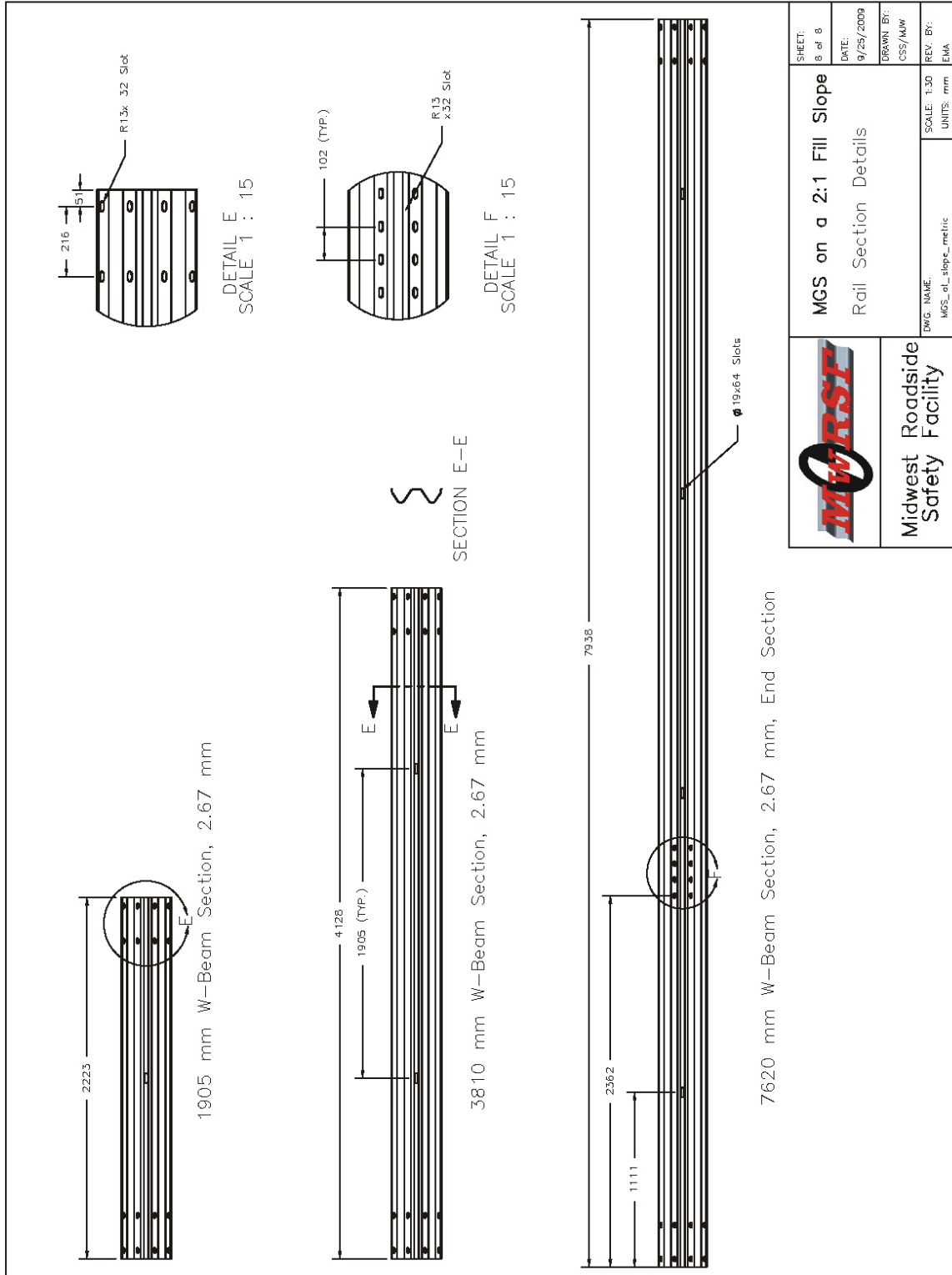


Figure 20. Rail Section Details, Test No. MGS221-1



Figure 21. MGS Installed Adjacent to a 2:1 Fill Slope, Test No. MGS221-1



Figure 22. MGS Installed Adjacent to a 2:1 Fill Slope, Test No. MGS221-1

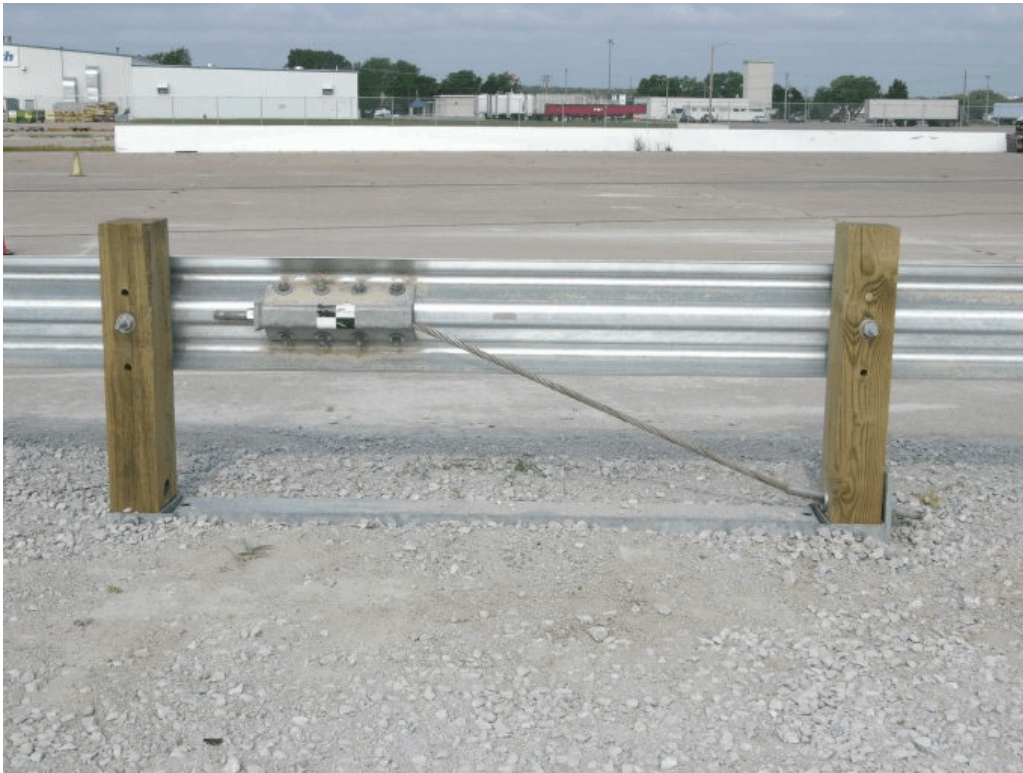


Figure 23. MGS Installed Adjacent to a 2:1 Fill Slope, Test No. MGS221-1

8 CRASH TEST NO. 1 (706-mm [27³/₄ in.] MGS)

8.1 Test MGS221-1

The 2,268-kg (5,000-lb) pickup truck impacted the MGS, with a 706-mm (27³/₄-in.) top mounting height, installed adjacent to a 2:1 fill slope system at a speed of 101.5 km/h (63.1 mph) and at an angle of 27.1 degrees. It should be noted that the actual rail top mounting height was measured to be 702 mm (27⁵/₈ in.) in the impact region prior to testing. A summary of the test results and sequential photographs are shown in Figure 24. A summary of the test results and sequential photographs in English units are shown in Appendix D. Additional sequential photographs are shown in Figures 25 through 28. Documentary photographs of the crash test are shown in Figure 29 and 30.

8.2 Weather Conditions

Test no. MGS221-1 was conducted on August 25, 2006 at approximately 12:45 pm. The weather conditions were reported as shown in Table 7.

Table 7. Weather Conditions, Test No. MGS221-1

Temperature	86° F
Humidity	55%
Wind Speed	8 mph
Wind Direction	South
Sky Conditions	Overcast
Visibility	10.0 Statute Miles
Pavement Surface	Dry
Previous 3-Day Precipitation	Trace
Previous 7-Day Precipitation	0.21 in.

8.3 Test Description

Initial vehicle impact was to occur 476 mm (18¾ in.) upstream from the centerline of post no. 13, as shown in Figure 31. Actual vehicle impact occurred 432 mm (17 in.) upstream from the centerline of post no. 13. At 0.010 sec after impact, the left corner of the bumper crushed inward, and post no. 13 deflected. At 0.018 sec, post no. 14 deflected, and the impacted rail flattened. At 0.024 sec, post no. 12 deflected. At 0.036 sec, the rail deformed around post no. 14. At 0.064 sec, post no. 15 deflected, and a buckle point formed at the midspan between post nos. 14 and 15. At 0.074 sec, the left corner of the front bumper was located at post no. 14 which was deflecting. At 0.096 sec, the guardrail released from post no. 14, and post no. 16 deflected. At 0.112 sec, the front of the vehicle was located at the midspan between post nos. 14 and 15. At 0.120 sec, the left-front tire disengaged from the vehicle. At 0.128 sec, buckling occurred at the midspan between post nos. 15 and 16. At this same time, the rail was located under the left corner of the front bumper. At 0.138 sec, the rail deformed around post no. 16, and post no. 17 deflected. At 0.146 sec, the guardrail released from post no. 15, and the right-front tire became airborne. At 0.154 sec, the left corner of the front bumper was located at post no. 15, which was deflecting. At 0.182 sec, the left corner of the bumper protruded over the top of the rail. At 0.206 sec, the front of the vehicle pitched upward. At 0.226 sec, the guardrail released from post no. 15. At this same time, the entire left side of the vehicle was in contact with the rail. At 0.250 sec, the front of the vehicle was located between post nos. 16 and 17. At 0.308 sec, the front of the vehicle was located on top of post no. 17. At 0.324 sec, the right-front tire overrode the rail, the truck stopped redirecting, and the right-rear tire became airborne. At 0.342 sec, the rail began to tear. At this same time, the left-rear tire contacted the rail. At 0.376 sec, the front of the vehicle overrode post no. 18, and the rail at post no. 15 tore. At 0.400

sec, the left-rear tire disengaged from the vehicle. At 0.412 sec, the front of the vehicle began to yaw away from the back of the system. At 0.450 sec, the vehicle was completely airborne. At 0.474 sec, the vehicle continued to yaw the same direction. At 0.592 sec, the vehicle began to descend toward the ground. At 0.790 sec, the front of the vehicle contacted the ground behind the system. At 0.838 sec, the vehicle continued to yaw the same direction. At 0.938 sec, the vehicle, positioned over the top of the barrier, appeared to be perpendicular to the system with the rear positioned toward the traffic side of the system. At 1.252 sec, the rear axle contacted the top of the system. At 1.462 sec, the vehicle continued to yaw and descended toward the ground. At 1.618 sec, the right-rear tire disengaged from the vehicle. At 1.856 sec, the front of the vehicle contacted the ground. The vehicle came to rest 26.3 m (86 ft - 4½ in.) downstream from impact and 2.0 m (6 ft - 7 in.) laterally away from the traffic-side face of the barrier. The trajectory and final position of the pickup truck are shown in Figures 24 and 32.

8.4 Barrier Damage

Damage to the barrier was moderate, as shown in Figures 33 through 41. Barrier damage consisted of deformed guardrail posts, disengaged wooden blockouts, contact marks on a guardrail section and posts, and deformed and fractured W-beam rail. The length of the vehicle contact along the MGS system was approximately 8.8 m (29 ft - 1½ in.), which spanned from 305 mm (12 in.) upstream from the centerline of post no. 13 through the midspan between post nos. 17 and 18.

Moderate deformation and flattening of the impacted section of W-beam rail occurred between post nos. 13 through 17. Contact marks were found on the guardrail between post nos. 12 and 18 and on the backside of the W-beam between post nos. 23 and 26. A 686-mm (27-in.) long diagonal tear in the rail occurred 127 mm (5 in.) downstream of post no. 5. A 25-mm (1-in.) long

tear in the rail occurred 229 mm (9 in.) upstream from the centerline of post no. 16. A buckle point in the guardrail occurred at post no. 17. The top corrugation of the W-beam was deformed downward between post nos. 25 and 26. The W-beam was pulled off post nos. 3 through 17, 20, and 23 through 26. Post bolts at post nos. 7 and 8 left minor tears in the rail. The rail between post nos. 18 through 23 remained undamaged.

Steel post nos. 3 through 12 encountered minor twisting. Steel post nos. 13 through 17 twisted and rotated backward with major soil failure visible at the ground level. Steel post nos. 18 through 20 were undamaged. Steel post nos. 21 and 22 bent slightly, while post no. 23 bent downstream and rotated clockwise. The rear flange of post no. 23 was bent toward the web due to vehicle contact. Steel post nos. 24 through 26 bent downstream and backward and twisted counter-clockwise. The front and back flanges were bent backward at the top of steel post nos. 24 and 25. The upstream and downstream anchorage systems moved longitudinally. For the upstream anchorage, soil gaps of 102 mm (4 in.) and 38 mm (1½ in.) were found on the upstream and downstream sides of post no. 1, respectively, and for post no. 2, soil gaps of 64 mm (2½ in.) and 51 mm (2 in.) were found on the upstream and downstream sides, respectively. For the downstream anchorage, soil gaps of 13 mm (½ in.) and 51 mm (2 in.) were found on the downstream side of post nos. 28 and 29, respectively, while no soil gaps were found on the upstream sides of these posts. In addition, post no. 28 and 29 were uplifted out of the ground 102 mm (4 in.) and 229 mm (9 in.), respectively. However, the wooden posts in both anchorage systems were not damaged.

The wooden blockout at post no. 14 encountered damage on the front face, but it remained attached. The wooden blockouts at post nos. 15 through 17 were fractured and mostly removed from the post. All other wooden blockouts remained undamaged.

The permanent set of the barrier system is shown in Figure 33. The maximum lateral permanent set rail and post deflections were 810 mm (31⁷/₈ in.) at the centerline of post no. 16 and 1,086 mm (42³/₄ in.) at post no. 15, respectively, as measured in the field. The maximum lateral dynamic rail and post deflections were 955 mm (37.6 in.) at the centerline of post no. 15 and 1,126 mm (44.3 in.) at post no. 15, respectively, as determined from high-speed digital video analysis.

8.5 Vehicle Damage

Exterior vehicle damage was moderate, as shown in Figures 42 through 44. Occupant compartment deformations to the left side and center of the floor pan were judged insufficient to cause serious injury to the vehicle occupants, as shown in Figure 45. Maximum longitudinal deflections of 6 mm (¹/₄ in.) were located throughout the left-side floor pan. Maximum lateral deflections of 13 mm (¹/₂ in.) were located at the rear-center of the left-side floor pan. Maximum vertical deflections of 13 mm (¹/₂ in.) were located on the floor pan near the left-side door. Complete occupant compartment deformations and the corresponding locations are provided in Appendix E.

Damage was concentrated on the left-front corner of the vehicle. The left-front corner was deformed inward toward the engine compartment. The left side of the grill was fractured and removed. The center of the front bumper buckled. The left-front, left-rear, and right-rear tires disengaged from the vehicle. Sheet metal tearing and major deformations were found along the lower portion of the left-side doors and the left-rear fender. The left side of the rear bumper was deformed upward. The left-side taillight was fractured, while the right-side taillight was slightly dislodged. The left-front, right-front, and right-rear brake lines were severed. The left-rear and right-rear shocks were fractured. The left-front upper control arm and left-front tie rod were fractured. The drive shaft was fractured and separated at the transmission yoke. The left-front sway bar linkage was

bent. Both ends of the rear axle fractured before the brake housing. The gas tank heat shield was deformed and bent. The roof, hood, and right side of the vehicle and all window glass remained undamaged.

8.6 Occupant Risk Values

The calculated occupant impact velocities (OIVs) and maximum 0.010-sec occupant ridedown accelerations (ORAs) in both the longitudinal and directions are shown in Table 8. It is noted that the OIVs and ORAs were within the suggested limits provided in MASH. The calculated THIV and PHD values are also shown in Table 8. The results of the occupant risk, as determined from the accelerometer data, are summarized in Figure 24. The recorded data from the accelerometers and the rate transducers are shown graphically in Appendix F.

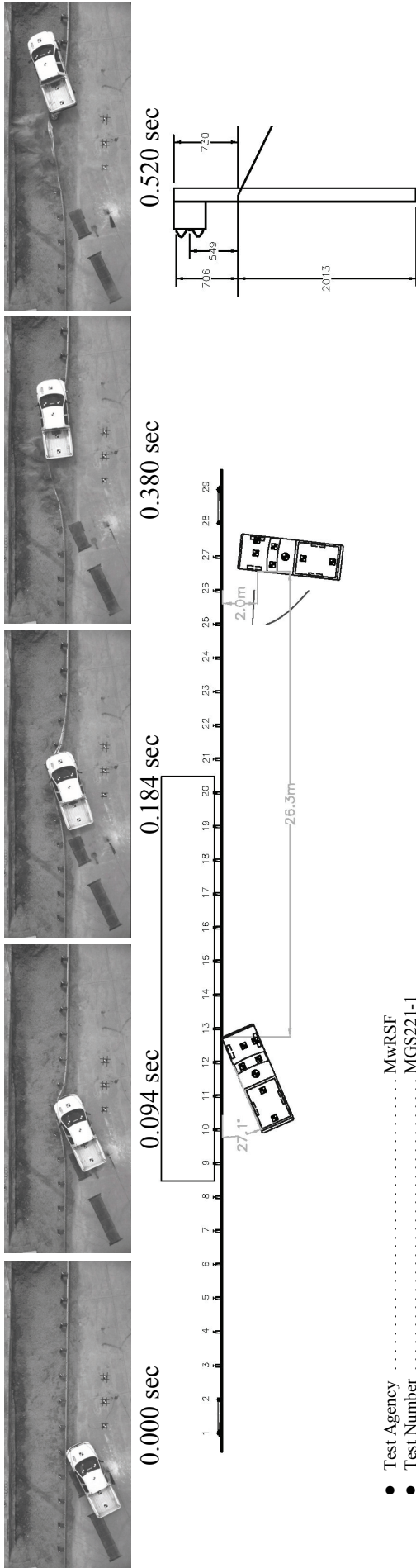
Table 8. Summary of OIV, ORA, THIV, and PHD Values, Test No. MGS221-1

Evaluation Criteria		Transducer	
		EDR-3	EDR-4
OIV ft/s (m/s)	Longitudinal	-4.93 (-16.18)	-4.32 (-14.18)
	Lateral	3.90 (12.80)	3.84 (-12.61)
ORA g's	Longitudinal	-11.66	-10.11
	Lateral	5.38	5.14
THIV		N/A	6.04 (19.83)
PHD		N/A	7.96

8.7 Discussion

The analysis of the test results for test no. MGS221-1 showed that the MGS, with a 706-mm (27³/₄-in.) top mounting height and installed adjacent to a 2:1 fill slope, did not adequately contain nor redirect the 2270P vehicle as the vehicle overrode the top of the system and subsequently landed behind the system. There were no detached elements nor fragments which showed potential for penetrating the occupant compartment nor presented undue hazard to other traffic. Deformations of, or intrusion into, the occupant compartment that could have caused serious injury did not occur. The test vehicle overrode and penetrated the guardrail system. It did remain upright during and after the collision. Vehicle roll, pitch, and yaw angular displacements were noted, but they were deemed acceptable because they did not adversely influence occupant risk safety criteria nor cause rollover. Therefore, test no. MGS221-1 conducted on the MGS installed adjacent to a 2:1 fill slope was determined to be unacceptable according to the TL-3 safety performance criteria found in MASH.

The vehicle override was attributed to the slow release of post no. 15 from the guardrail, thus causing the W-beam to be pulled downward. In addition, the vehicle override was also attributed to the failure of the vehicle's front suspension shortly after impact, thus preventing the guardrail from capturing the pickup truck's left-front tire.



- Test Agency MwRSF
- Test Number MGS221-1
- Date 8/25/2006
- MASH Test Designation 3-11
- Appearance MGS adjacent to a 2:1 Foreslope
- Total Length 53.34 m
- Key Elements - Steel W-beam
 - Thickness 2.66 mm
 - Top Mounting Height 706 mm
- Key Elements - Steel Posts
 - Post Nos. 3-8, 21-27 W152x13.4 by 1,829 mm long
 - Post Nos. 9-20 W152x13.4 by 2,743 mm long
 - Post Location Centerline of posts at slope break point
 - Spacing 1,905 mm
- Key Elements - Wood Posts
 - Post Nos. 1-2, 28-29 140 mm x 190 mm by 1,080 mm long
- Key Elements - Steel Foundation Tube
 - Post Nos. 3-27 152 mm x 305 mm x 362 mm long
- Key Elements - Wood Spacer Blocks
 - Post Nos. 3-27 Grading B-AASHTO M 147-65 (1990)
- Type of Soil 2270P
- Test Vehicle
 - Type/Designation 2003 Dodge Ram 1500 Quad Cab
 - Make and Model 2,316 kg
 - Curb 2,268 kg
 - Test Inertial 2,268 kg
 - Gross Static 101.5 km/h
- Impact Conditions
 - Speed 27.1 degrees
 - Angle 432 mm upstream of centerline of post no. 13
 - Impact Location 432 mm upstream of centerline of post no. 13
- Exit Conditions
 - Speed N/A
 - Angle N/A
 - Exit Box Criterion N/A
- Post-Impact Trajectory
 - Vehicle Stability Satisfactory
 - Stopping distance 26.3 m downstream
 - 2.0 m laterally in front
- Occupant Impact Velocity (EDR-3)
 - Longitudinal -4.93 m/s < 12.2 m/s
 - Lateral 3.90 m/s < 12.2 m/s
- Occupant Ride Down Deceleration (EDR-3)
 - Longitudinal -11.66 g's < 20.49 g's
 - Lateral 5.38 g's < 20.49 g's
- Occupant Impact Velocity (EDR-4)
 - Longitudinal -4.32 m/s < 12.2 m/s
 - Lateral 3.84 m/s < 12.2 m/s
- Occupant Ride Down Deceleration (EDR-4)
 - Longitudinal -10.11 g's < 20.49 g's
 - Lateral 5.14 g's < 20.49 g's
- THIV (EDR-4 - not required) 6.04 m/s
- PHD (EDR-4 - not required) 11.77 g's < 20 g's
- Test Article Damage Moderate
- Test Article Deflections
 - Permanent Set 1,086 mm
 - Dynamic 1,126 mm
 - Working Width N/A
- Vehicle Damage
 - VDS²⁶ Moderate
 - CDC²⁷ 11-LFQ-3
 - 11-LYENS
 - Maximum Deformation 13 mm left-side floor pan
 - Angular Displacement
 - Roll -32.2 degrees
 - Pitch -23.7 degrees
 - Yaw -34.3 degrees

Figure 24. Summary of Test Results and Sequential Photographs, Test No. MGS221-1



0.000 sec



0.790 sec



0.094 sec



1.252 sec



0.278 sec



1.462 sec



0.474 sec



1.856 sec

Figure 25. Additional Sequential Photographs, Test No. MGS221-1



0.000 sec



0.308 sec



0.096 sec



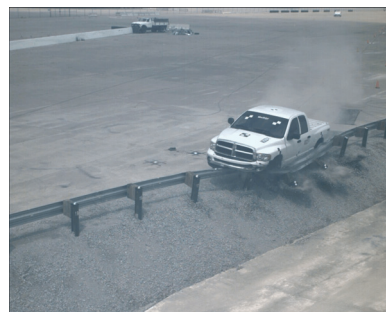
0.400 sec



0.182 sec



0.516 sec



0.246 sec



0.742 sec

Figure 26. Additional Sequential Photographs, Test No. MGS221-1



0.000 sec



0.226 sec



0.028 sec



0.300 sec



0.064 sec



0.376 sec



0.146 sec



0.450 sec

Figure 27. Additional Sequential Photographs, Test No. MGS221-1



0.000 sec



0.725 sec



0.104 sec



1.036 sec



0.380 sec



1.450 sec



0.518 sec



1.760 sec

Figure 28. Additional Sequential Photographs, Test No. MGS221-1



Figure 29. Documentary Photographs, Test No. MGS221-1



Figure 30. Documentary Photographs, Test No. MGS221-1



Figure 31. Impact Location, Test No. MGS221-1



Figure 32. Vehicle Final Position and Trajectory Marks, Test No. MGS221-1



Figure 33. System Damage, Test No. MGS221-1



Figure 34. Post Nos. 3 through 6 Damage, Test No. MGS221-1



Figure 35. Post Nos. 7 through 10 Damage, Test No. MGS221-1



Figure 36. Post Nos. 11 through 14 Damage, Test No. MGS221-1



Figure 37. Post Nos. 15 through 17 Damage, Test No. MGS221-1



Figure 38. Post Nos. 20, and 22 through 24 Damage, Test No. MGS221-1



Figure 39. Post Nos. 25 through 27 Damage, Test No. MGS221-1



Figure 40. Upstream Anchorage Damage, Test No. MGS221-1



Figure 41. Downstream Anchorage Damage, Test No. MGS221-1



Figure 42. Vehicle Damage, Test No. MGS221-1



Figure 43. Vehicle Damage, Test No. MGS221-1



Figure 44. Undercarriage Damage, Test No. MGS221-1



Figure 45. Occupant Compartment Damage, Test No. MGS221-1

9 MGS INSTALLED ADJACENT TO A 2:1 FILL SLOPE (DESIGN NO. 2) DETAILS

Following the unsuccessful performance of the 706-mm (27³/₄ in.) high, MGS installed adjacent to a steep slope, it was believed that raising the rail height to 787 mm (31 in.) would allow for improved engagement between the barrier system and the vehicle. Therefore, the second design of the MGS installed adjacent to a 2:1 fill slope system was identical to the system in test no. MGS221-1 except for the guardrail's top mounting height. The first installation's height was set at the design's anticipated minimum height tolerance of 706 mm (27³/₄ in.). For the second installation, the top W-beam guardrail height was raised to 787 mm (31 in.) with a 632-mm (24⁷/₈-in.) center mounting height. Additionally, post nos. 1 through 29 were still spaced 1,905 mm (75 in.) on center but were embedded to a depth of 1,930 mm (76 in.), as shown in Figures 46 and 47.

Once again, the posts installed adjacent to the 2:1 foreslope, post nos. 9 through 20, were still ASTM A36 steel W152x13.4 (W6x9) sections measuring 2,743 mm (9 ft) long. As used in the previous system, the rail splices were placed at the center span locations and were configured to reduce vehicle snag at the splice during the crash test. Photographs of the test installation are shown in Figures 48 and 49. The complete system drawings in metric and English units are shown in Appendix G.

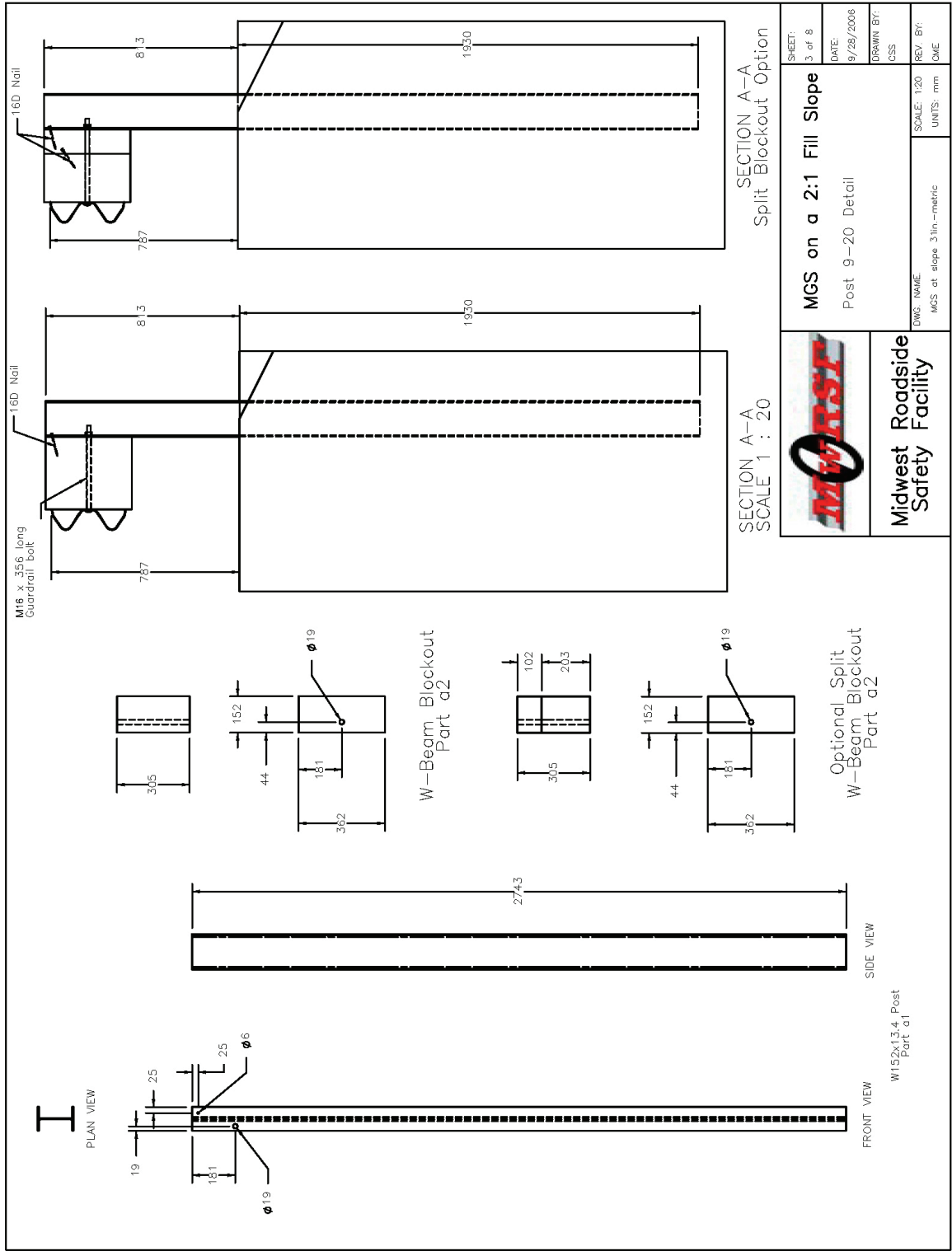


Figure 46. MGS Installed Adjacent to a 2:1 Fill Slope System Modifications, Test No. MGS221-2

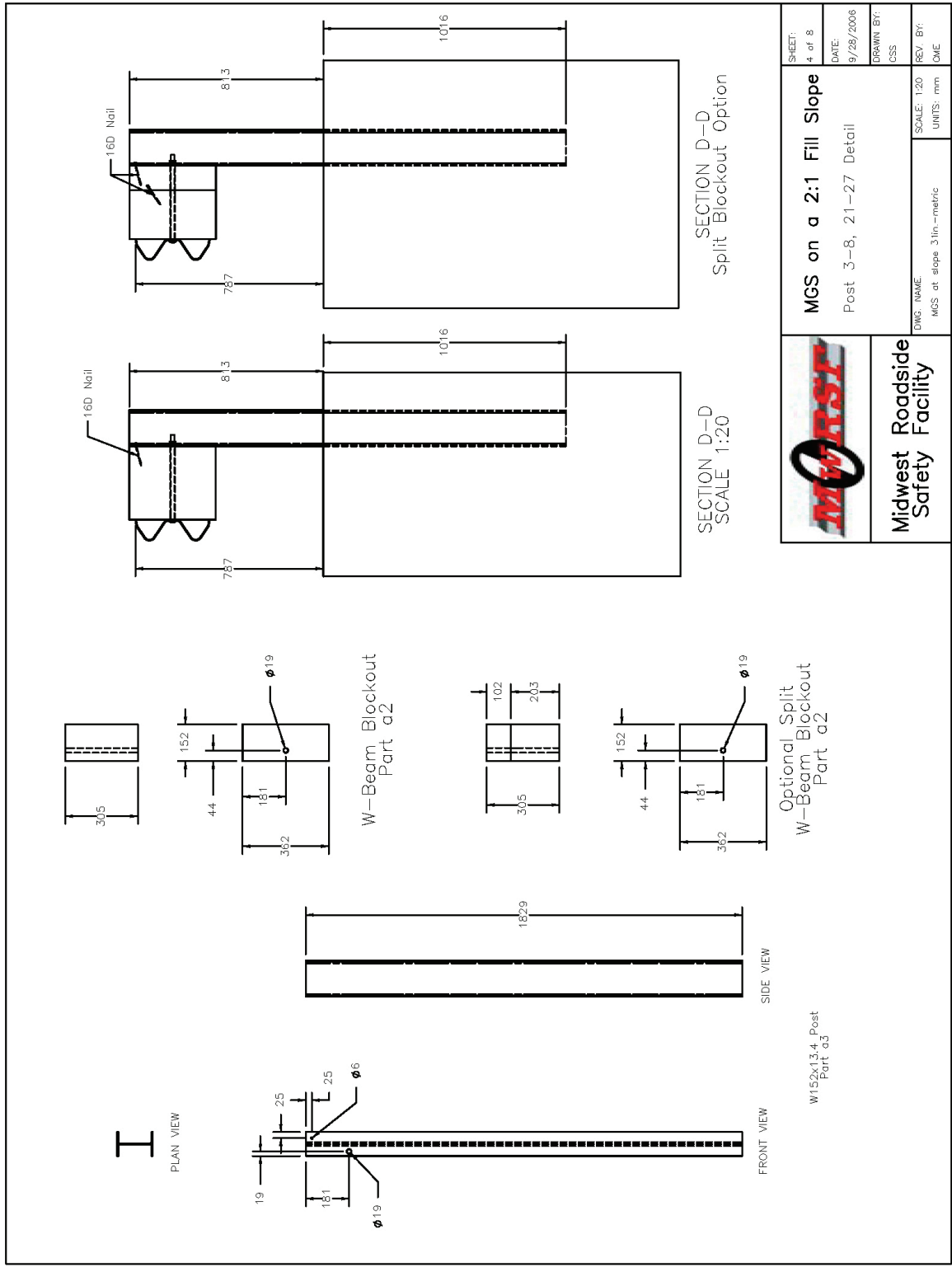


Figure 47. MGS Installed Adjacent to a 2:1 Fill Slope System Modifications, Test No. MGS221-2



Figure 48. MGS Installed Adjacent to a 2:1 Fill Slope, Test No. MGS221-2



Figure 49. MGS Installed Adjacent to a 2:1 Fill Slope, Test No. MGS221-2

10 CRASH TEST NO. 2 (787-mm [31-in.] MGS)

10.1 Test MGS221-2

The 2,274-kg (5,013-lb) pickup truck impacted the MGS, with a 787-mm (31-in.) top mounting height, installed adjacent to a 2:1 fill slope system at a speed of 101.5 km/h (63.1 mph) and at an angle of 25.5 degrees. A summary of the test results and sequential photographs are shown in Figure 50. A summary of the test results and sequential photographs in English units are shown in Appendix D. Additional sequential photographs are shown in Figures 51 through 54. Documentary photographs of the crash test are shown in Figure 55.

10.2 Weather Conditions

Test no. MGS221-2 was conducted on December 15, 2006 at approximately 2:00 pm. The weather conditions were reported as shown in Table 9.

Table 9. Weather Conditions, Test No. MGS221-2

Temperature	51° F
Humidity	35%
Wind Speed	10 mph
Wind Direction	Southeast
Sky Conditions	Clear
Visibility	10.0 Statute Miles
Pavement Surface	Dry
Previous 3-Day Precipitation	0.00 in.
Previous 7-Day Precipitation	0.03 in.

10.3 Test Description

Initial vehicle impact was to occur 476 mm (18¾ in.) upstream from the centerline of post no. 13, as shown in Figure 56. Actual vehicle impact occurred 394 mm (15½ in.) upstream from the centerline of post no. 13. At 0.014 sec after impact, post no. 13 deflected. At 0.022 sec, post no. 12 twisted downstream, and the left-front corner of the vehicle crushed inward toward the engine compartment. At this same time, post no. 14 deflected. At 0.030 sec, the soil heaved behind post no. 13. At 0.044 sec, post nos. 14 through 19 twisted downstream. At 0.050 sec, the rail buckled upstream of post no. 5, and the soil heaved behind post no. 14. At 0.076 sec, the left-front tire protruded past the slope break point, and post no. 15 deflected. At this same time, the rail buckled downstream of post no. 15. At 0.084 sec, the left corner of the front bumper was located at post no. 14. At this same time, the left-front corner of the vehicle crushed inward, and the left-side headlight fractured. At 0.090 sec, the rail released from post no. 14 as the post deflected. At this same time, the soil heaved behind post no. 15. At 0.112 sec, the rail buckled at post no. 16. At 0.126 sec, the vehicle began to redirect. At 0.150 sec, the rail released from post no. 15 as the vehicle traversed over it. At this same time, the left-front wheel deformed due to contact with post no. 14. At 0.166 sec, the rail released from post nos. 10 and 11. At 0.208 sec, the deformed left-front wheel contacted post no. 15. At 0.220 sec, the entire left side of the vehicle was in contact with the rail, and both left-side tires protruded past the slope break point. At 0.236 sec, the rail released from post no. 16. At 0.266 sec, post no. 17 deflected. At 0.298 sec, the left-front tire contacted post no. 16. At 0.306 sec, the vehicle became parallel to the system with a resultant velocity of 68.1 km/h (42.3 mph). At 0.322 sec, the left-front corner of the vehicle contacted post no. 17 as the vehicle redirected away from the system. At this same time, the left-rear tire was airborne above the slope. At 0.330 sec, the left-front

wheel disengaged from the vehicle. At 0.428 sec, the left-front corner of the vehicle was located at post no. 18 as the vehicle continued to redirect out of the system. At 0.552 sec, the left-front corner of the vehicle was no longer in contact with the rail. At 0.726 sec, the vehicle exited the guardrail at a trajectory angle of 17.4 degrees and a resultant velocity of 62.1 km/h (38.6 mph). The vehicle continued to travel downstream away from the system until it was redirected behind the end of the system. The vehicle came to rest 39.0 m (127 ft - 11½ in.) downstream from impact and 11.3 m (37 ft) laterally behind the traffic-side face of the rail. The trajectory and final position of the vehicle are shown in Figures 50 and 57.

10.4 Barrier Damage

Damage to the barrier was moderate, as shown in Figures 58 through 64. Barrier damage consisted of deformed W-beam and guardrail posts, disengaged wooden blockouts, and contact marks on a guardrail section and posts. The length of the vehicle contact along the MGS system was approximately 12.42 m (40 ft - 9 in.), which spanned from 394 mm (15½ in.) upstream of the centerline of post no. 13 through 597 mm (23½ in.) downstream from the centerline of post no. 19.

Moderate deformation and flattening of the impacted section of W-beam rail occurred between post nos. 14 through 17. Contact marks were found on the guardrail between post nos. 12 and 20. Buckling in the rail occurred around the upstream cable anchor bracket. The guardrail buckled at post nos. 12 through 18. Rail buckle points also occurred at the midspans between post nos. 13 and 14, 14 and 15, and 15 and 16, at 229 mm (9 in.) and 508 mm (20 in.) downstream from post no. 15, at 330 mm (13 in.) downstream from post no. 16, and at 508 mm (20 in.) upstream from post no. 19. The W-beam rail sustained yielding around the post bolt slots at post nos. 2 through 19. The W-beam was pulled off post nos. 2 through 18.

Steel post nos. 12 through 14 twisted and rotated backward. Post no. 14 also bent downstream to the ground. Post nos. 15 through 18 are bent and twisted downstream in the soil. Post no. 15 also encountered minor scraping and denting on the traffic face of the post. Post no. 16 encountered tearing in the flange at the bolt hole. The upstream and downstream anchorage systems moved slightly longitudinally. For the upstream anchorage, soil gaps of 121 mm (4¾ in.) and 89 mm (3½ in.) were found on the upstream sides of post nos. 1 and 2, respectively. For the downstream anchorage, a soil gap of 25 mm (1 in.) was found on the downstream side of post no. 29. However, the wooden posts in both anchorage systems were not damaged.

The wooden blockouts at post nos. 12, 13, and 18 encountered minor crush on the upstream traffic-side face. The wooden blockouts at post nos. 15 through 17 were fractured and removed from the posts. All other wooden blockouts remained undamaged.

The permanent set of the barrier system is shown in Figure 58. The maximum lateral permanent set rail and post deflections were 1,067 mm (42 in.) at the midspan between post nos. 15 and 16 and 864 mm (34 in.) at post no. 14, respectively, as measured in the field. The maximum lateral dynamic rail and post deflections were 1,463 mm (57.6 in.) at the centerline of post no. 15 and 805 mm (31.7 in.) at post no. 14, respectively, as determined from high-speed digital video analysis. The working width of the system was found to be 1,631 mm (64.2 in.).

10.5 Vehicle Damage

Exterior vehicle damage was moderate, as shown in Figures 65 and 66. Occupant compartment deformations to the left side and center of the floor pan were judged insufficient to cause serious injury to the vehicle occupants. Maximum longitudinal deflections of 6 mm (¼ in.) were located throughout the left-side floor pan. Maximum lateral deflections of 13 mm (½ in.) were

located at the front-center of the left-side floor pan. Maximum vertical deflections of 6 mm ($\frac{1}{4}$ in.) were located throughout the left-side floor pan. Complete occupant compartment deformations and the corresponding locations are provided in Appendix H.

Damage was concentrated on the left-front corner of the vehicle. The left-front corner was deformed inward toward the engine compartment. The left-front tire disengaged from the vehicle. The left-rear tire was deflated. Sheet metal tearing and major deformations were found along the lower portion of the left-side doors and the left-rear fender. The left-side taillight was fractured, while the right-side taillight was slightly dislodged. The roof, hood, and right side of the vehicle and all window glass remained undamaged.

10.6 Occupant Risk Values

The calculated occupant impact velocities (OIVs) and maximum 0.010-sec occupant ridedown accelerations (ORAs) in both the longitudinal and directions are shown in Table 10. It is noted that the OIVs and ORAs were within the suggested limits provided in MASH. The calculated THIV and PHD values are also shown in Table 10. The results of the occupant risk, as determined from the accelerometer data, are summarized in Figure 50. The recorded data from the accelerometers and the rate transducers are shown graphically in Appendix I. Due to technical difficulties, the EDR-4 unit did not collect angular data from the rate transducer, but did collect acceleration data.

10.7 Discussion

The analysis of the test results for test no. MGS221-2 showed that the MGS, with a 787-mm (31-in.) top mounting height and installed adjacent to a 2:1 fill slope, adequately contained and redirected the 2270P vehicle. There were no detached elements nor fragments which showed

potential for penetrating the occupant compartment nor presented undue hazard to other traffic. Deformations of, or intrusion into, the occupant compartment that could have caused serious injury did not occur. The test vehicle did not penetrate nor ride over the guardrail system and remained upright during and after the collision. Vehicle roll, pitch, and yaw angular displacements were noted, but they were deemed acceptable because they did not adversely influence occupant risk safety criteria nor cause rollover. After collision, the vehicle's trajectory revealed minimum intrusion into adjacent traffic lanes. In addition, the vehicle exited the barrier within the exit box. Therefore, test no. MGS221-2 was determined to be acceptable according to the TL-3 safety performance criteria of test designation no. 3-11 found in MASH.

Table 10. Summary of OIV, ORA, THIV, and PHD Values, Test No. MGS221-2

Evaluation Criteria		Transducer	
		EDR-3	EDR-4
OIV ft/s (m/s)	Longitudinal	-4.24 (-13.90)	-4.10 (-13.46)
	Lateral	4.15 (13.61)	4.06 (13.31)
ORA g's	Longitudinal	-5.36	-5.13
	Lateral	5.28	5.73
THIV		N/A	6.26 (20.54)
PHD		N/A	6.93

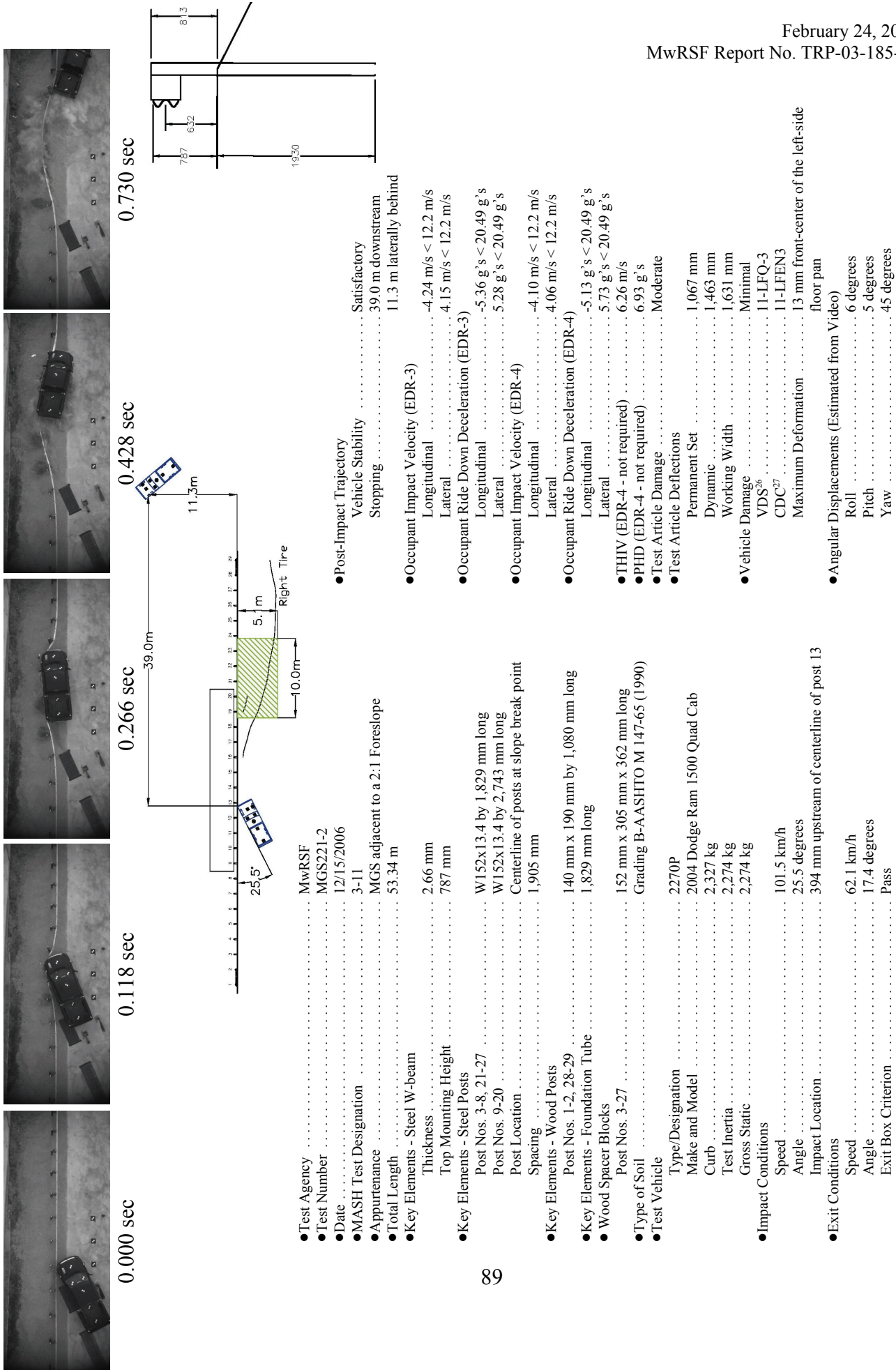


Figure 50. Summary of Test Results and Sequential Photographs, Test No. MGS221-2



0.000 sec



0.220 sec



0.034 sec



0.306 sec



0.084 sec



0.512 sec



0.110 sec



0.700 sec

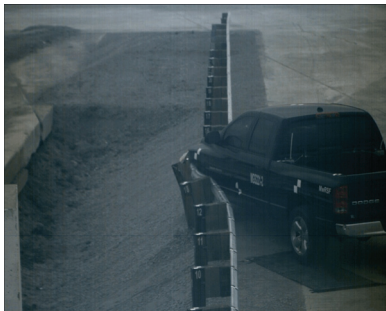
Figure 51. Additional Sequential Photographs, Test No. MGS221-2



0.000 sec



0.304 sec



0.076 sec



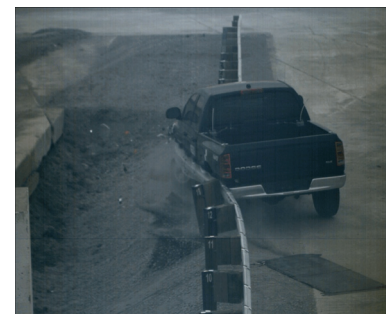
0.346 sec



0.142 sec



0.504 sec



0.220 sec



0.704 sec

Figure 52. Additional Sequential Photographs, Test No. MGS221-2



0.000 sec



0.208 sec



0.070 sec



0.298 sec



0.166 sec



0.330 sec



0.154 sec



0.478 sec

Figure 53. Additional Sequential Photographs, Test No. MGS221-2



0.000 sec



0.167 sec



0.033 sec



0.300 sec



0.067 sec



0.501 sec



0.100 sec



0.767 sec

Figure 54. Additional Sequential Photographs, Test No. MGS221-2

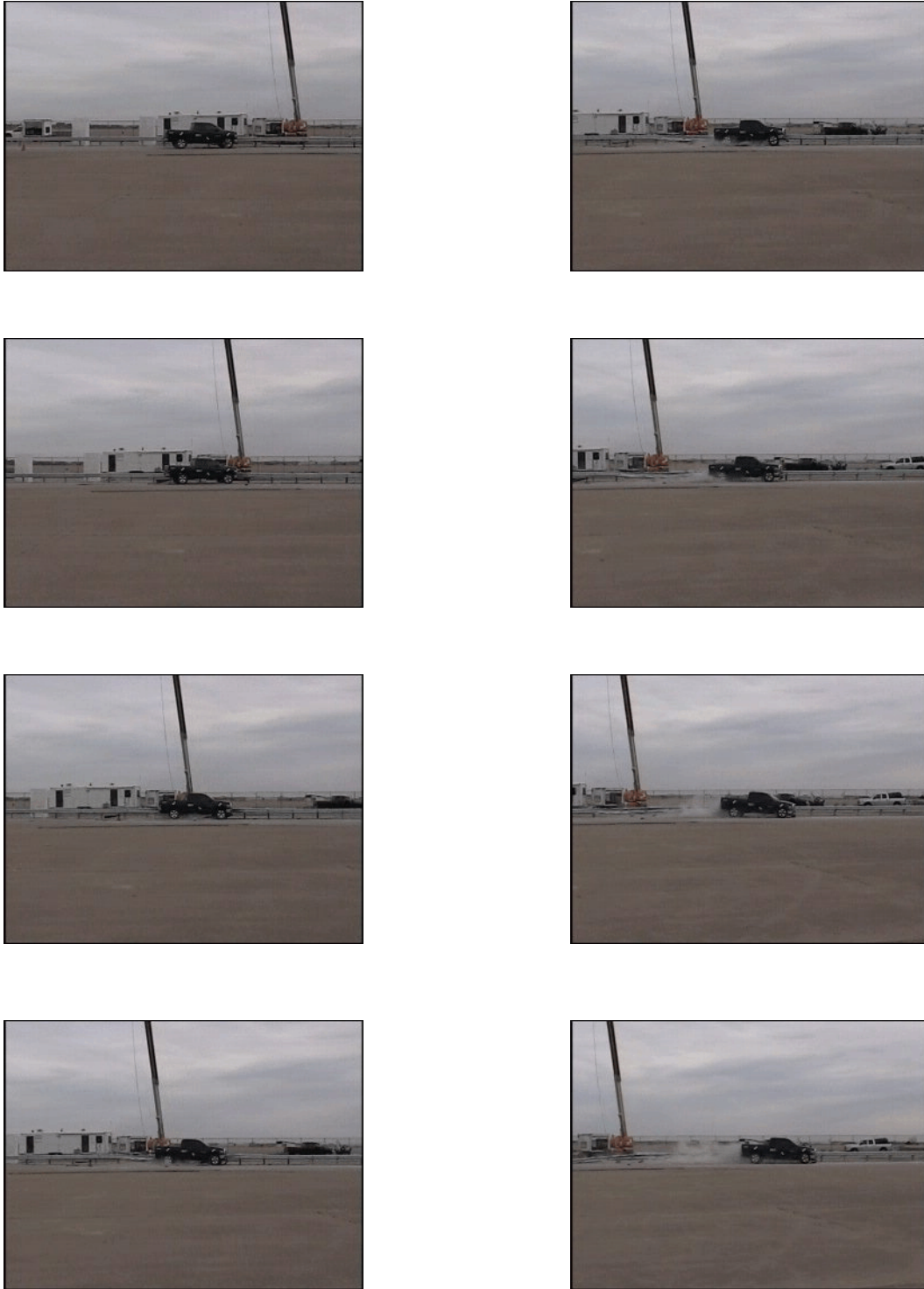


Figure 55. Documentary Photographs, Test No. MGS221-2



Figure 56. Impact Location, Test No. MGS221-2



Figure 57. Vehicle Final Position and Trajectory Marks, Test No. MGS221-2



Figure 58. System Damage, Test No. MGS221-2



Figure 59. System Damage, Test No. MGS221-2



Figure 60. Post Nos. 9 through 12 Damage, Test No. MGS221-2



Figure 61. Post Nos. 13 through 15 Damage, Test No. MGS221-2



Figure 62. Post Nos. 16 through 18 Damage, Test No. MGS221-2



Figure 63. Upstream Anchorage Damage, Test No. MGS221-2



Figure 64. Downstream Anchorage Damage, Test No. MGS221-2



Figure 65. Vehicle Damage, Test No. MGS221-2



Figure 66. Vehicle Damage, Test No. MGS221-2

11 SUMMARY AND CONCLUSIONS

This study set out to evaluate the performance of the MGS system installed adjacent to a 2:1 fill slope. The strong-post, W-beam system utilized W152x13.4 (W6x9) steel post measuring 2,743 mm (9 ft) in length. Two full-scale crash tests were performed on the MGS system placed adjacent to a 2:1 fill slope. A summary of the safety performance evaluation is provided in Table 11.

The first full-scale crash test, test no. MGS221-1, was performed on the MGS system adjacent to a 2:1 fill slope, with a 706-mm (27³/₄-in.) top mounting height, according to test designation 3-11 of MASH. The test consisted of a 2,268-kg (5,000-lb) pickup truck impacting the W-beam at a speed of 101.5 km/h (63.1 mph) and at an angle of 27.1 degrees. The impact point for this test was 432 mm (17 in.) upstream of the centerline of post no. 13. During the test the W-beam barrier did not adequately contain nor redirect the 2270P vehicle as the vehicle overrode the top of the system and subsequently landed behind the system. The test results were determined to be unacceptable according to MASH safety requirements.

The second full-scale crash test, test no. MGS221-2, was performed on the MGS system adjacent to a 2:1 fill slope, with a 787-mm (31-in.) top mounting height, according to test designation 3-11 of MASH. The test consisted of a 2,274-kg (5,013-lb) pickup truck impacting the W-beam at a speed of 101.5 km/h (63.1 mph) and at an angle of 25.5 degrees. The impact point for this test was 394 mm (15¹/₂ in.) upstream of the centerline of post no. 13. The test results were determined to be acceptable according to MASH safety requirements as the pickup truck was contained, redirected, and safely brought to a controlled stop.

Table 11. Summary of Safety Performance Evaluation Results

Evaluation Factors	Evaluation Criteria	Test No. MGS221-1	Test No. MGS221-2	
Structural Adequacy	A. Test article should contain and redirect the vehicle or bring the vehicle to a controlled stop; the vehicle should not penetrate, underide, or override the installation although controlled lateral deflection of the test article is acceptable.	U	S	
	D. Detached elements, fragments or other debris from the test article should not penetrate or show potential for penetrating the occupant compartment, or present an undue hazard to other traffic, pedestrians, or personnel in a work zone. Deformations of, or intrusions into, the occupant compartment should not exceed limits set forth in Section 5.3 and Appendix E of MASH.	S	S	
Occupant Risk	F. The vehicle should remain upright during and after collision. The maximum roll and pitch angles are not to exceed 75 degrees.	S	S	
	H. Occupant Impact Velocity (OIV) (see Appendix A, Section A5.3 of MASH for calculation procedure) should satisfy the following limits:	S	S	
	Occupant Impact Velocity Limits			
	Component			Preferred
	Lateral and Longitudinal	30 ft/s (9.1 m/s)	40 ft/s (12.2 m/s)	
I. The Occupant Ridedown Acceleration (ORA) (see Appendix A, Section A5.3 of MASH for calculation procedure) should satisfy the following limits:	S	S		
Occupant Ridedown Acceleration Limits				
Component			Preferred	Maximum
Longitudinal and Lateral	15.0 g's	20.49 g's		

S - Satisfactory
U - Unsatisfactory
NA - Not Applicable

12 RECOMMENDATIONS

A stiffened version of the MGS was developed for use adjacent to steep roadside slopes. The new design incorporates 2,743-mm (9-ft) long W152x13.4 (W6x9) steel posts spaced on 1,905 mm (75 in.) centers. With the top of the W-beam mounted at a height of 787 mm (31 in.), this guardrail system was successfully crash tested according to the safety performance evaluation criteria found in MASH. Hence, the stiffened MGS guardrail design with full post spacing is acceptable for use on the National Highway System. This new guardrail design will provide a safe and economical alternative for use along highways with steep slopes very close the travelway.

Full-scale crash testing of the MGS installed adjacent to a 2:1 fill slope has demonstrated a working width of 1,631 mm (64.2 in.). Therefore, it is recommended that a minimum lateral distance of 1.65 m (5 ft - 6 in.) be provided between the front face of any fixed object and the front face of the MGS adjacent to a 2:1 fill slope.

A follow-on research study has been funded to determine the appropriate size and length of a wood post to serve as a substitute for the 2,743-mm (9-ft) long W152x13.4 (W6x9) steel post used within the MGS near 2:1 fill slopes.

13 REFERENCES

1. Stout, D., Hinch, J., and Yang, T-L., *Force-Deflection Characteristics of Guardrail Posts*, Report No. FHWA-RD-88-195, Submitted to the Safety Design Division, Federal Highway Administration, Performed by ENSCO, Inc., August 31, 1988.
2. Polivka, K.A., Faller, R.K., Sicking, D.L., Rohde, J.R., Holloway, J.C., and Keller, E.A., *Development of a W-beam Guardrail System for Use on a 2:1 Slope*, Final Report to the Midwest States Regional Pooled Fund Program, Transportation Research Report No. TRP-03-99-00, Midwest Roadside Safety Facility, University of Nebraska-Lincoln, October 16, 2000.
3. Polivka, K.A., Sicking, D.L., Faller, R.K., and Rohde, J.R., *A W-beam Guardrail Adjacent to a Slope*, Paper No. 01-0343, Transportation Research Record No. 1743, Transportation Research Board, Washington, D.C., January 2001.
4. Stolle, C.S., Polivka, K.A., Reid, J.D., Faller, R.K., Sicking, D.L., Bielenberg, R.W., and Rohde, J.R., *Evaluation of Critical Flare Rates for The Midwest Guardrail System (MGS)*, Final Report in to the Midwest States Regional Pooled Fund Program, Transportation Report No. TRP-03-191-08, Project No.: SPR-3(017), Project Code: RPFPP-04-03 and RPFPR-05-05 - Years 14 and 15, Midwest Roadside Safety Facility, University of Nebraska-Lincoln, Lincoln, Nebraska, July 15, 2008.
5. Reid, J.D., Kuipers, B.D., Sicking, D.L., and Faller, R.K., *Impact Performance of W-Beam Guardrail Installed at various Flare Rates*, International Journal of Impact Engineering, Volume 36, Issue 3, March 2009, pages 476-485.
6. Sicking, D.L., Mak, K.K., Rohde, J.R., and Reid, J.D., *Manual for Assessing Safety Hardware - Draft Report*, National Cooperative Research Program (NCHRP), Project 22-14(2) Panel, 2008.
7. Michie, J.D., *Recommended Procedures for the Safety Performance Evaluation of Highway Appurtenances*, National Cooperative Highway Research Program (NCHRP) Report No. 230, Transportation Research Board, Washington, D.C., March 1981.
8. Ross, H.E., Sicking, D.L., Zimmer, R.A., and Michie, J.D., *Recommended Procedures for the Safety Performance Evaluation of Highway Features*, National Cooperative Research Program (NCHRP) Report 350, Transportation Research Board, Washington, D.C., 1993.
9. Powell, G.H., *BARRIER VII - A Computer Program for Evaluation of Automobile Barrier Systems*, Report No. FHWA-RD-73-51, University of California - Berkeley, Federal Highway Administration, Washington, D.C. April 1973.

10. Dey, G., Faller, R.K., Hascall, J.A., Bielenberg, R.W., Polivka, K.A., and Molacek, K., *Dynamic Impact Testing of W152x13.4 (W6x9) Steel Posts on a 2:1 Slope*, Final Report to the Midwest States Regional Pooled Fund Program, Transportation Research Report No. TRP-03-165-07, Project No. SPR-3(017)-Year 15, Project Code: RFPF-05-09, Midwest Roadside Safety Facility, University of Nebraska-Lincoln, Lincoln, Nebraska, March 23, 2007.
11. Kuipers, B.D., and Reid, J.D., *Testing of W152X23.8 (W6X16) Steel Posts-Soil Embedment Depth Study for the Midwest Guardrail System*, Final Report to the Midwest States Regional Pooled Fund Program, Transportation Research Report No. TRP-03-136-03, Midwest Roadside Safety Facility, The University of Nebraska-Lincoln, Lincoln, Nebraska, June 12, 2003.
12. Polivka, K.A., Faller, R.K., Sicking, D.L., Reid, J.D., Rohde, J.R., Holloway, J.C., Bielenberg, R.W., and Kuipers, B.D., *Development of the Midwest Guardrail System (MGS) for Standard and Reduced Post Spacing and in Combination with Curbs*, Final Report to the Midwest States Regional Pooled Fund Program, Transportation Research Report No. TRP-03-139-04, Project No. SPR-3(017)-Years 10, and 12-13, Project Code: RFPF-00-02, 02-01, and 03-05, Midwest Roadside Safety Facility, University of Nebraska-Lincoln, Lincoln, Nebraska, September 1, 2004.
13. Faller, R.K., Polivka, K.A., Kuipers, B.D., Bielenberg, B.W., Reid, J.D., Rohde, J.R., and Sicking, D.L., *Midwest Guardrail System for Standard and Special Applications*, Transportation Research Record No. 1890, Transportation Research Board, Washington, D.C., January 2004.
14. Sicking, D.L., Reid, J.D., and Rohde, J.R., *Development of the Midwest Guardrail System*, Paper No. 02-3157, Transportation Research Record No. 1797, Transportation Research Board, Washington D.C., 2002.
15. Faller, R.K., Sicking, D.L., Bielenberg, R.W., Rohde, J.R., Polivka, K.A., and Reid, J.D., *Performance of Steel-Post W-Beam Guardrail Systems*, Paper No. 07-2642, Transportation Research Record No. 2025, Transportation Research Board, Washington D.C., January 2007.
16. Polivka, K.A., Faller, R.K., Sicking, D.L., Rohde, J.R., Bielenberg, B.W., and Reid, J.D., *Performance Evaluation of the Midwest Guardrail System - Update to NCHRP 350 Test No. 3-11 with 28" C.G. Height (2214MG-2)*, Final Report to the National Cooperative Highway Research Program (NCHRP), Transportation Research Board, Transportation Research Report No. TRP-03-171-06, Midwest Roadside Safety Facility, University of Nebraska-Lincoln, October 11, 2006.
17. Reid, J.D., Sicking, D.L., and Bligh R., *Critical Impact Point for Longitudinal Barriers*, American Society of Civil Engineering (ASCE) Journal of Transportation Engineering, Vol 124, No. 1, January/February 1998.

18. Eller, C.M., Polivka, K.A., Faller, R.K., Sicking, D.L., Rohde, J.R., Reid, J.D., Bielenberg, R.W., and Allison, E.M., *Development of the Midwest Guardrail System (MGS) W-Beam to Thrie Beam Transition Element*, Final Report to the Midwest States Regional Pooled Fund Program, Transportation Research Report No. TRP-03-167-07, Project No. SPR-3(017)-Years 11-12, 16, Project Code: RFPF-01-04, 02-05, and 06-04, Midwest Roadside Safety Facility, University of Nebraska-Lincoln, Lincoln, Nebraska, November 26, 2007.
19. Polivka, K.A., Coon, B.A., Sicking, D.L., Faller, R.K., Bielenberg, R.W., Rohde, J.R. and Reid, J.D., *Development of the Midwest Guardrail System (MGS) W-Beam to Thrie-Beam Transition*, Paper No. 07-2628, Transportation Research Record No. 2025, Transportation Research Board, Washington, D.C., January 2007.
20. Buth, C.E., Campise, W.L., Griffin, III, L.I., Love, M.L., and Sicking, D.L., *Performance Limits of Longitudinal Barrier Systems - Volume I - Summary Report*, Report No. FHWA/RD-86/153, Submitted to the Office of Safety and Traffic Operations, Federal Highway Administration, Performed by Texas Transportation Institute, May 1986.
21. Ivey, D.L., Robertson, R., and Buth, C.E., *Test and Evaluation of W-Beam and Thrie-Beam Guardrails*, Report No. FHWA/RD-82/071, Submitted to the Office of Research, Federal Highway Administration, Performed by Texas Transportation Institute, March 1986.
22. Ross, H.E., Jr., Perera, H.S., Sicking, D.L., and Bligh, R.P., *Roadside Safety Design for Small Vehicles*, National Cooperative Highway Research Program (NCHRP) Report No. 318, Transportation Research Board, Washington, D.C., May 1989.
23. Polivka, K.A., Faller, R.K., Sicking, D.L., Rohde, J.R., Bielenberg, B.W., and Reid, J.D., *Performance Evaluation of the Midwest Guardrail System—Update to NCHRP 350 Test No. 3-10 (2214MG-3)*. Final Report to the National Cooperative Highway Research Program, MwRSF Research Report No. TRP-03-172-06, Midwest Roadside Safety Facility, University of Nebraska-Lincoln, October 11, 2006.
24. Hinch, J., Yang, T.L., and Owings, R., *Guidance Systems for Vehicle Testing*, ENSCO, Inc., Springfield, VA, 1986.
25. *Center of Gravity Test Code* - SAE J874 March 1981, SAE Handbook Vol. 4, Society of Automotive Engineers, Inc., Warrendale, Pennsylvania, 1986.
26. *Vehicle Damage Scale for Traffic Investigators*, Second Edition, Technical Bulletin No. 1, Traffic Accident Data (TAD) Project, National Safety Council, Chicago, Illinois, 1971.
27. *Collision Deformation Classification - Recommended Practice J224 March 1980*, Handbook Volume 4, Society of Automotive Engineers (SAE), Warrendale, Pennsylvania, 1985.

14 APPENDICES

APPENDIX A
Barrier VII Finite Element Model CAD Drawing

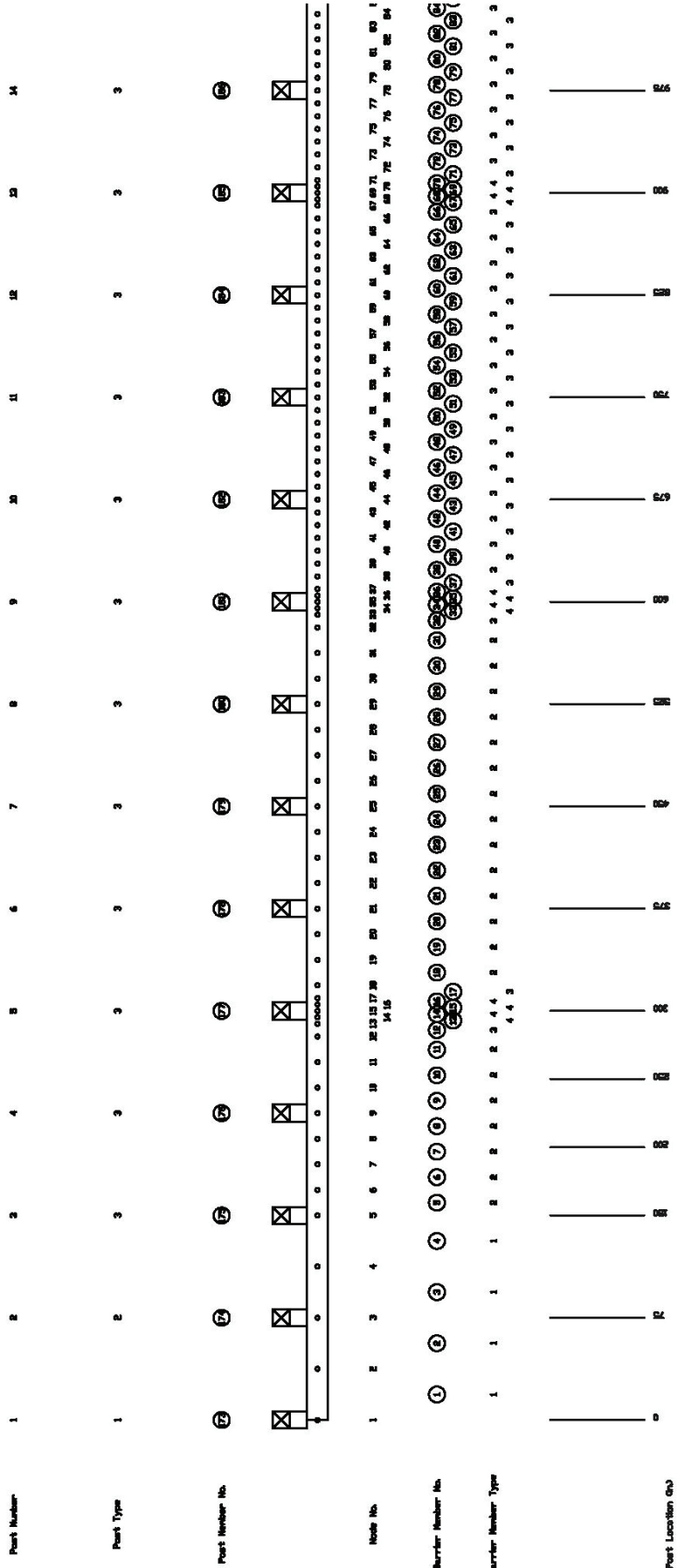


Figure A-1. Barrier VII Finite Element Model CAD Drawing

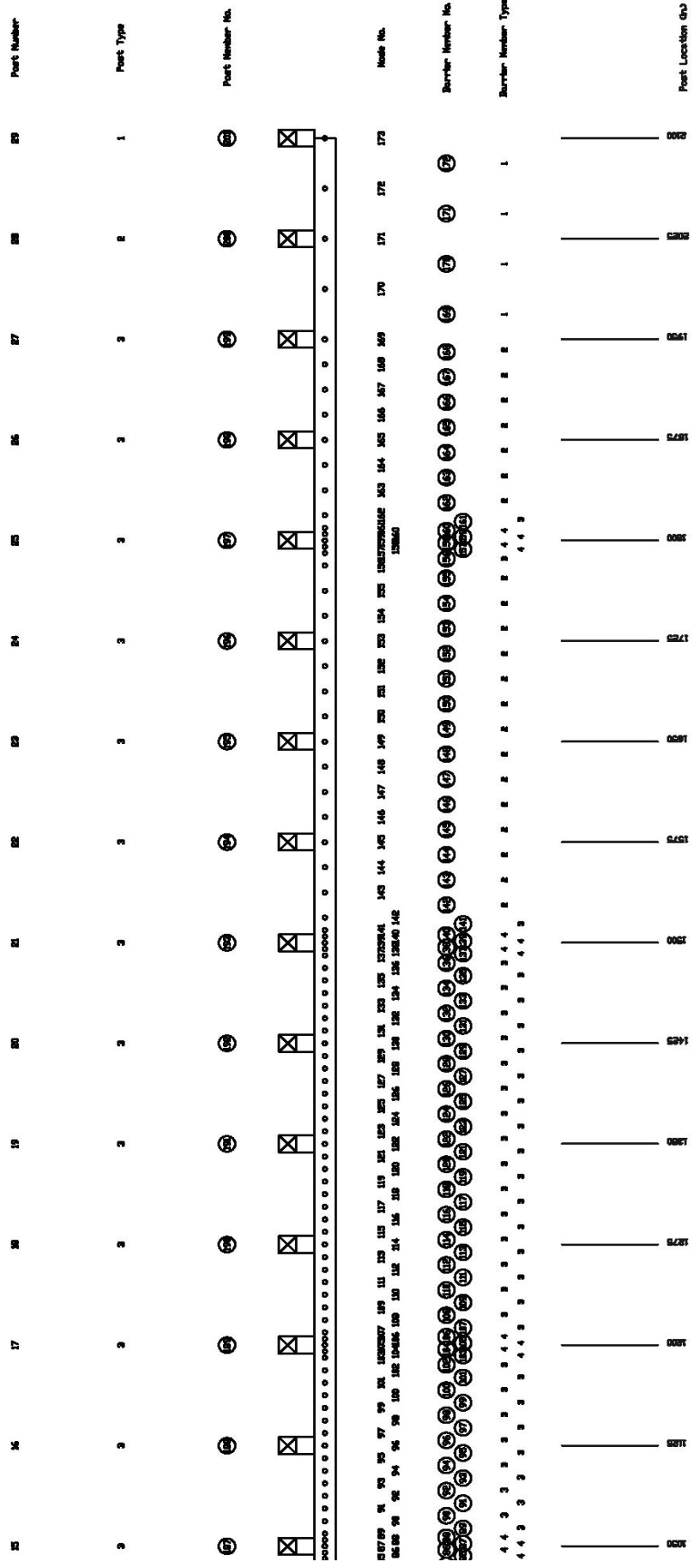


Figure A-2. Barrier VII Finite Element Model CAD Drawing

APPENDIX B
Barrier VII Input Deck

```

MGS21 W152x13.5 (6x9) mgs2-1_run3.b7
173 71 28 1 201 73 2 0
0.0001 0.0001 2.000 2000 0 1.0 1
2 10 10 10 10 500 1
1 0.0 0.0
3 75.00 0.0
5 150.00 0.0
9 225.00 0.0
12 281.25 0.0
13 290.625 0.0
14 295.3125 0.0
15 300.00 0.0
16 304.6875 0.0
17 309.375 0.0
18 318.75 0.0
21 375.00 0.0
25 450.00 0.0
29 525.00 0.0
32 581.25 0.0
33 590.625 0.0
34 595.3125 0.0
35 600.00 0.0
36 604.6875 0.0
37 609.375 0.0
38 618.75 0.0
44 675.00 0.0
52 750.00 0.0
60 825.00 0.0
66 881.25 0.0
67 890.625 0.0
68 895.3125 0.0
69 900.00 0.0
70 904.6875 0.0
71 909.375 0.0
72 918.75 0.0
78 975.00 0.0
84 1031.25 0.0
85 1040.625 0.0
86 1045.3125 0.0
87 1050.00 0.0
88 1054.6875 0.0
89 1059.375 0.0
90 1068.75 0.0
96 1125.00 0.0
102 1181.25 0.0
103 1190.625 0.0
104 1195.3125 0.0
105 1200.00 0.0
106 1204.6875 0.0
107 1209.375 0.0
108 1218.75 0.0
114 1275.00 0.0
122 1350.00 0.0
130 1425.00 0.0
136 1481.25 0.0

```


137	1490.625			0.0					
138	1495.3125			0.0					
139	1500.00			0.0					
140	1504.6875			0.0					
141	1509.375			0.0					
142	1518.75			0.0					
145	1575.00			0.0					
149	1650.00			0.0					
153	1725.00			0.0					
156	1781.25			0.0					
157	1790.625			0.0					
158	1795.3125			0.0					
159	1800.00			0.0					
160	1804.6875			0.0					
161	1809.375			0.0					
162	1818.75			0.0					
165	1875.00			0.0					
169	1950.00			0.0					
171	2025.00			0.0					
173	2100.00			0.0					
1	3	1	1	0.0					
3	5	1	1	0.0					
5	9	3	1	0.0					
9	12	2	1	0.0					
18	21	2	1	0.0					
21	25	3	1	0.0					
25	29	3	1	0.0					
29	32	2	1	0.0					
38	44	5	1	0.0					
44	52	7	1	0.0					
52	60	7	1	0.0					
60	66	5	1	0.0					
72	78	5	1	0.0					
78	84	5	1	0.0					
90	96	5	1	0.0					
96	102	5	1	0.0					
108	114	5	1	0.0					
114	122	7	1	0.0					
122	130	7	1	0.0					
130	136	5	1	0.0					
142	145	2	1	0.0					
145	149	3	1	0.0					
149	153	3	1	0.0					
153	156	2	1	0.0					
162	165	2	1	0.0					
165	169	3	1	0.0					
169	171	1	1	0.0					
171	173	1	1	0.0					
1	173								
		0.35							
173	172	171	170	169	168	167	166	165	164
163	162	161	160	159	158	157	156	155	154
153	152	151	150	149	148	147	146	145	144
143	142	141	140	139	138	137	136	135	134
133	132	131	130	129	128	127	126	125	124
123	122	121	120	119	118	117	116	115	114
113	112	111	110	109	108	107	106	105	104
103	102	101	100	99	98	97	96	95	94
93	92	91	90	89	88	87	86	85	84

83	82	81	80	79	78	77	76	75	74
73	72	71	70	69	68	67	66	65	64
63	62	61	60	59	58	57	56	55	54
53	52	51	50	49	48	47	46	45	44
43	42	41	40	39	38	37	36	35	34
33	32	31	30	29	28	27	26	25	24
23	22	21	20	19	18	17	16	15	14
13	12	11	10	9	8	7	6	5	4
3	2	1							
100	4								
1	2.29	1.99	37.50		30000.0	6.92	99.5	68.5	0.05 12-Gauge W-Beam
2	2.29	1.99	18.75		30000.0	6.92	99.5	68.5	0.05 12-Gauge W-Beam
3	2.29	1.99	9.375		30000.0	6.92	99.5	68.5	0.05 12-Gauge W-Beam
4	2.29	1.99	4.6875		30000.0	6.92	99.5	68.5	0.05 12-Gauge W-Beam
300	3								
1	24.875	0.00	6.0	6.0	100.0	675.0	675.0	0.05	Simulated Strong Anchor Post
	100.0		100.0		15.0		15.0		
2	24.875	0.00	3.0	3.0	100.0	150.0	225.00	0.05	Second BCT Post
	50.0		50.0		15.0		15.0		
3	24.875	0.0	4.00	5.21	81.0	92.88	126.86	0.05	W6x9 by 6' Long
	6.0		15.0		15.0		15.0		
1	1	2	4	1	101	0.0	0.0	0.0	0.0
5	5	6	11	1	102	0.0	0.0	0.0	0.0
12	12	13			103	0.0	0.0	0.0	0.0
13	13	14			104	0.0	0.0	0.0	0.0
14	14	15			104	0.0	0.0	0.0	0.0
15	15	16			104	0.0	0.0	0.0	0.0
16	16	17			104	0.0	0.0	0.0	0.0
17	17	18			103	0.0	0.0	0.0	0.0
18	18	19	31	1	102	0.0	0.0	0.0	0.0
32	32	33			103	0.0	0.0	0.0	0.0
33	33	34			104	0.0	0.0	0.0	0.0
34	34	35			104	0.0	0.0	0.0	0.0
35	35	36			104	0.0	0.0	0.0	0.0
36	36	37			104	0.0	0.0	0.0	0.0
37	37	38	66	1	103	0.0	0.0	0.0	0.0
67	67	68			104	0.0	0.0	0.0	0.0
68	68	69			104	0.0	0.0	0.0	0.0
69	69	70			104	0.0	0.0	0.0	0.0
70	70	71			104	0.0	0.0	0.0	0.0
71	71	72	84	1	103	0.0	0.0	0.0	0.0
85	85	86			104	0.0	0.0	0.0	0.0
86	86	87			104	0.0	0.0	0.0	0.0
87	87	88			104	0.0	0.0	0.0	0.0
88	88	89			104	0.0	0.0	0.0	0.0
89	89	90	102	1	103	0.0	0.0	0.0	0.0
103	103	104			104	0.0	0.0	0.0	0.0
104	104	105			104	0.0	0.0	0.0	0.0
105	105	106			104	0.0	0.0	0.0	0.0
106	106	107			104	0.0	0.0	0.0	0.0
107	107	108	136	1	103	0.0	0.0	0.0	0.0
137	137	138			104	0.0	0.0	0.0	0.0
138	138	139			104	0.0	0.0	0.0	0.0
139	139	140			104	0.0	0.0	0.0	0.0
140	140	141			104	0.0	0.0	0.0	0.0
141	141	142			103	0.0	0.0	0.0	0.0
142	142	143	155	1	102	0.0	0.0	0.0	0.0
156	156	157			103	0.0	0.0	0.0	0.0

157	157	158			104	0.0	0.0	0.0		
158	158	159			104	0.0	0.0	0.0		
159	159	160			104	0.0	0.0	0.0		
160	160	161			104	0.0	0.0	0.0		
161	161	162			103	0.0	0.0	0.0		
162	162	163	168	1	102	0.0	0.0	0.0		
169	169	170	172	1	101	0.0	0.0	0.0		
173	1				301	0.0	0.0	0.0	0.0	0.0
174	3				302	0.0	0.0	0.0	0.0	0.0
175	5				303	0.0	0.0	0.0	0.0	0.0
176	9				303	0.0	0.0	0.0	0.0	0.0
177	15				303	0.0	0.0	0.0	0.0	0.0
178	21				303	0.0	0.0	0.0	0.0	0.0
179	25				303	0.0	0.0	0.0	0.0	0.0
180	29				303	0.0	0.0	0.0	0.0	0.0
181	35				303	0.0	0.0	0.0	0.0	0.0
182	44				303	0.0	0.0	0.0	0.0	0.0
183	52				303	0.0	0.0	0.0	0.0	0.0
184	60				303	0.0	0.0	0.0	0.0	0.0
185	69				303	0.0	0.0	0.0	0.0	0.0
186	78				303	0.0	0.0	0.0	0.0	0.0
187	87				303	0.0	0.0	0.0	0.0	0.0
188	96				303	0.0	0.0	0.0	0.0	0.0
189	105				303	0.0	0.0	0.0	0.0	0.0
190	114				303	0.0	0.0	0.0	0.0	0.0
191	122				303	0.0	0.0	0.0	0.0	0.0
192	130				303	0.0	0.0	0.0	0.0	0.0
193	139				303	0.0	0.0	0.0	0.0	0.0
194	145				303	0.0	0.0	0.0	0.0	0.0
195	149				303	0.0	0.0	0.0	0.0	0.0
196	153				303	0.0	0.0	0.0	0.0	0.0
197	159				303	0.0	0.0	0.0	0.0	0.0
198	165				303	0.0	0.0	0.0	0.0	0.0
199	169				303	0.0	0.0	0.0	0.0	0.0
200	171				302	0.0	0.0	0.0	0.0	0.0
201	173				301	0.0	0.0	0.0	0.0	0.0
	5000.0	58310.0	20		6	4	0	1		
1	0.055	0.12			6.00			17.0		
2	0.057	0.15			7.00			18.0		
3	0.062	0.18			10.00			12.0		
4	0.110	0.35			12.00			6.0		
5	0.35	0.45			6.00			5.0		
6	1.45	1.50			15.00			1.0		
1	102.50	15.875	1		12.0	1	1	0	0	
2	102.50	27.875	1		12.0	1	1	0	0	
3	102.50	39.000	2		12.0	1	1	0	0	
4	88.75	39.000	2		12.0	1	1	0	0	
5	76.75	39.000	2		12.0	1	1	0	0	
6	64.75	39.000	2		12.0	1	1	0	0	
7	52.75	39.000	2		12.0	1	1	0	0	
8	40.75	39.000	2		12.0	1	1	0	0	
9	28.75	39.000	2		12.0	1	1	0	0	
10	16.75	39.000	2		12.0	1	1	0	0	
11	-13.25	39.000	3		12.0	1	1	0	0	
12	-33.25	39.000	3		12.0	1	1	0	0	
13	-53.25	39.000	3		12.0	1	1	0	0	
14	-73.25	39.000	3		12.0	1	1	0	0	
15	-93.25	39.000	3		12.0	1	1	0	0	

16	-125.35	39.000	4	12.0	1	1	0	0
17	-125.35	-39.000	4	12.0	0	0	0	0
18	102.50	-39.000	1	12.0	0	0	0	0
19	62.40	33.90	5	1.0	1	1	0	0
20	-77.85	33.90	6	1.0	1	1	0	0
1	62.40	33.90		0.0	608.			
2	62.40	-33.90		0.0	608.			
3	-77.85	33.90		0.0	492.			
4	-77.85	-33.90		0.0	492.			
1	0.0	0.0						
3	825.000	0.0	25.00	62.14		0.0	0.0	1.0

APPENDIX C
English-Unit System Details - Test No. MGS221-1

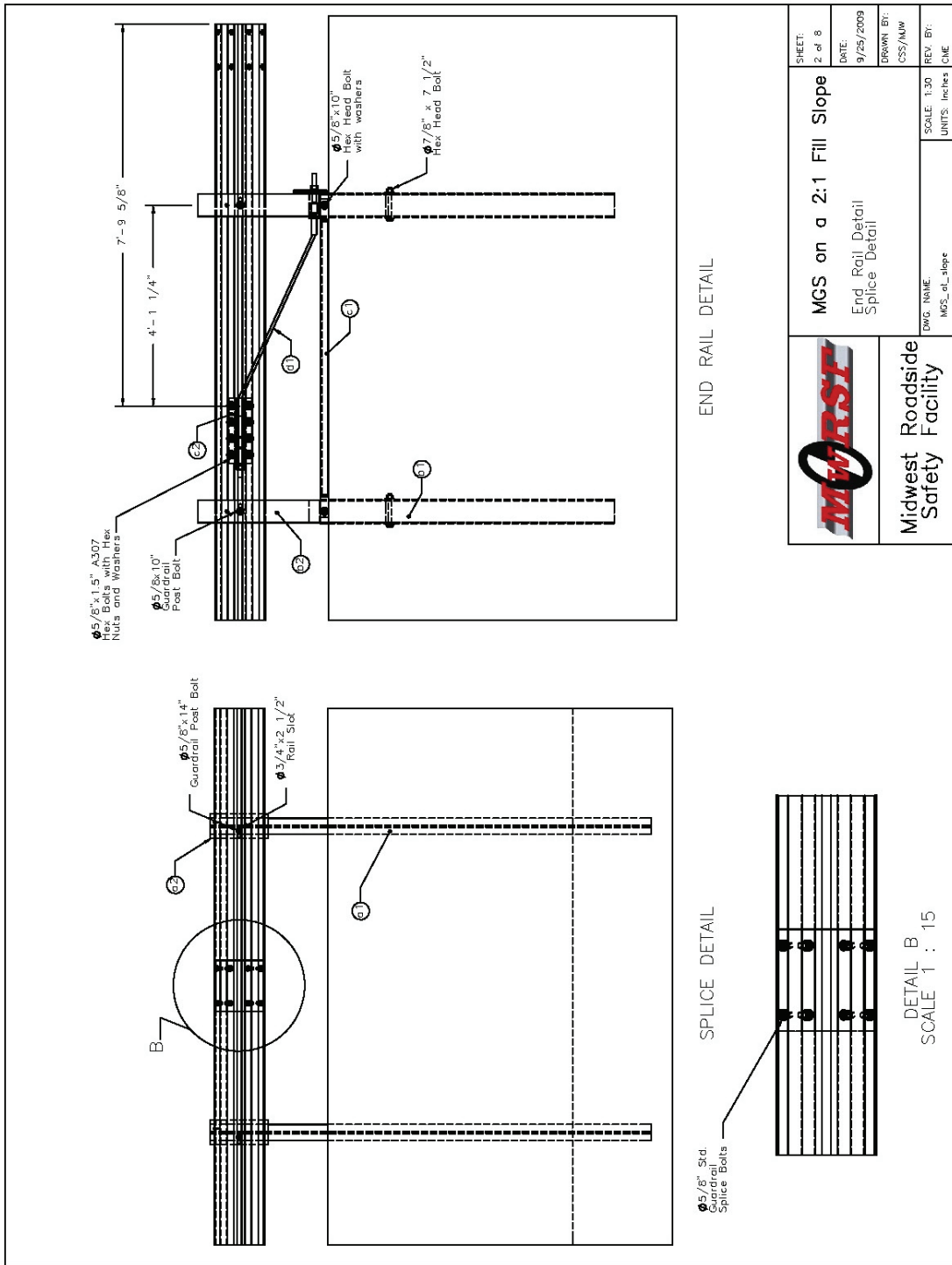


Figure C-2. Rail Detail, Test No. MGS221-1 (English)

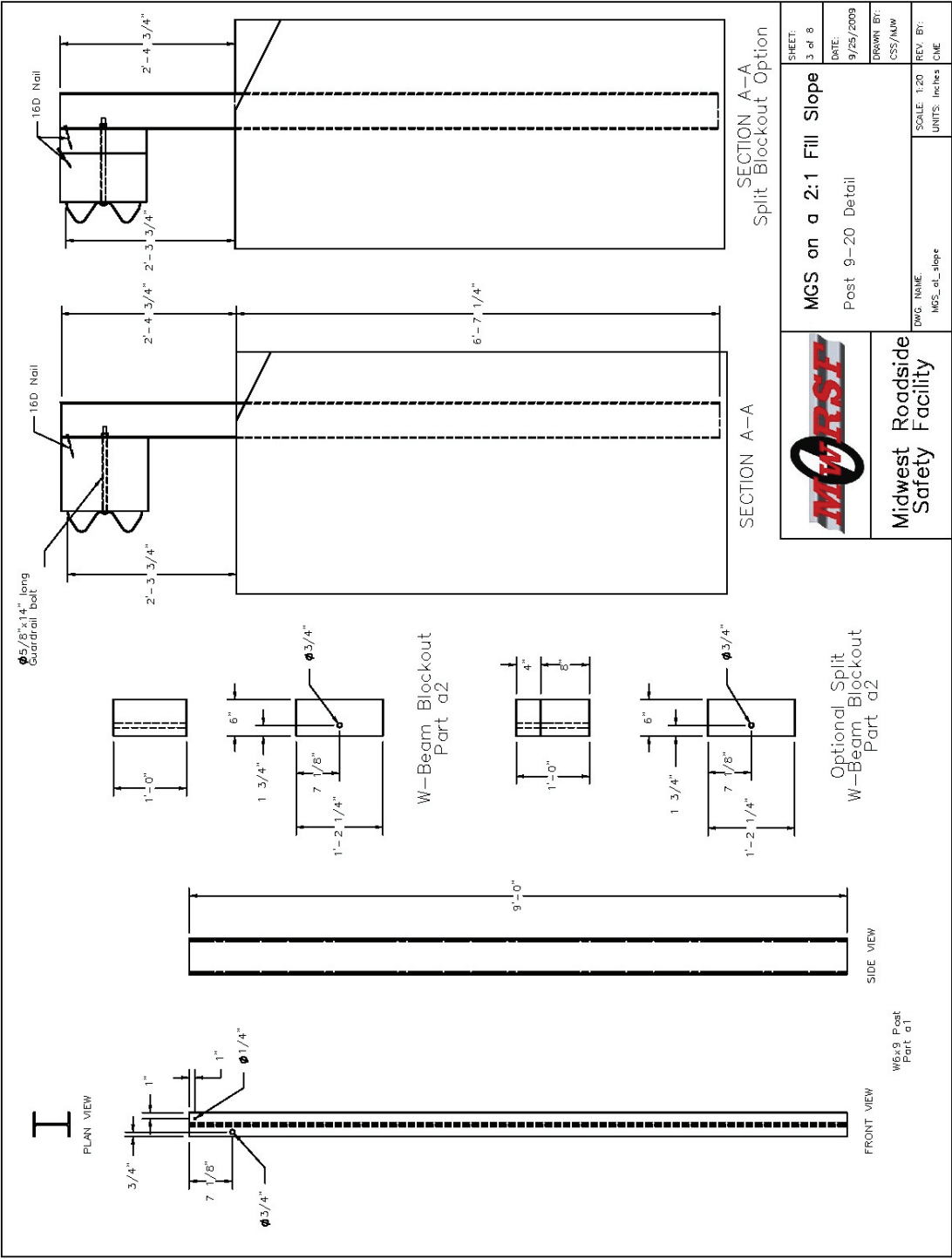


Figure C-3. Post Details, Test No. MGS221-1 (English)

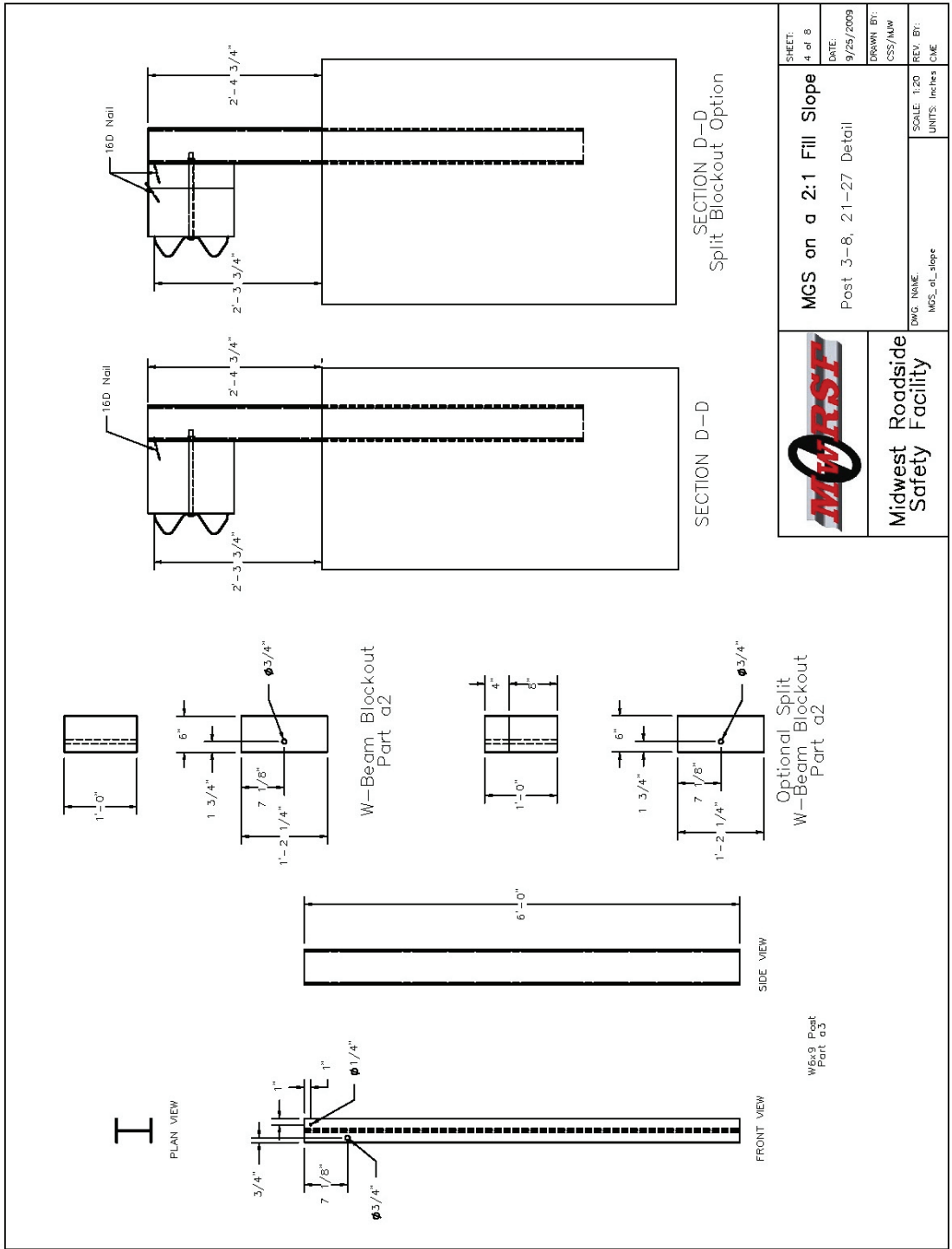


Figure C-4. Post Details, Test No. MGS221-1 (English)

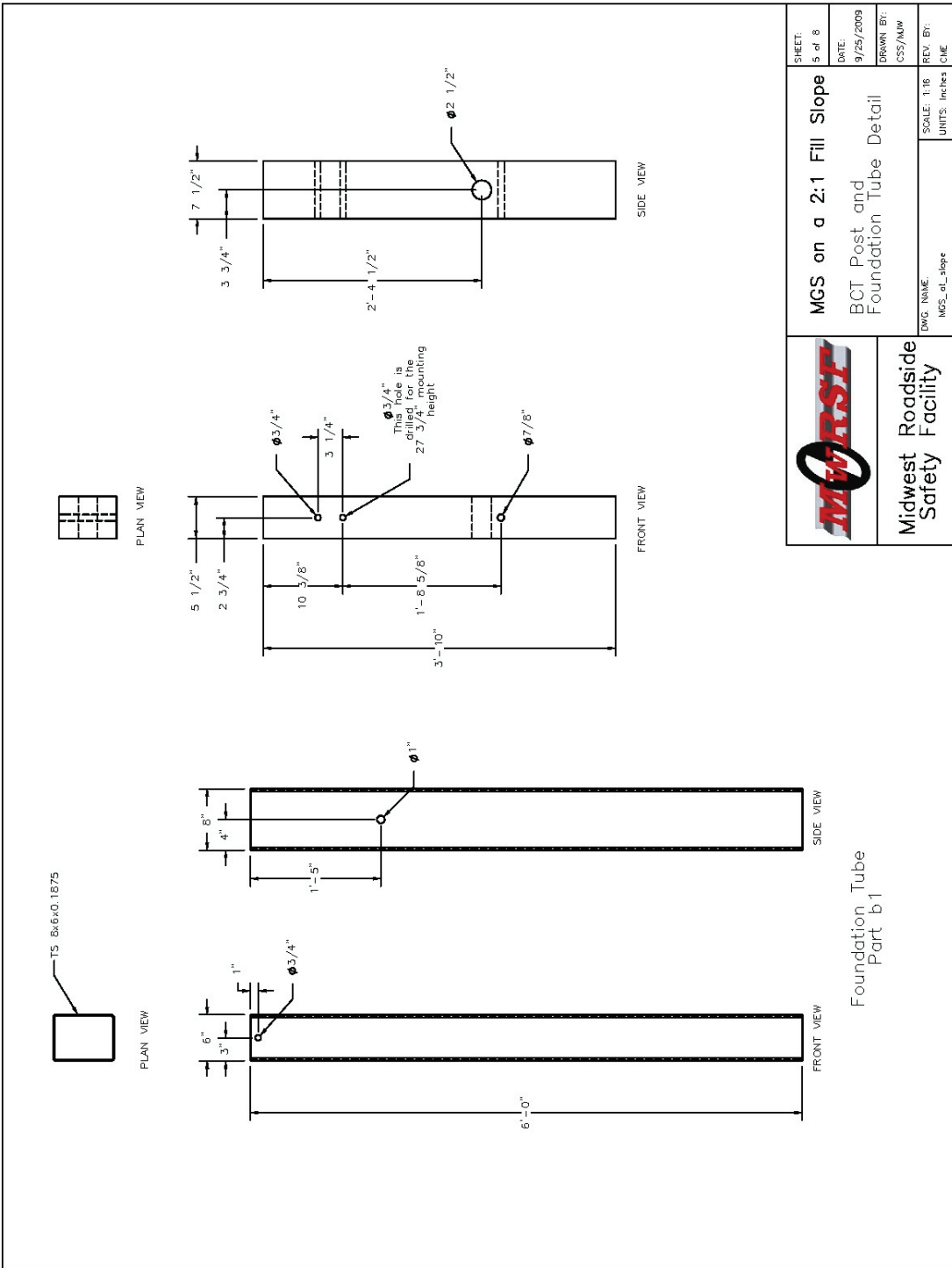
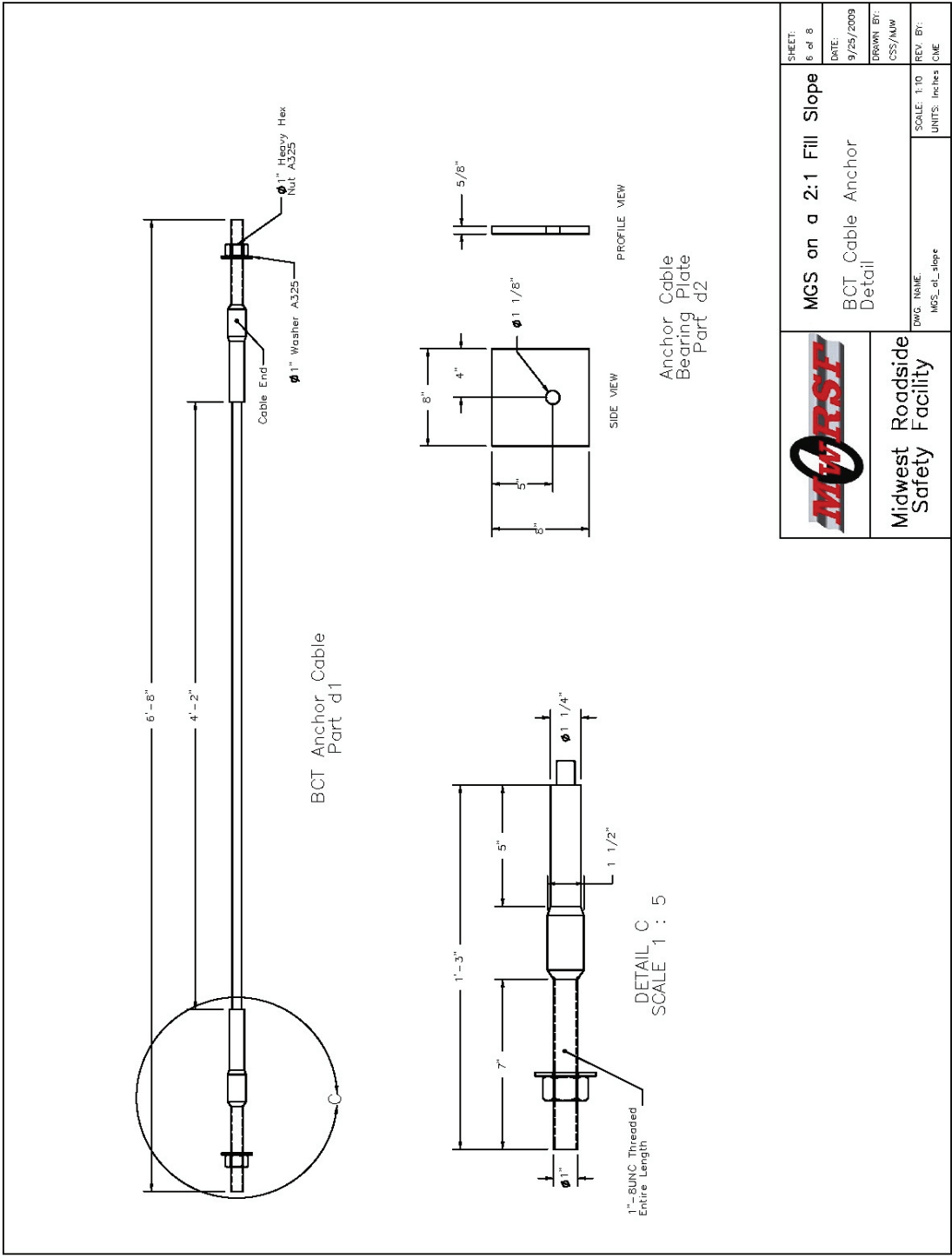


Figure C-5. Post and Foundation Tube Details, Test No. MGS221-1 (English)




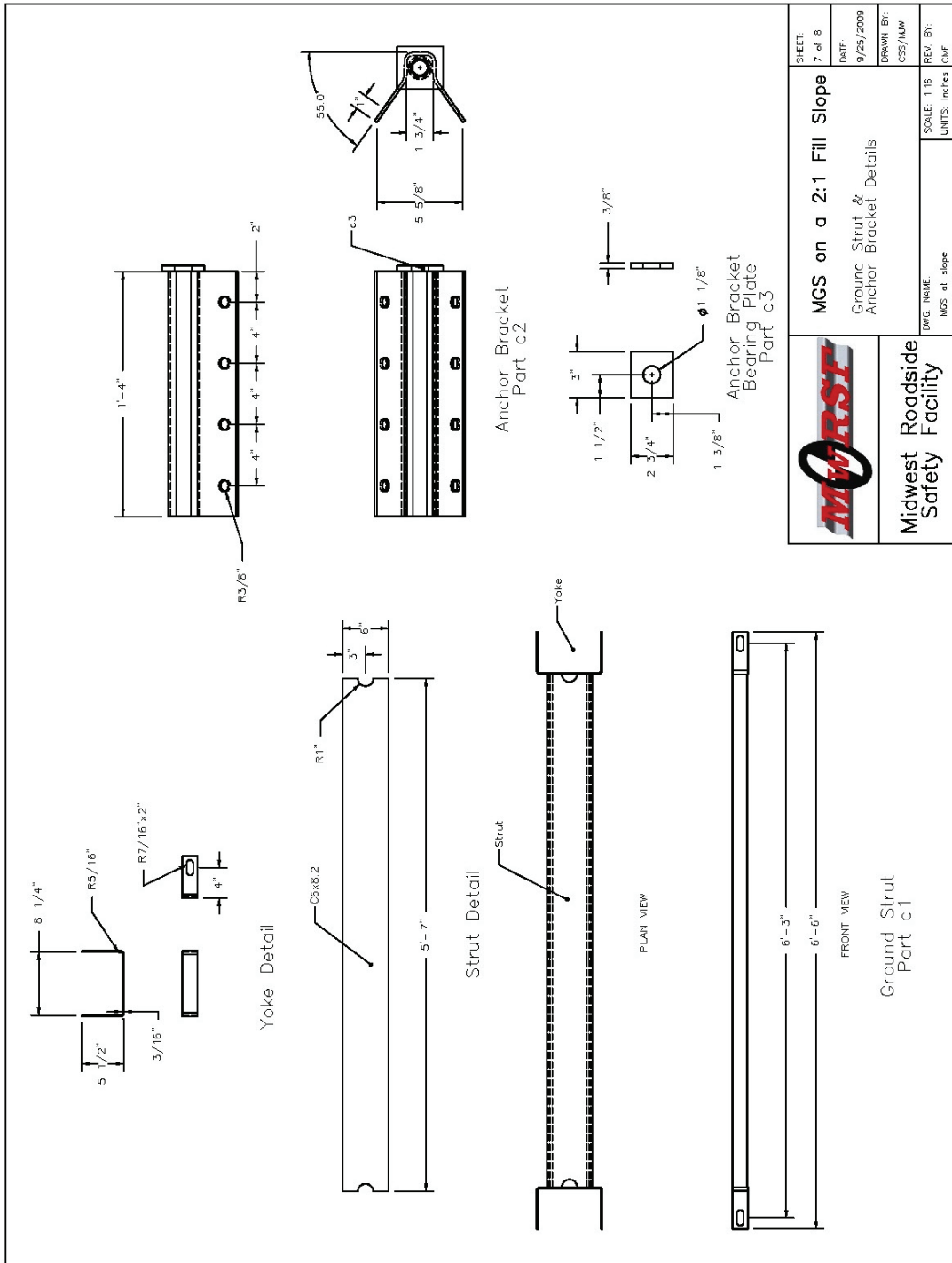
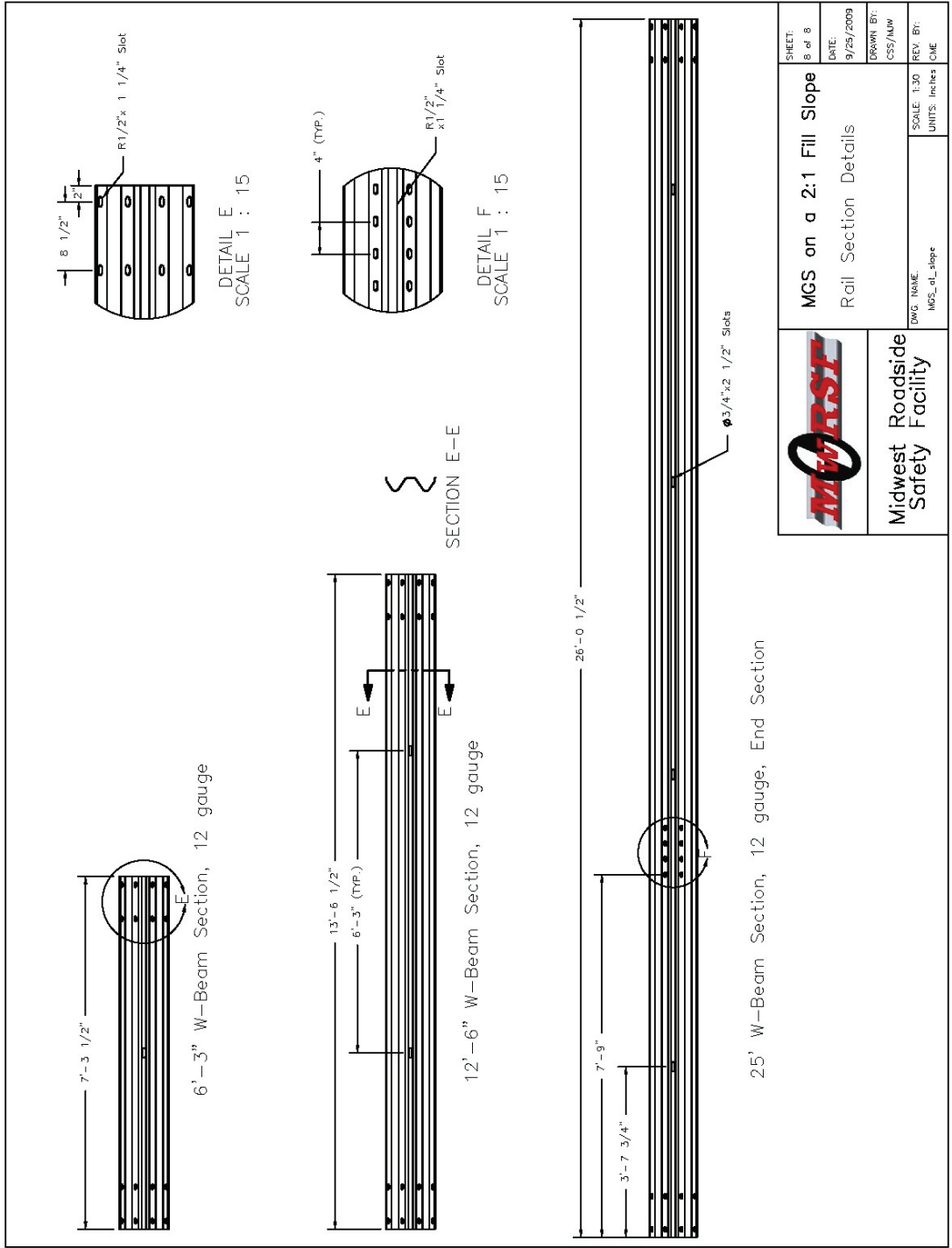
 Midwest Roadside Safety Facility	MGS on a 2:1 Fill Slope BCT Cable Anchor Detail	SHEET: 6 of 8
	DWG. NAME: MGS_el_slope	DATE: 9/25/2009
SCALE: 1:10 UNITS: Inches	DRAWN BY: CSS/AMW	REV. BY: ONE

Figure C-6. Anchor Cable Details, Test No. MGS221-1 (English)



	Midwest Safety Facility	DMG NAME: MGS_sl_slope	SCALE: 1:16 UNITS: Inches
	MGS on a 2:1 Fill Slope Ground Strut & Anchor Bracket Details	SHEET: 7 of 8 DATE: 9/25/2009 DRAWN BY: CSS/MW REV. BY: CME	

Figure C-7. Ground Strut and Anchor Bracket Details, Test No. MGS221-1 (English)




	MGS on a 2:1 Fill Slope Rail Section Details	SHEET: 8 of 8
	DATE: 9/25/2009	DRAWN BY: CCS/ALW
DWG NAME: MGS_01_slope	SCALE: 1:30 UNITS: Inches	REV. BY: CME

Figure C-8. Rail Details, Test No. MGS221-1 (English)

APPENDIX D
Test Summary Sheets - English Units

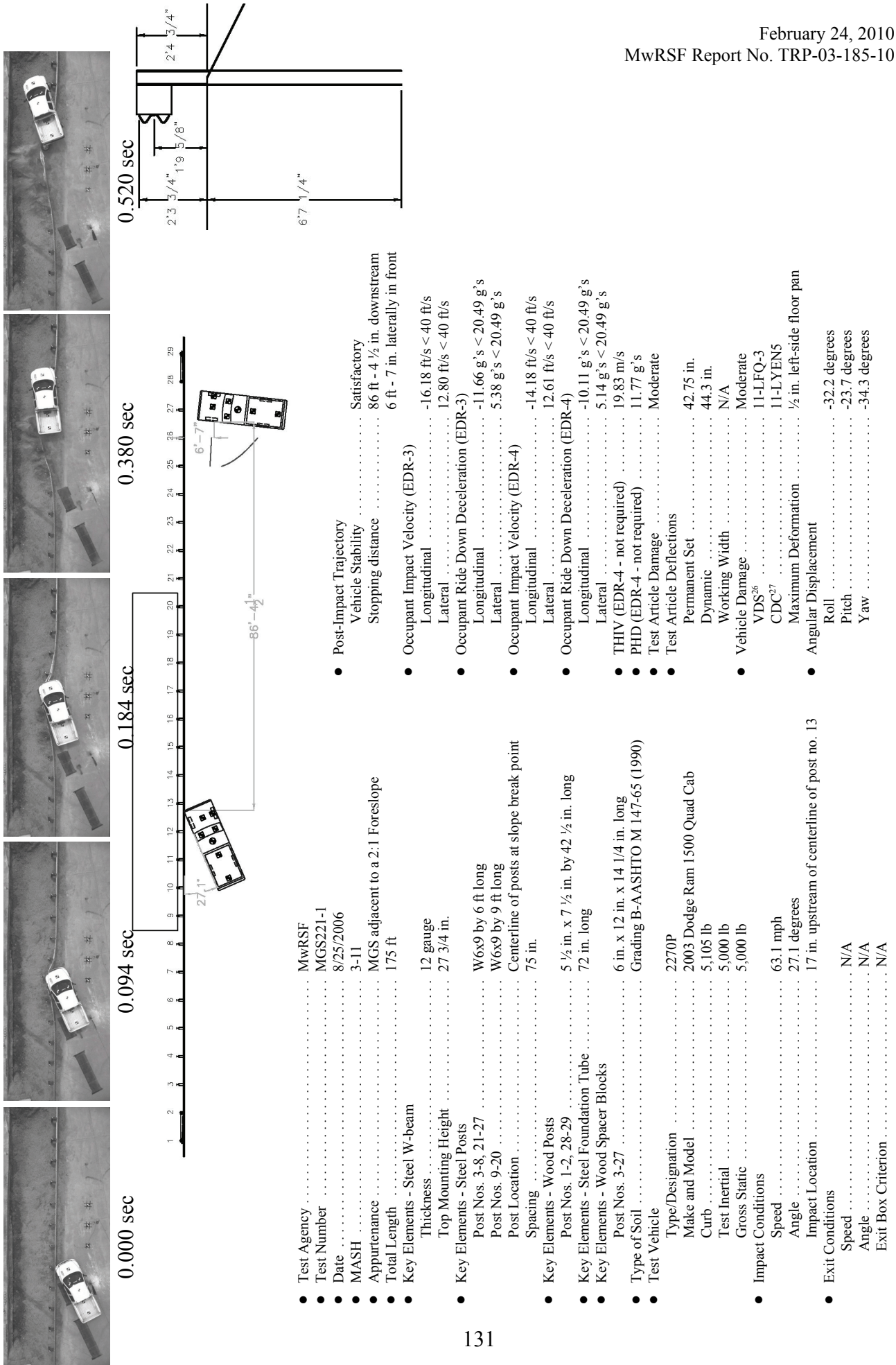
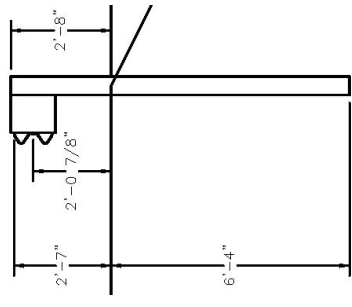
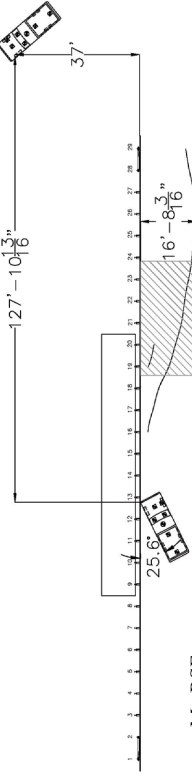


Figure D-1. Summary of Test Results and Sequential Photographs (English), Test No. MGS221-1



0.000 sec 0.118 sec 0.266 sec 0.428 sec 0.730 sec



● Test Agency	MwRSF	Vehicle Stability	Satisfactory
● Test Number	MG221-2	Stopping	127 ft - 10.75 in. downstream 37 ft laterally behind
● Date	12/15/2006	● Occupant Impact Velocity (EDR-3)	
● MASH	3-11	Longitudinal	-16.18 ft/s < 40 ft/s
● Appurtenance	MG2 adjacent to a 2:1 Foreslope	Lateral	12.80 ft/s < 40 ft/s
● Total Length	175 ft	● Occupant Ride Down Deceleration (EDR-3)	
● Key Elements - Steel W-beam		Longitudinal	-11.66 g's < 20.49 g's
Thickness	12 gauge	Lateral	5.38 g's < 20.49 g's
Top Mounting Height	31 in.	● Occupant Impact Velocity (EDR-4)	
● Key Elements - Steel Posts		Longitudinal	-13.90 < 40 ft/s
Post Nos. 3-8, 21-27	W6x9.4 by 6 ft long	Lateral	13.61 ft/s < 40 ft/s
Post Nos. 9-20	W6x9 by 9 ft long	● Occupant Ride Down Deceleration (EDR-4)	
Post Location	Centerline of posts at slope break point	Longitudinal	-5.36 g's < 20.49 g's
Spacing	75 in	Lateral	5.28 g's < 20.49 g's
● Key Elements - Wood Posts		● THIV (not required)	20.5 ft/s
Post Nos. 1-2, 28-29	5 1/2 in. x 7 1/2 in. by 42 1/2 in. long	● PHD (not required)	6.93 g's
● Key Elements - Foundation Tube		● Test Article Damage	Moderate
Wood Spacer Blocks		● Test Article Deflections	
Post Nos. 3-27	6 in. x 12 in. x 14 1/4 in. long	Permanent Set	42 in.
● Type of Soil	Grading B-AAASHTO M 147-65 (1990)	Dynamic	57.6 in.
● Test Vehicle		Working Width	64.2 in
Type/Designation	2270P	● Vehicle Damage	Minimal
Make and Model	2004 Dodge Ram 1500 Quad Cab	VDS ²⁶	11-LFO-3
Curb	5,130 lb	CDC ²⁷	11-LFEN3
Test Inertia	5,013 lb	Maximum Deformation	1/2 in. front-center of the left-side floor pan
Gross Static	5,013 lb	● Angular Displacements (Estimated from Video)	
● Impact Conditions		Roll	6
Speed	61.3 mph	Pitch	5
Angle	25.5 degrees	Yaw	45
Impact Location	15 1/2 in. upstream of centerline of post 13		
● Exit Conditions			
Speed	38.6 mph		
Angle	17.4 degrees		
Exit Box Criterion	Pass		

Figure D-2. Summary of Test Results and Sequential Photographs (English), Test No. MG221-2

APPENDIX E
Occupant Compartment Deformation Data, Test No. MGS221-1

VEHICLE PRE/POST CRUSH INFO
Set-1

TEST: MGS221-1
VEHICLE: 2003 Dodge Ram 1500 QC

Note: If impact is on driver side need to
enter negative number for Y

POINT	X	Y	Z	X'	Y'	Z'	DEL X	DEL Y	DEL Z
1	28.5	-27.75	-1.75	28.5	-28	-1.5	0	-0.25	0.25
2	29.5	-23.75	-3.5	29.5	-23.75	-3.5	0	0	0
3	27.75	-16.5	-4.5	28	-16.25	-4.5	0.25	0.25	0
4	23.75	-7.25	-0.25	23.75	-7.5	-0.25	0	-0.25	0
5	26.25	-29.5	-5.25	26.25	-29.5	-5.5	0	0	-0.25
6	25	-22	-6	25.25	-21.75	-6	0.25	0.25	0
7	24.75	-16.25	-6	24.75	-16.25	-6	0	0	0
8	20.75	-9	-4.25	20.75	-8.75	-4.25	0	0.25	0
9	21.5	-29.75	-8.25	21.25	-30	-8.5	-0.25	-0.25	-0.25
10	21	-23.25	-8.25	21	-23	-8.5	0	0.25	-0.25
11	21	-15.5	-8	21	-15.5	-8.25	0	0	-0.25
12	17.5	-9.5	-6	17.5	-9.5	-6	0	0	0
13	15	-6.5	-1	15	-6.25	-1	0	0.25	0
14	13.25	-29	-8.75	13.25	-28.75	-8.25	0	0.25	0.5
15	13.25	-23	-8.5	13.5	-22.75	-8.75	0.25	0.25	-0.25
16	13.5	-16.5	-8.5	13.5	-16.5	-8.5	0	0	0
17	13.25	-11	-8	13.25	-10.75	-8.25	0	0.25	-0.25
18	11	-6	-1	11	-6	-1.25	0	0	-0.25
19	6	-29.25	-8.5	6	-29.25	-8.5	0	0	0
20	6.25	-23	-8.5	6.25	-23	-8.5	0	0	0
21	6.5	-16	-8.5	6.25	-15.75	-8.5	-0.25	0.25	0
22	6.5	-10.5	-8.75	6.5	-10.25	-8.75	0	0.25	0
23	6	-7.5	-2.25	6	-7.5	-2.25	0	0	0
24	0.5	-27.5	-4.5	0.5	-27.25	-4.5	0	0.25	0
25	0.5	-22	-4.5	0.5	-21.5	-4.5	0	0.5	0
26	0.5	-15.25	-4.5	0.5	-15	-4.5	0	0.25	0
27	1	-8.5	-2	1	-8.5	-2	0	0	0
28	1	-3.5	-1.25	1	-3.5	-1.25	0	0	0
29							0	0	0
30							0	0	0

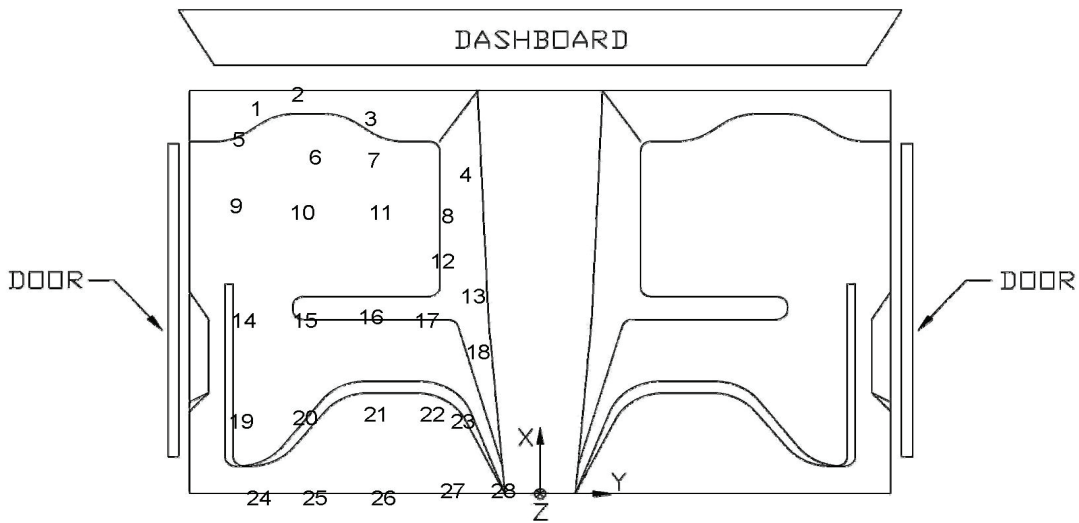


Figure E-1. Occupant Compartment Deformation Data - Set 1, Test MGS221-1

VEHICLE PRE/POST CRUSH INFO
Set-2

TEST: MGS221-1
VEHICLE: 2003 Dodge Ram 1500 QC

Note: If impact is on driver side need to enter negative number for Y

POINT	X	Y	Z	X'	Y'	Z'	DEL X	DEL Y	DEL Z
1	46.5	-32.25	-0.75	46.5	-32.5	-0.5	0	-0.25	0.25
2	47.5	-28.25	-3	47.5	-28.25	-3	0	0	0
3	45.75	-21	-4.25	46	-20.75	-4.5	0.25	0.25	-0.25
4	41.75	-11.75	-0.5	41.75	-12	-0.5	0	-0.25	0
5	44.25	-34	-4.5	44.25	-34	-4.75	0	0	-0.25
6	43	-26.5	-5.75	43.25	-26.25	-5.5	0.25	0.25	0.25
7	42.75	-20.75	-6	42.75	-20.75	-6.25	0	0	-0.25
8	38.75	-13.5	-4.75	38.75	-13.25	-4.75	0	0.25	0
9	39.5	-34.25	-7.5	39.25	-34.5	-7.5	-0.25	-0.25	0
10	39	-27.75	-7.75	39	-27.5	-7.75	0	0.25	0
11	39	-20	-8	39	-20	-8	0	0	0
12	35.5	-14	-6	35.5	-14	-6.25	0	0	-0.25
13	33	-11	-1.25	33	-10.75	-1.5	0	0.25	-0.25
14	31.25	-33.5	-7.75	31.25	-33.25	-7.75	0	0.25	0
15	31.25	-27.5	-8	31.5	-27.25	-8	0.25	0.25	0
16	31.5	-21	-8.25	31.5	-21	-8.25	0	0	0
17	31.25	-15.5	-8.25	31.25	-15.25	-8.25	0	0.25	0
18	29	-10.5	-1.5	29	-10.5	-1.75	0	0	-0.25
19	24	-33.75	-7.5	24	-33.75	-7.5	0	0	0
20	24.25	-27.5	-8	24.25	-27.5	-8	0	0	0
21	24.5	-20.5	-8.25	24.25	-20.25	-8.25	-0.25	0.25	0
22	24.5	-15	-7.75	24.5	-14.75	-8	0	0.25	-0.25
23	24	-12	-2.5	24	-12	-2.75	0	0	-0.25
24	18.5	-32	-3.5	18.5	-31.75	-3.25	0	0.25	0.25
25	18.5	-26.5	-3.75	18.5	-26	-3.75	0	0.5	0
26	18.5	-19.75	-4.25	18.5	-19.5	-4.25	0	0.25	0
27	19	-13	-2.25	19	-13	-2.25	0	0	0
28	19	-8	-2	19	-8	-2	0	0	0
29							0	0	0
30							0	0	0

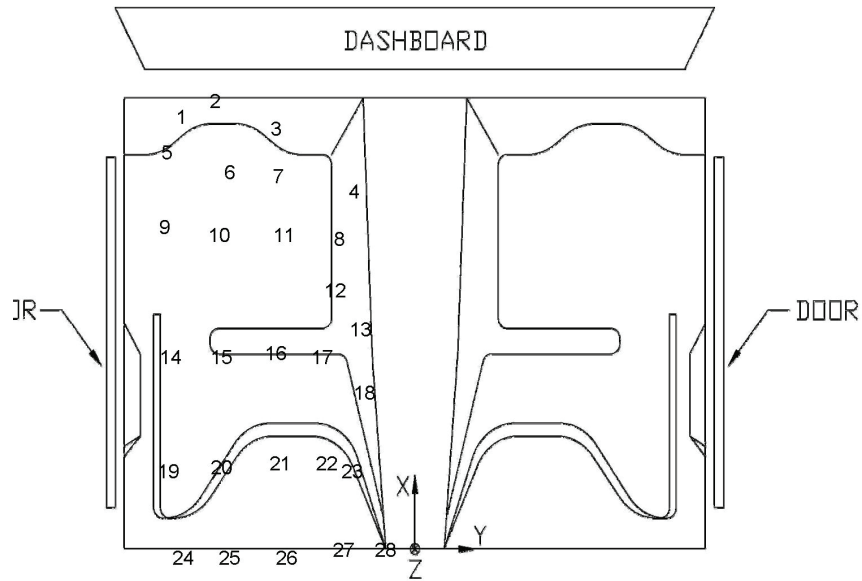


Figure E-2. Occupant Compartment Deformation Data - Set 2, Test MGS221-1

Occupant Compartment Deformation Index (OCDI)

Test No. MSG221-1
Vehicle Type: 2003 Dodge Ram 1500 QC

OCDI = XXABCDEFGHI

XX = location of occupant compartment deformation

A = distance between the dashboard and a reference point at the rear of the occupant compartment, such as the top of the rear seat or the rear of the cab on a pickup

B = distance between the roof and the floor panel

C = distance between a reference point at the rear of the occupant compartment and the motor panel

D = distance between the lower dashboard and the floor panel

E = interior width

F = distance between the lower edge of right window and the upper edge of left window

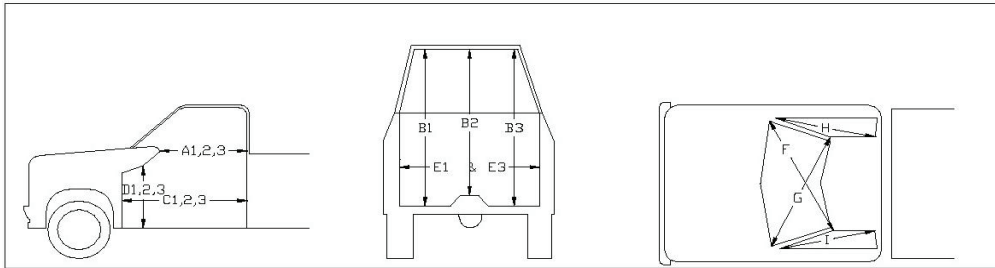
G = distance between the lower edge of left window and the upper edge of right window

H = distance between bottom front corner and top rear corner of the passenger side window

I = distance between bottom front corner and top rear corner of the driver side window

Severity Indices

- 0 - if the reduction is less than 3%
- 1 - if the reduction is greater than 3% and less than or equal to 10%
- 2 - if the reduction is greater than 10% and less than or equal to 20%
- 3 - if the reduction is greater than 20% and less than or equal to 30%
- 4 - if the reduction is greater than 30% and less than or equal to 40%



where,
1 = Passenger Side
2 = Middle
3 = Driver Side

Location:

Measurement	Pre-Test (in.)	Post-Test (in.)	Change (in.)	% Difference	Severity Index
A1	55.25	55.25	0.00	0.00	0
A2	50.25	50.25	0.00	0.00	0
A3	55.25	55.00	-0.25	-0.45	0
B1	48.25	48.50	0.25	0.52	0
B2	41.75	41.75	0.00	0.00	0
B3	47.25	47.50	0.25	0.53	0
C1	66.50	66.50	0.00	0.00	0
C2	47.75	47.75	0.00	0.00	0
C3	64.25	64.50	0.25	0.39	0
D1	18.25	18.25	0.00	0.00	0
D2	13.00	13.00	0.00	0.00	0
D3	16.00	16.00	0.00	0.00	0
E1	65.00	65.00	0.00	0.00	0
E3	64.75	64.75	0.00	0.00	0
F	56.25	56.25	0.00	0.00	0
G	57.75	57.50	-0.25	-0.43	0
H	37.50	37.50	0.00	0.00	0
I	37.00	37.00	0.00	0.00	0

Note: Maximum severity index for each variable (A-I) is used for determination of final OCDI value

Final OCDI: XXABCDEFGHI
LF 0 0 0 0 0 0 0 0 0

Figure E-3. Occupant Compartment Deformation Index (OCDI), Test MGS221-1

APPENDIX F
Accelerometer and Rate Transducer Data Analysis, Test No. MGS221-1

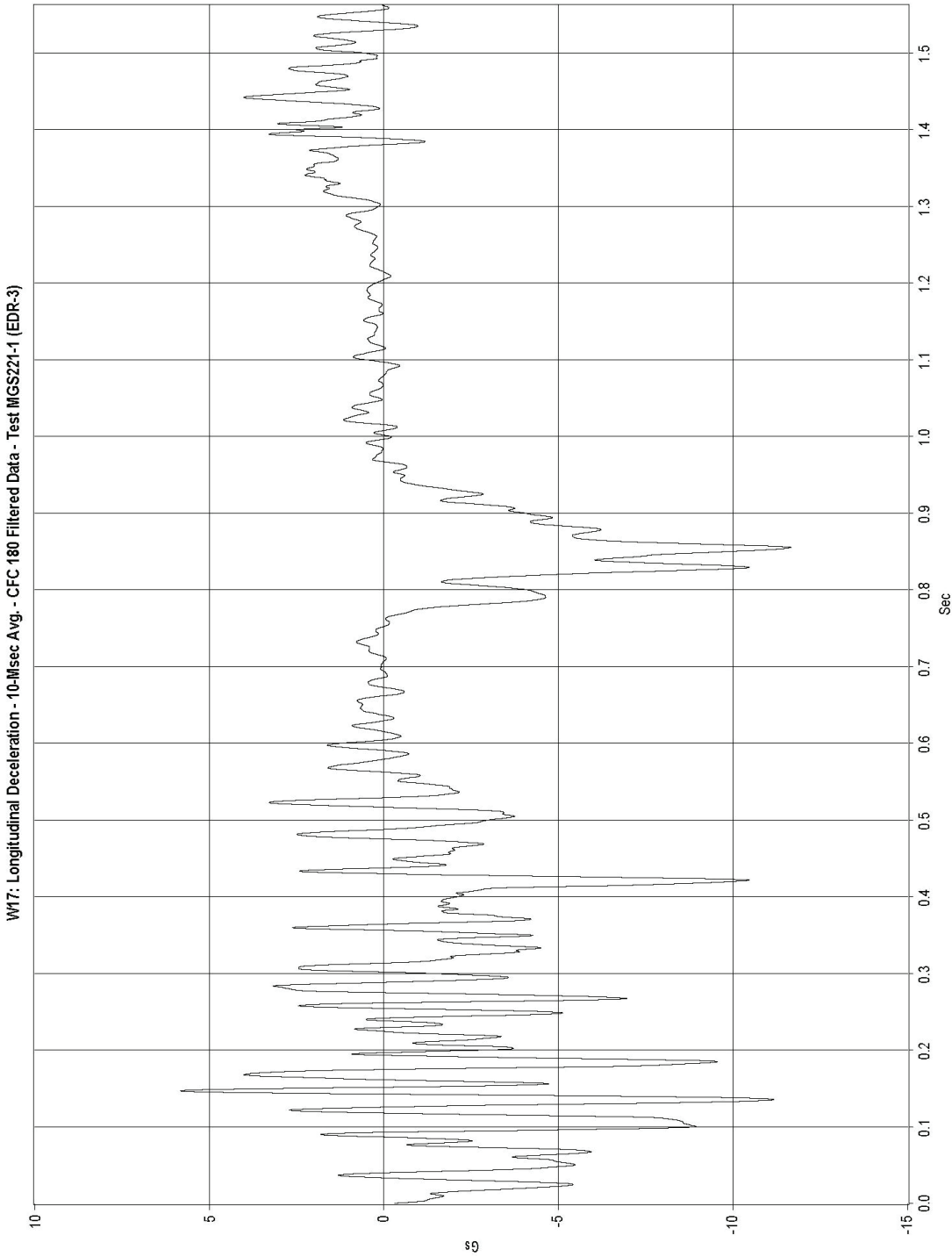


Figure F-1. Graph of Longitudinal Deceleration, Test MGS221-1

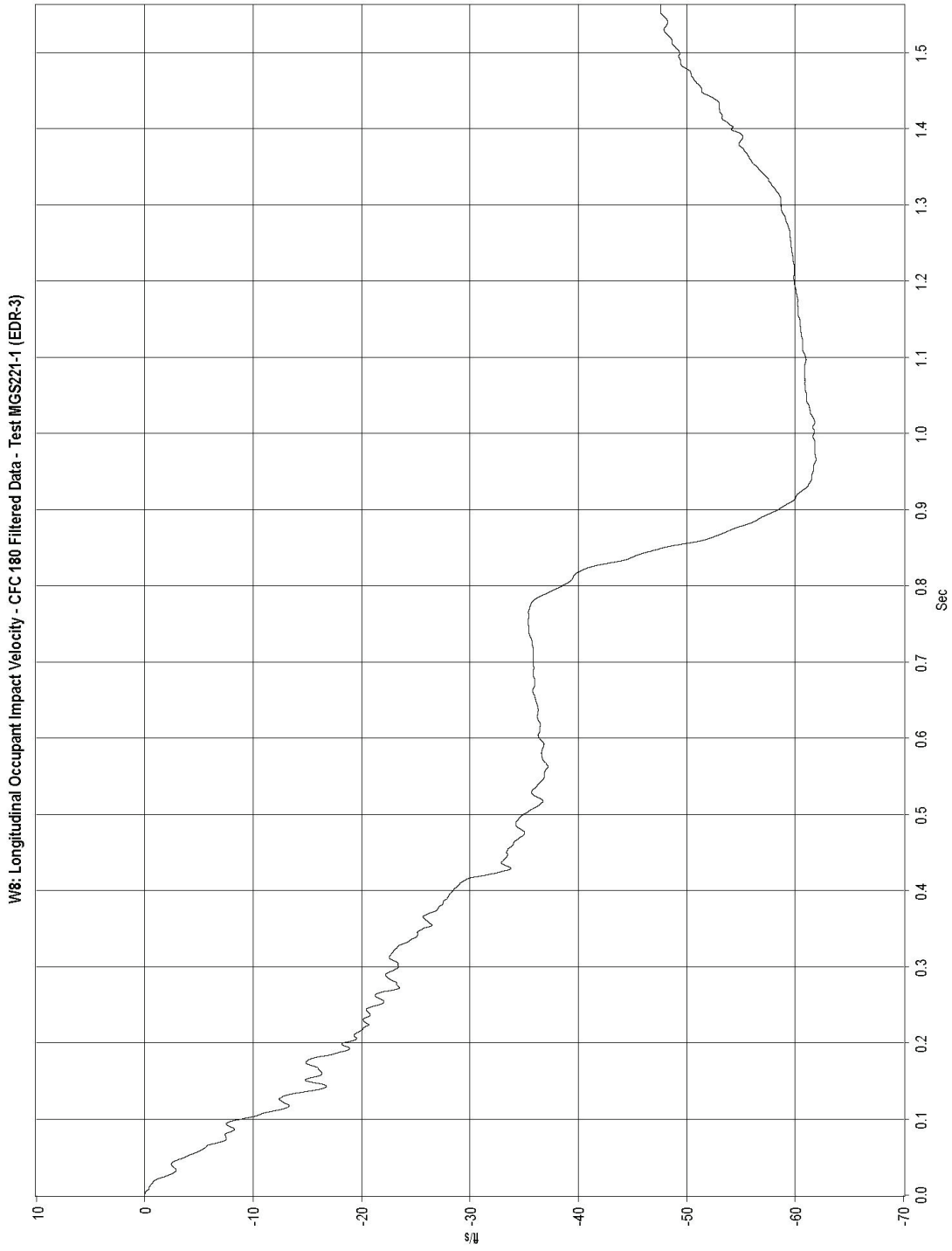


Figure F-2. Graph of Longitudinal Occupant Impact Velocity, Test MGS221-1

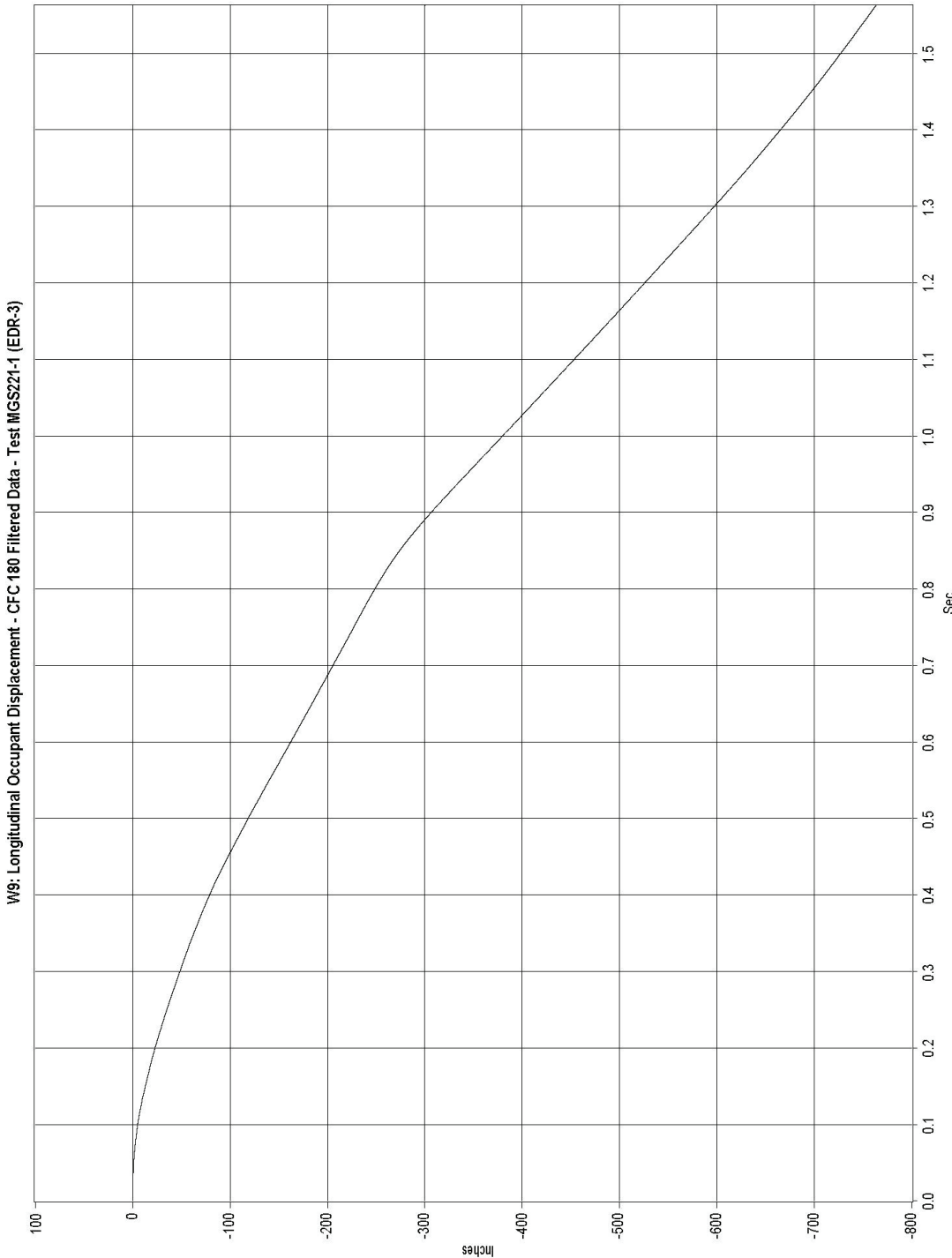


Figure F-3. Graph of Longitudinal Occupant Displacement, Test MGS221-1

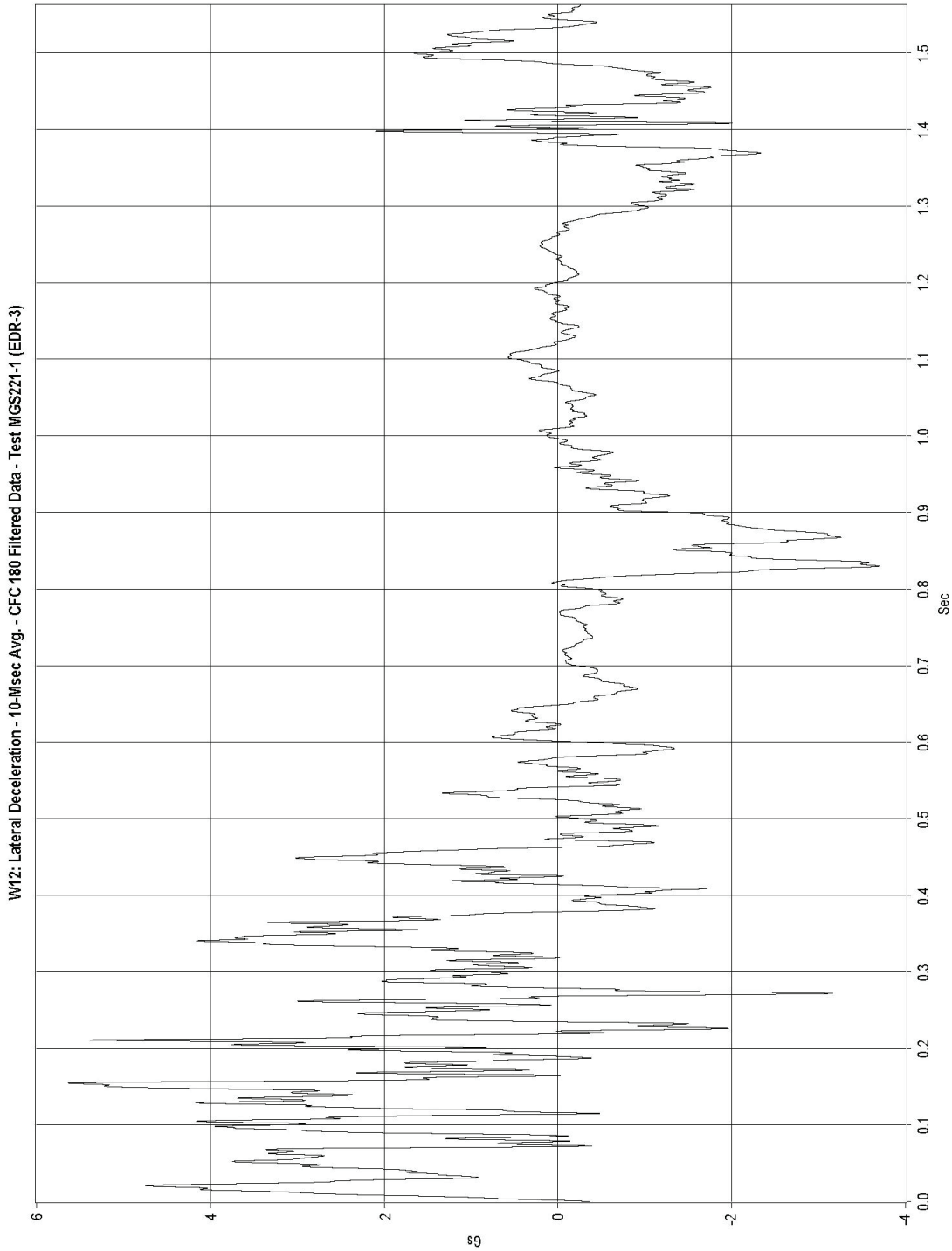


Figure F-4. Graph of Lateral Deceleration, Test MGS221-1

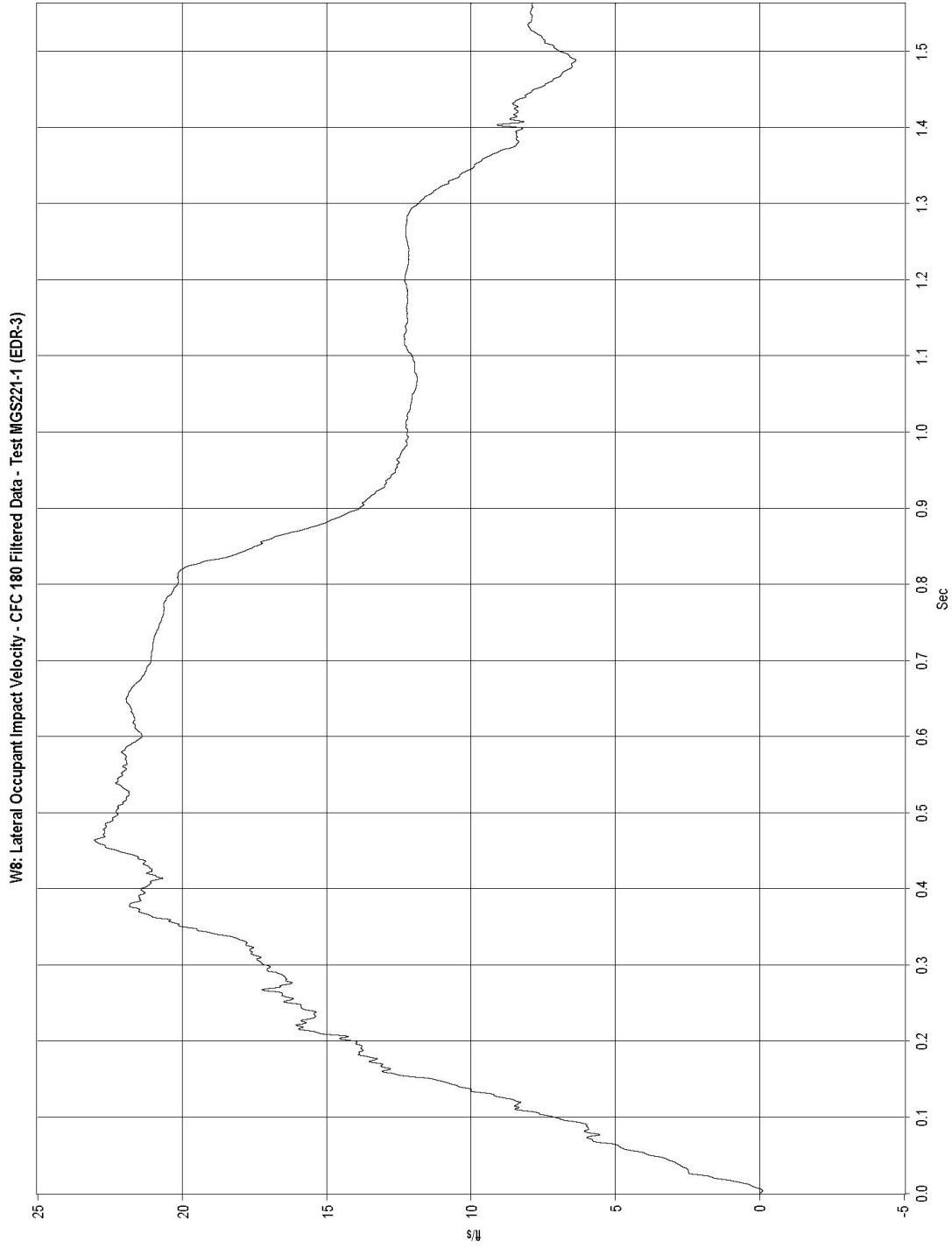


Figure F-5. Graph of Lateral Occupant Impact Velocity, Test MGS221-1

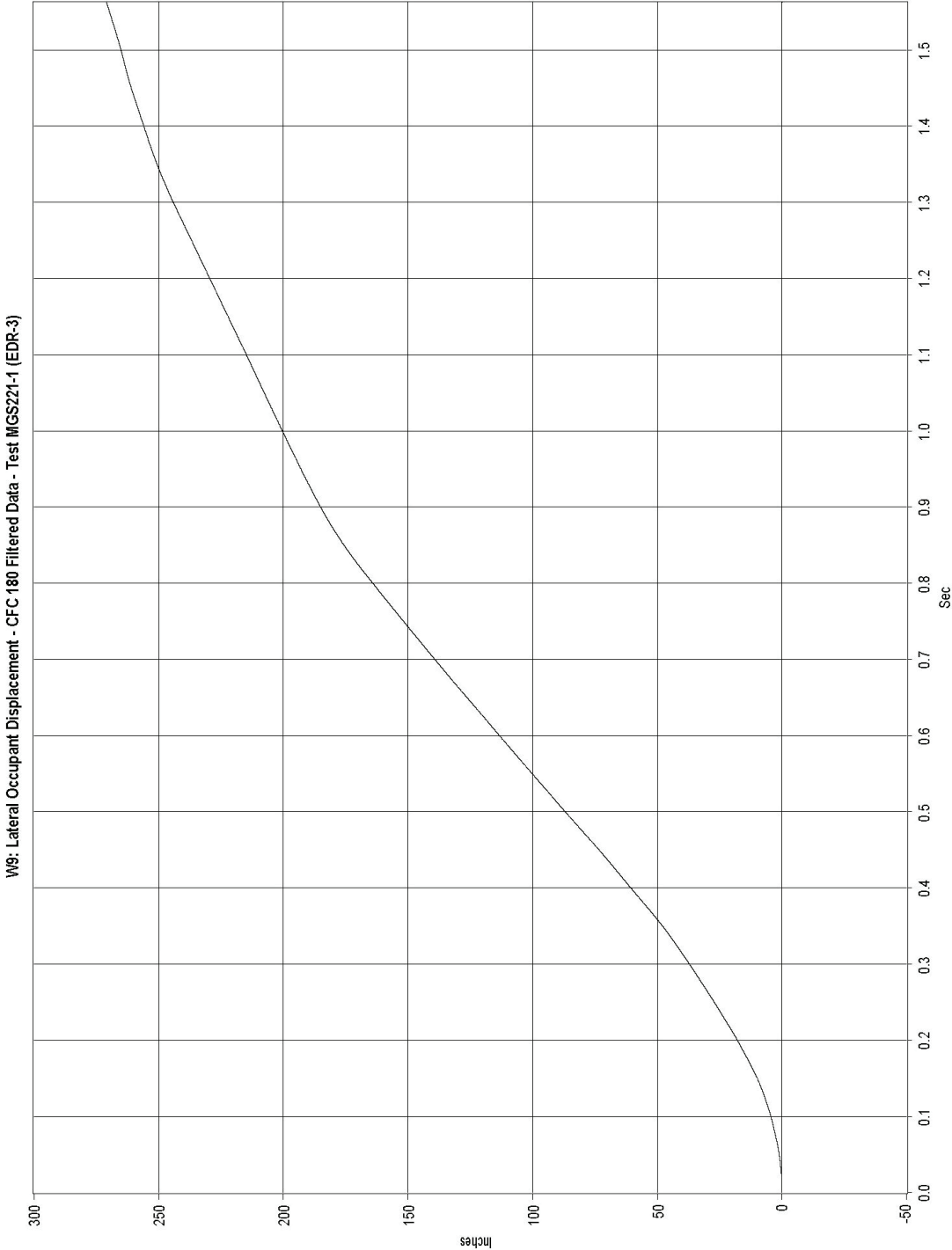


Figure F-6. Graph of Lateral Occupant Displacement, Test MGS221-1

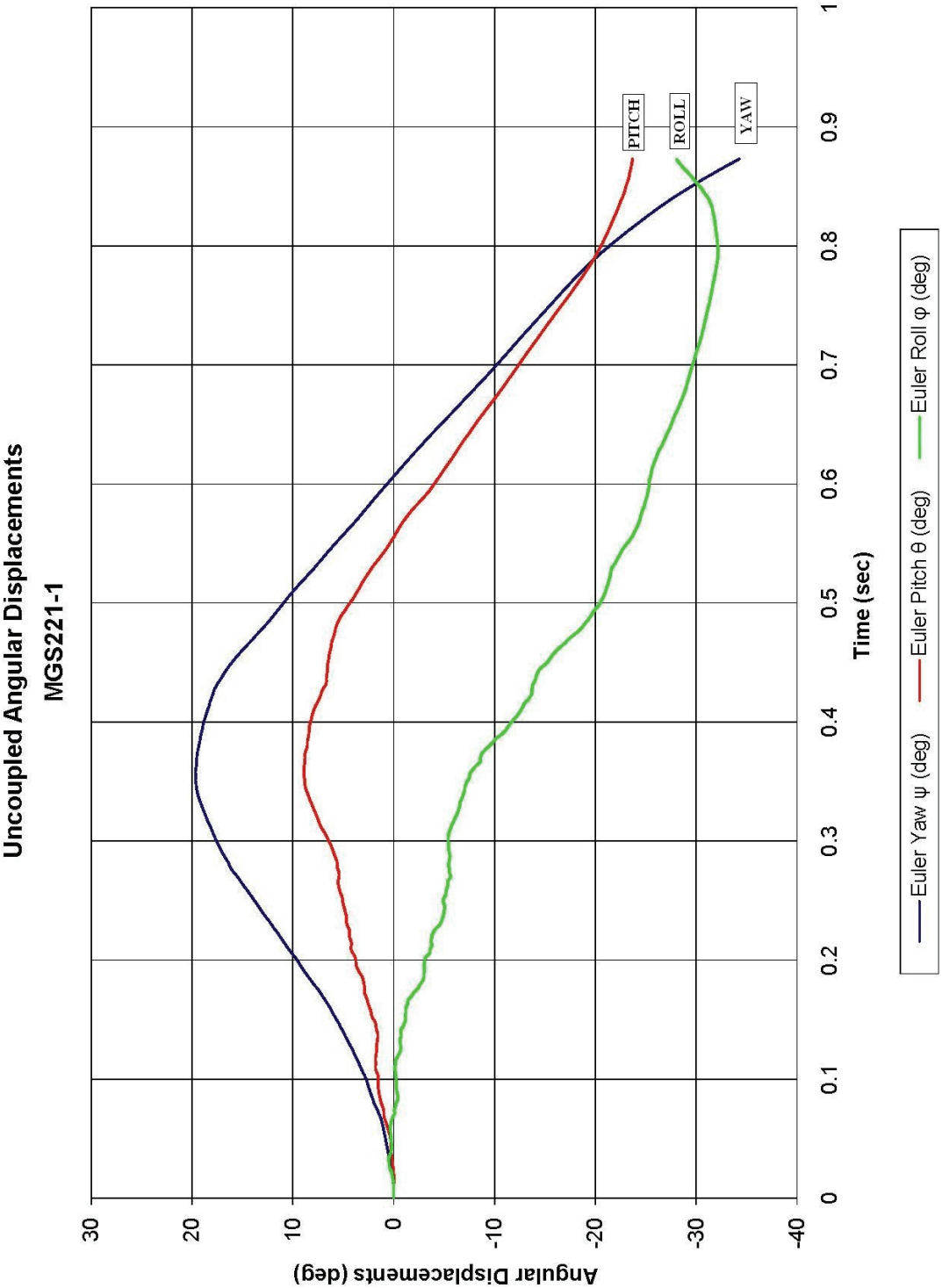


Figure F-7. Graph of Roll, Pitch, and Yaw Angular Displacement, Test No. MGS221-1

APPENDIX G
Metric-Unit and English-Unit System Details - Test No. MGS221-2

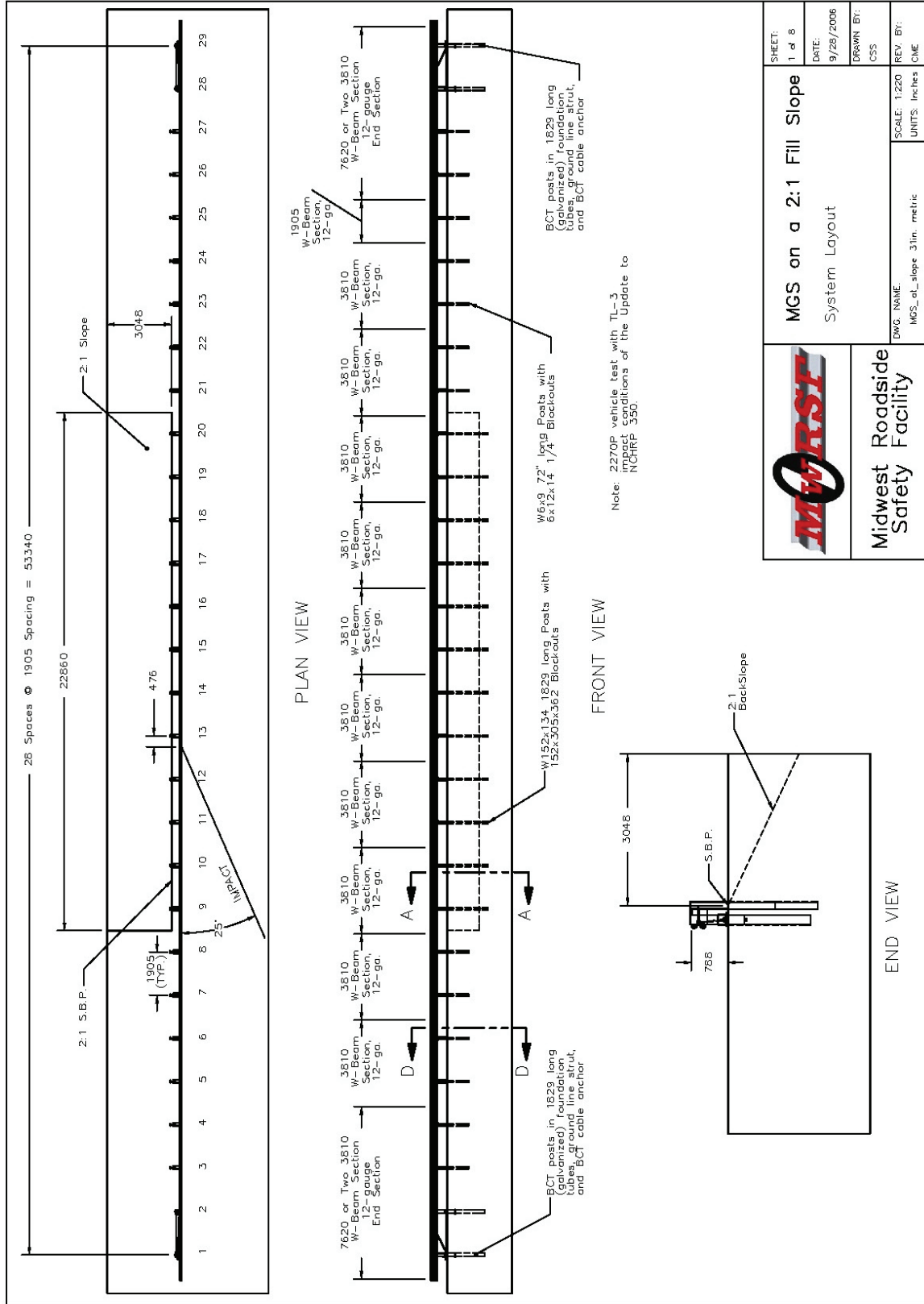


Figure G-1. System Layout Details, Test No. MGS221-2 (Metric)

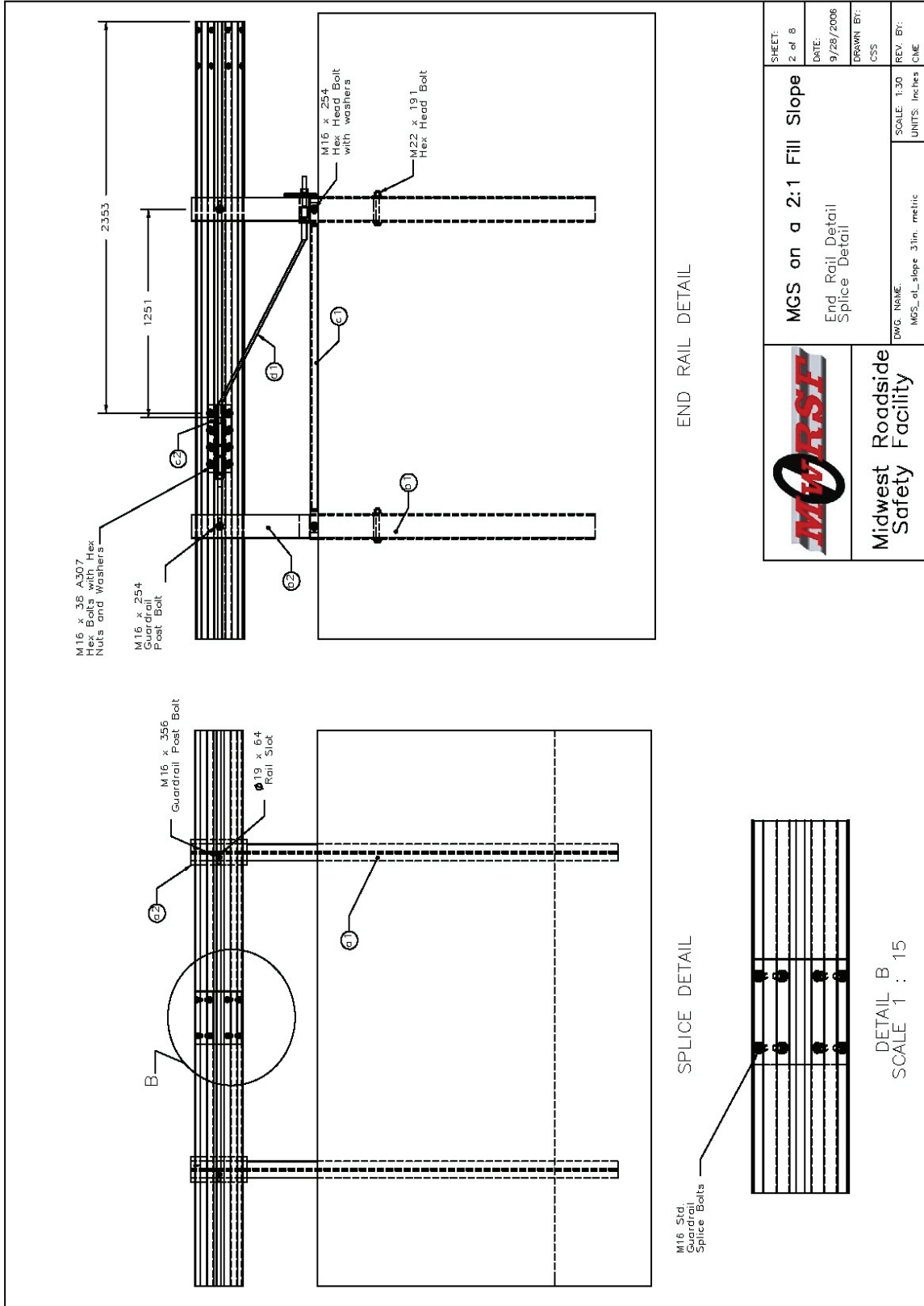


Figure G-2. Rail Detail, Test No. MGS221-2 (Metric)

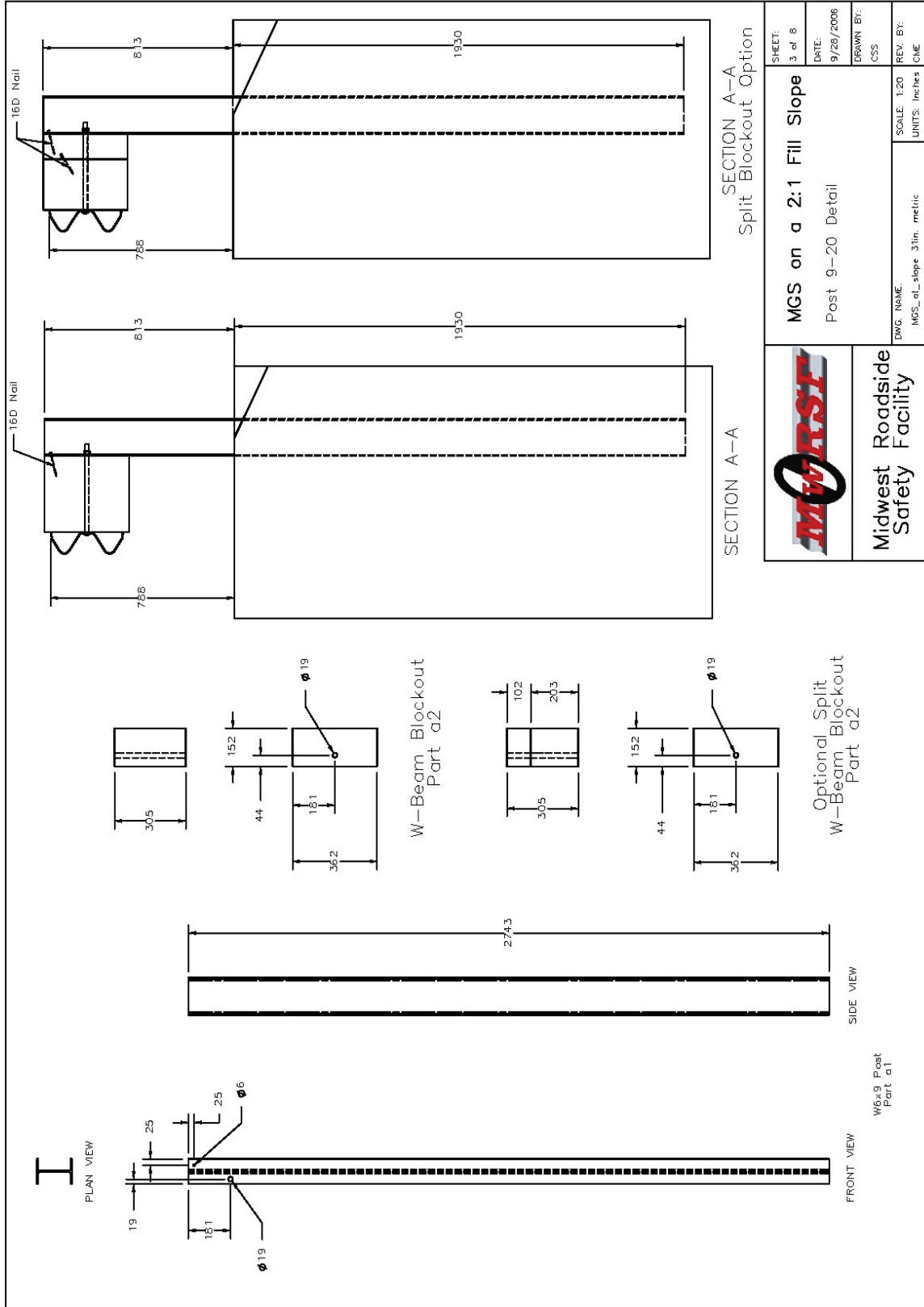
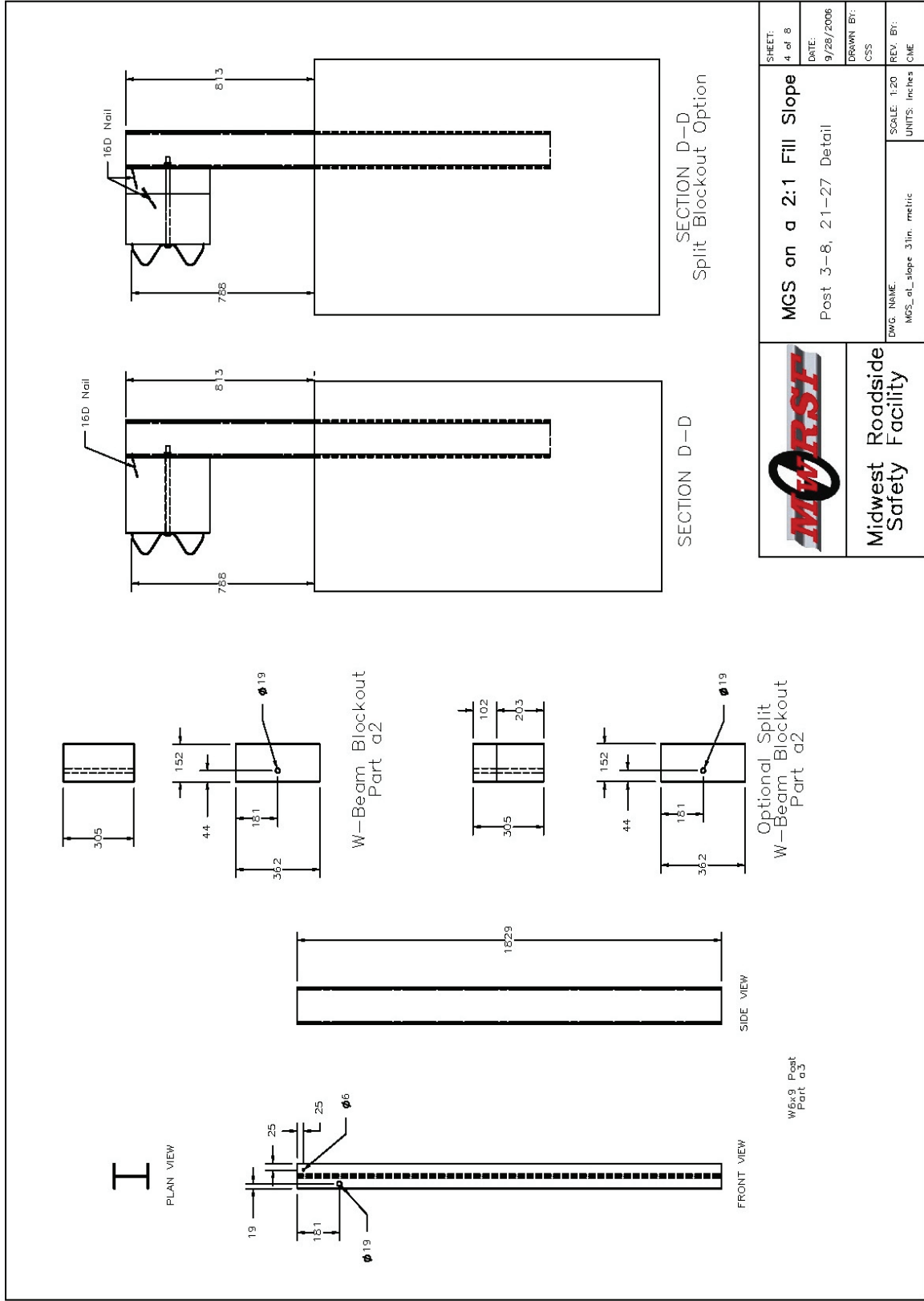


Figure G-3. Post Details, Test No. MGS221-2 (Metric)




	MGS on a 2:1 Fill Slope Post 3-8, 21-27 Detail	SHEET: 4 of 8 DATE: 9/28/2006 DRAWN BY: CSS
	DWG. NAME: MGS_sl_slope_31m_metric	SCALE: 1:20 UNITS: inches metric
Midwest Roadside Safety Facility		

Figure G-4. Post Details, Test No. MGS221-2 (Metric)

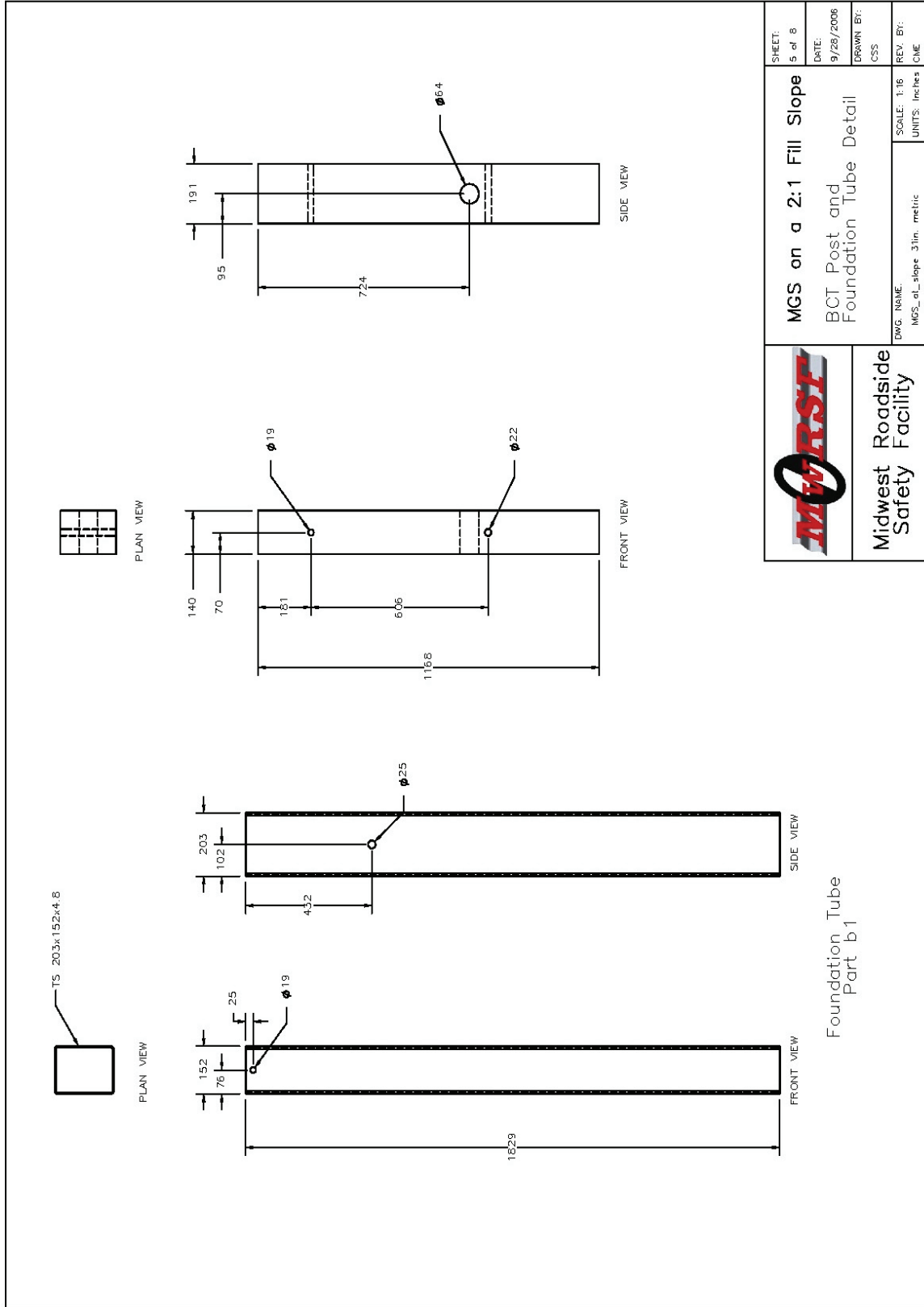


Figure G-5. Post and Foundation Tube Details, Test No. MGS221-2 (Metric)

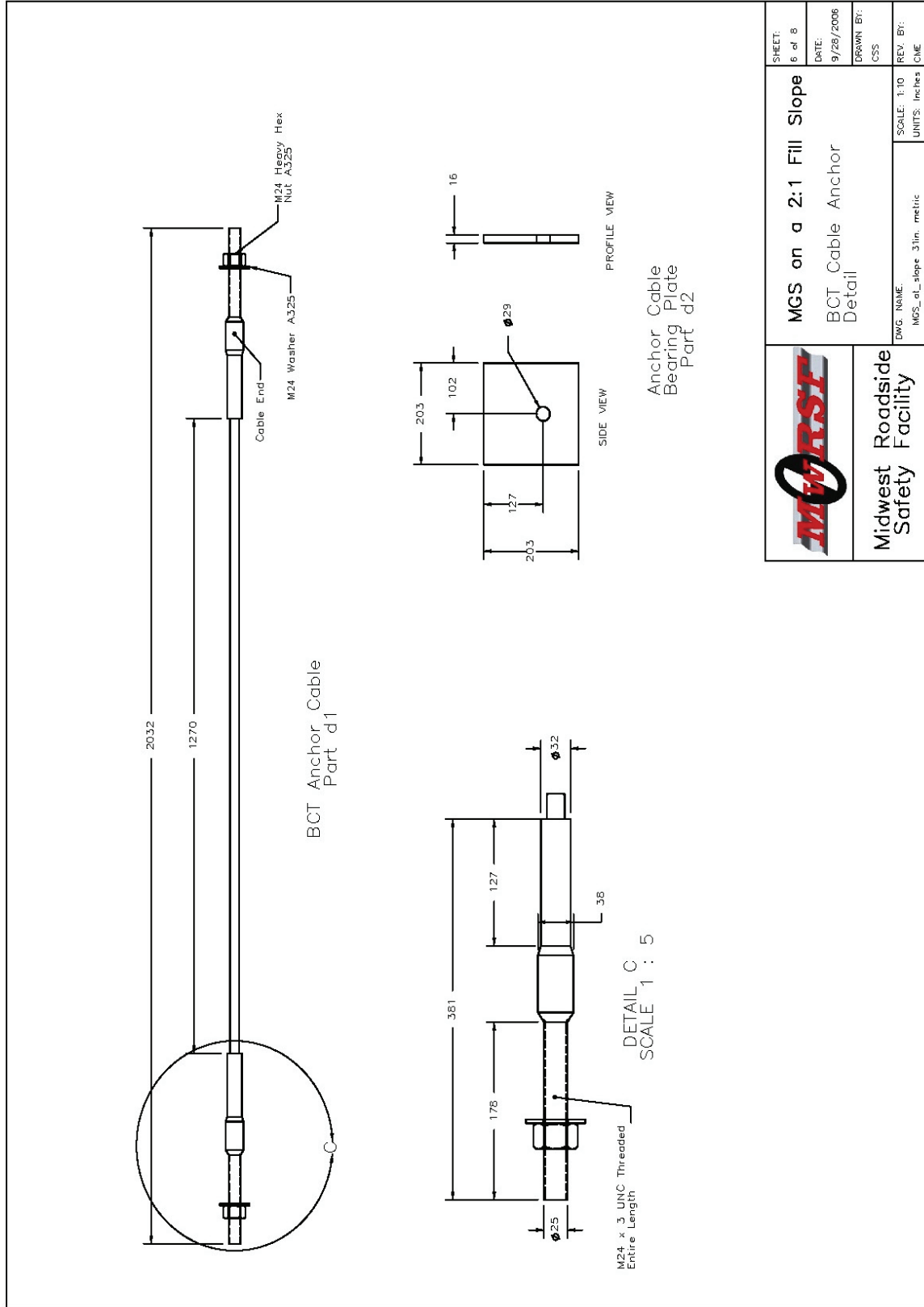


Figure G-6. Anchor Cable Details, Test No. MGS221-2 (Metric)

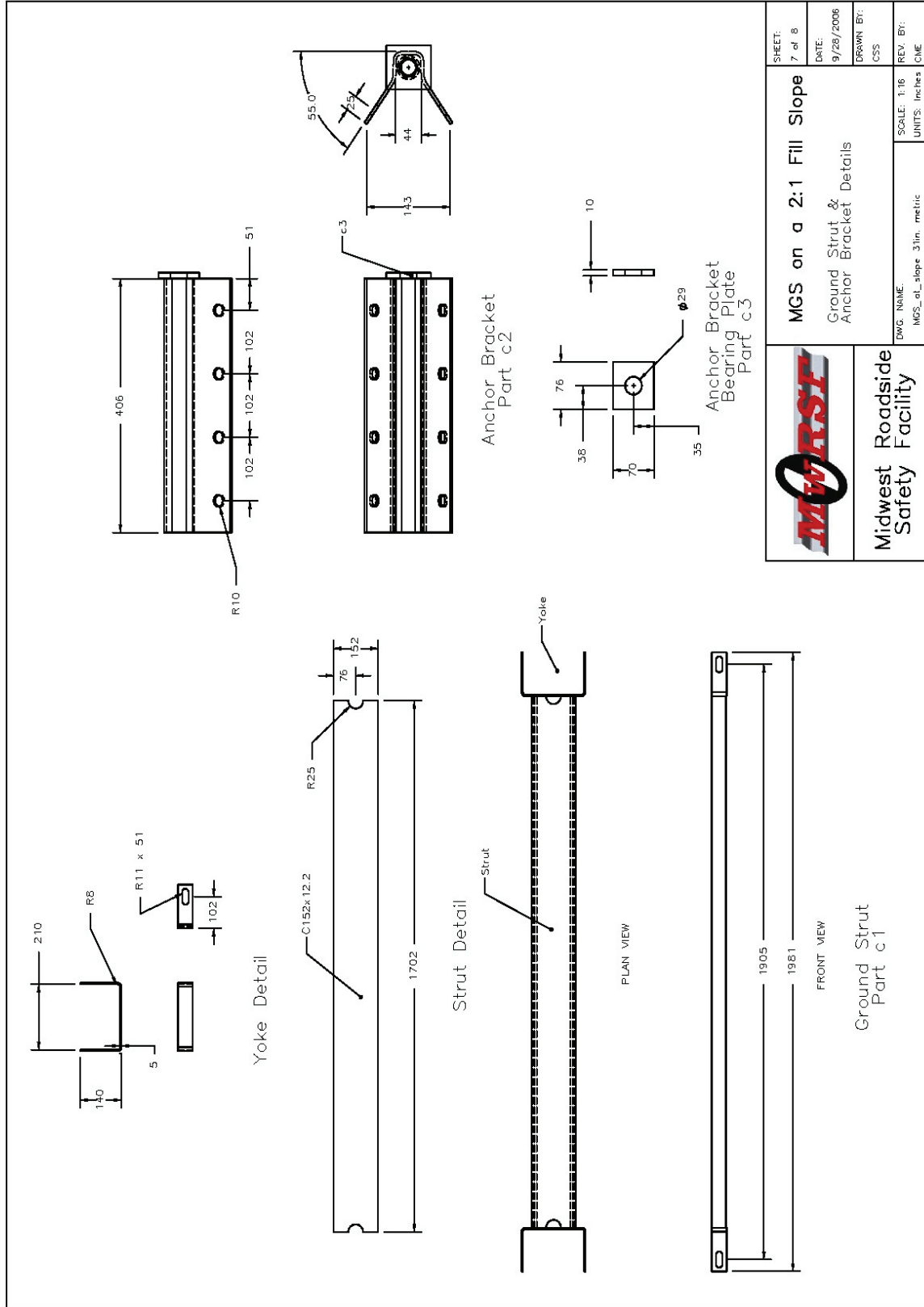


Figure G-7. Ground Strut and Anchor Bracket Details, Test No. MGS221-2 (Metric)

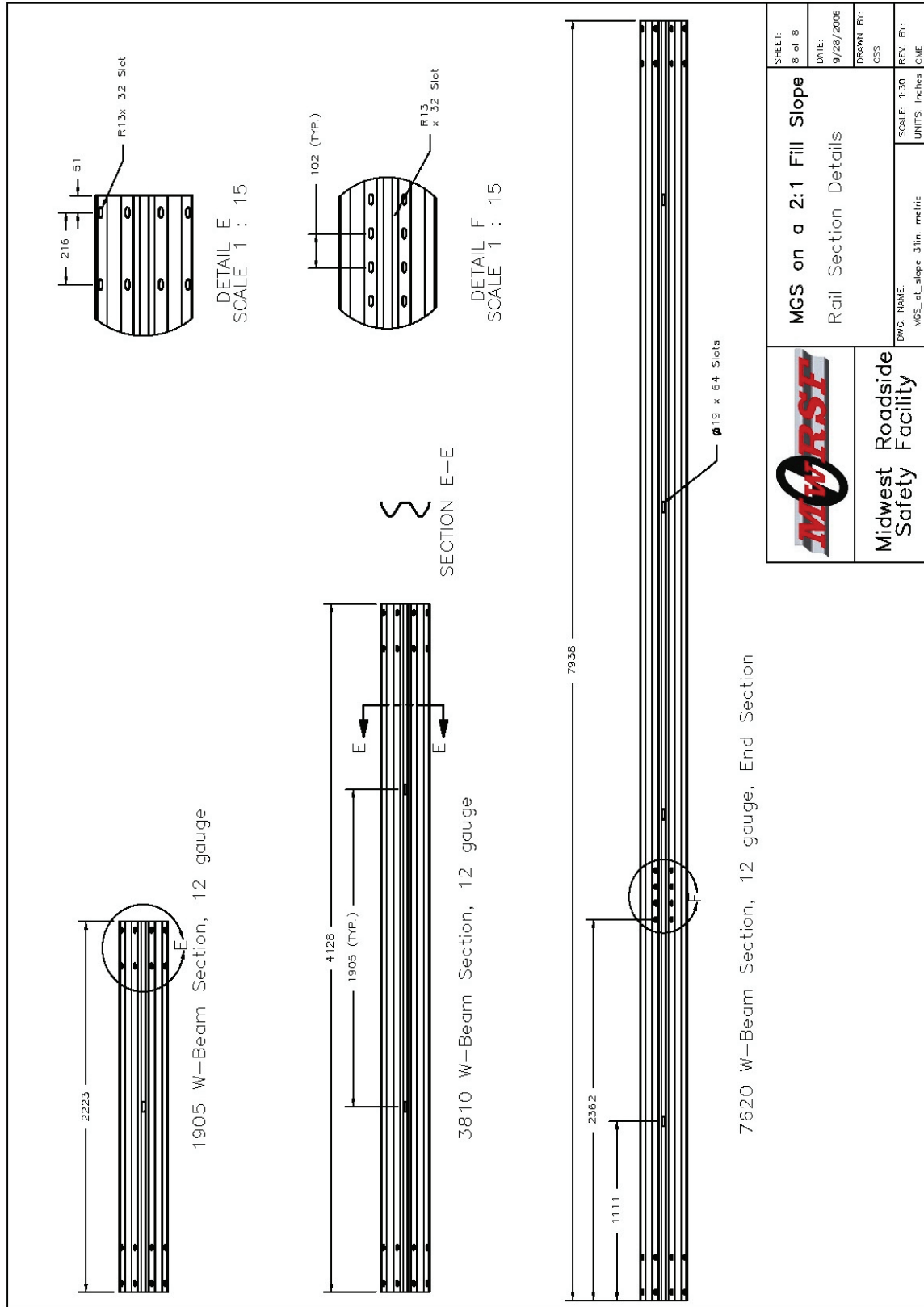


Figure G-8. Rail Details, Test No. MGS221-2 (Metric)

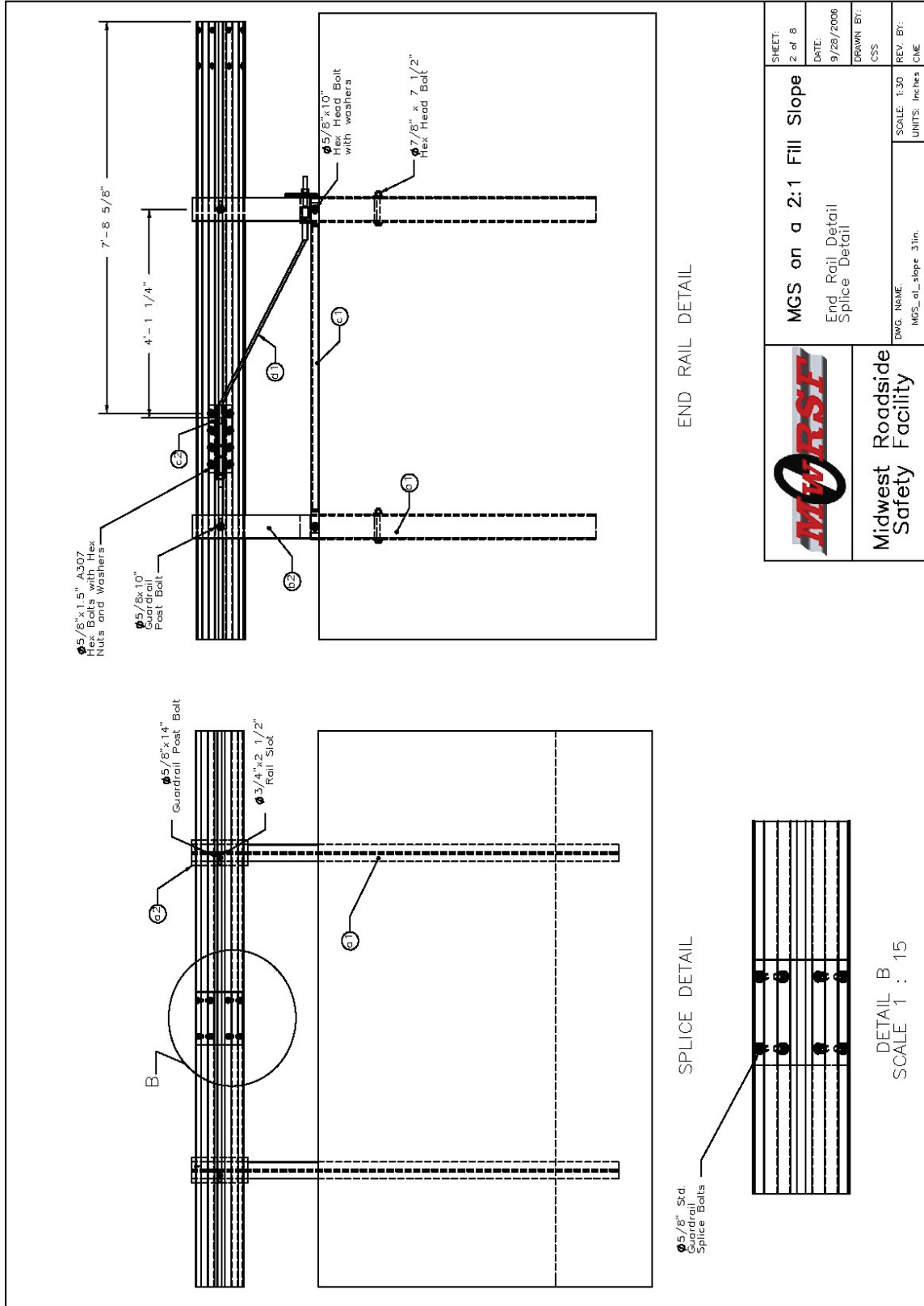


Figure G-10. Rail Detail, Test No. MGS221-2 (English)

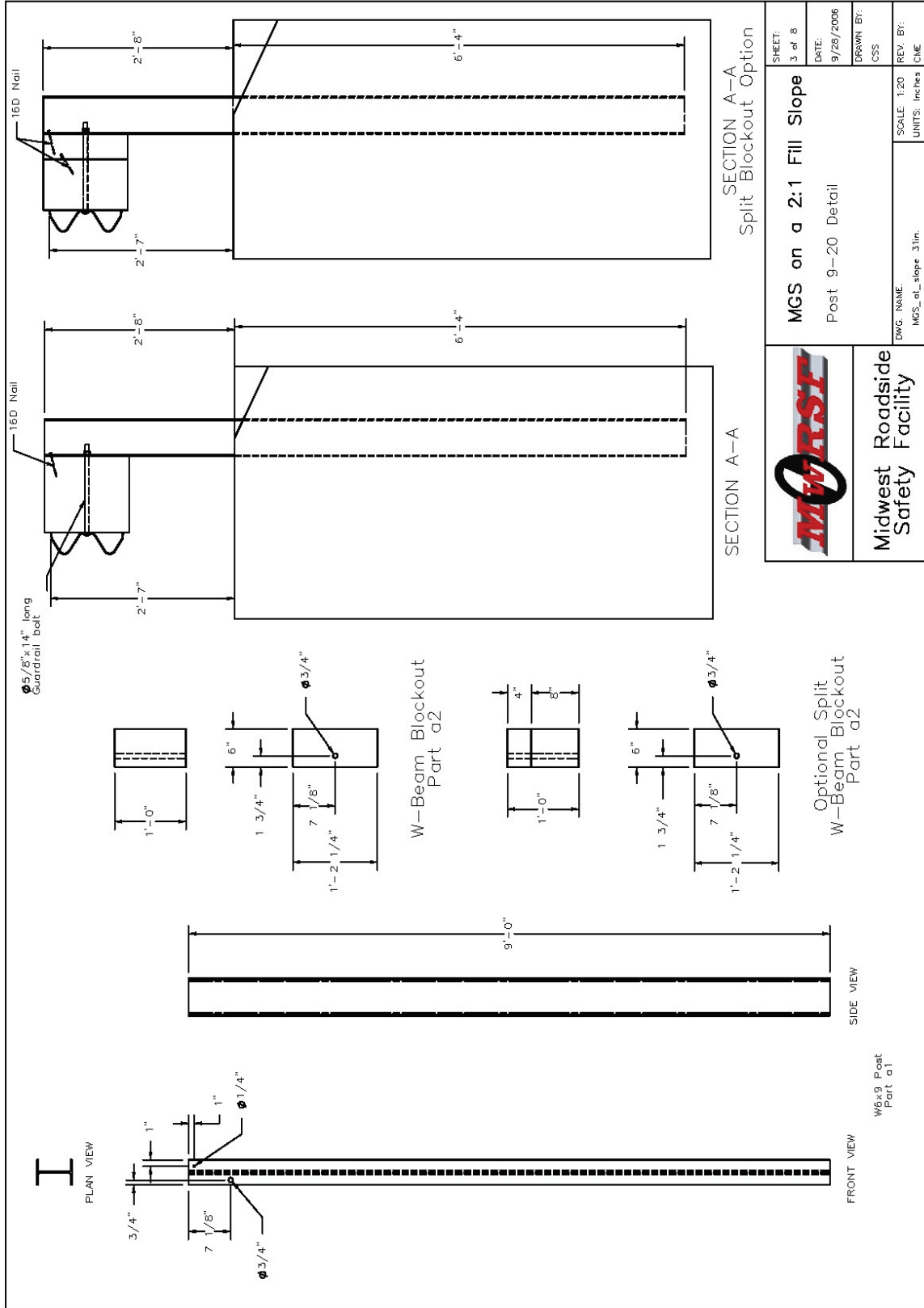


Figure G-11. Post Details, Test No. MGS221-2 (English)

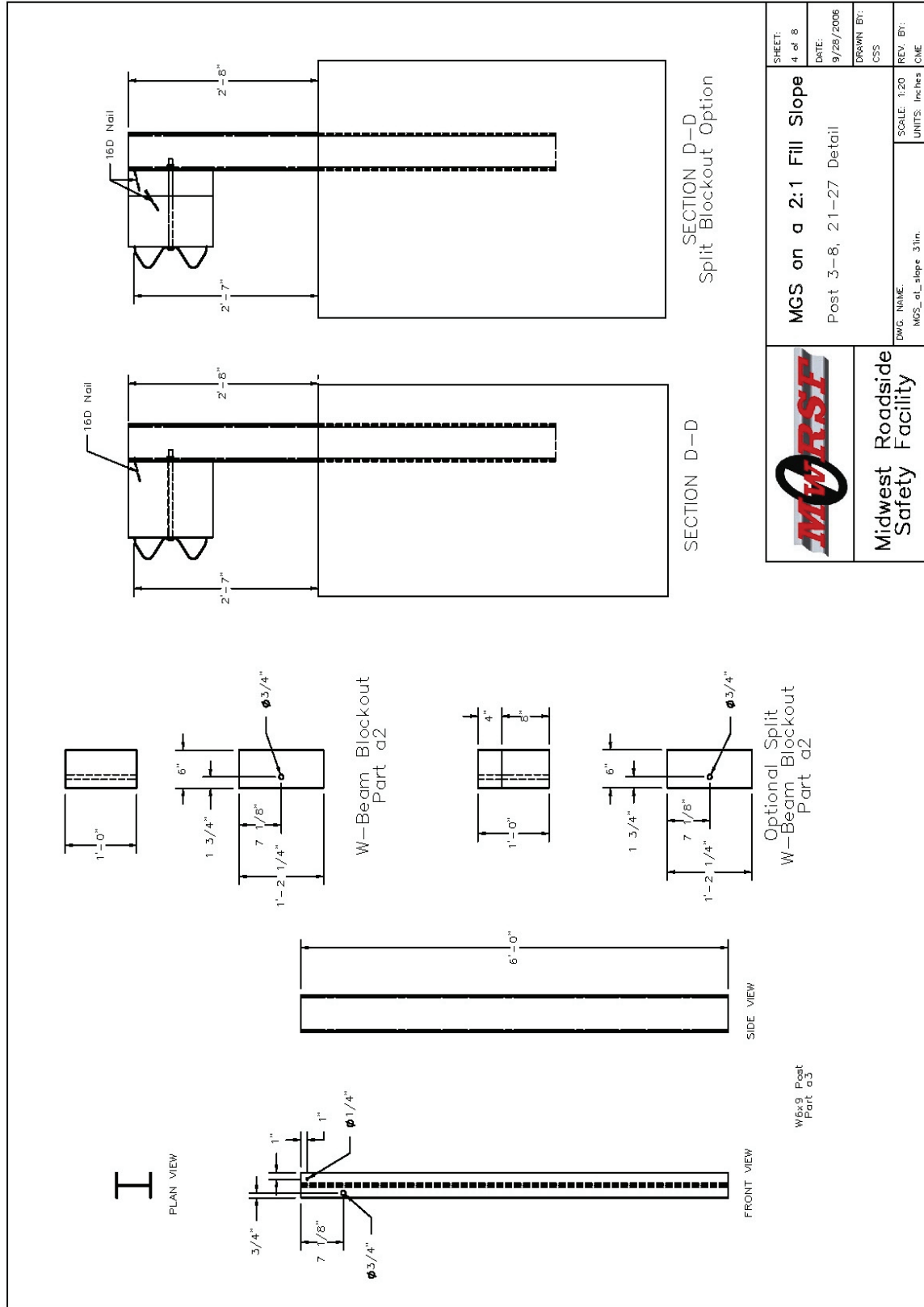
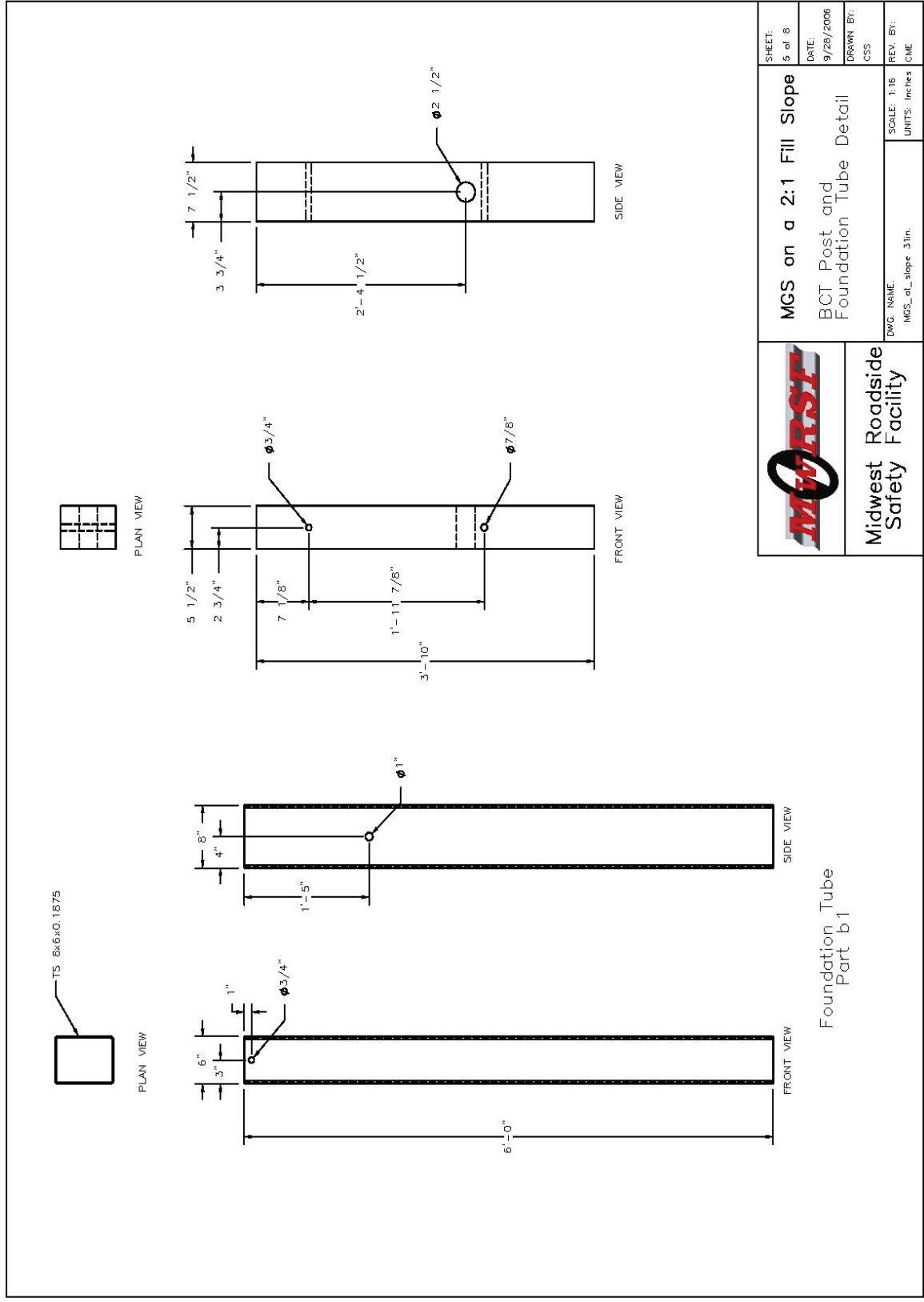


Figure G-12. Post Details, Test No. MGS221-2 (English)




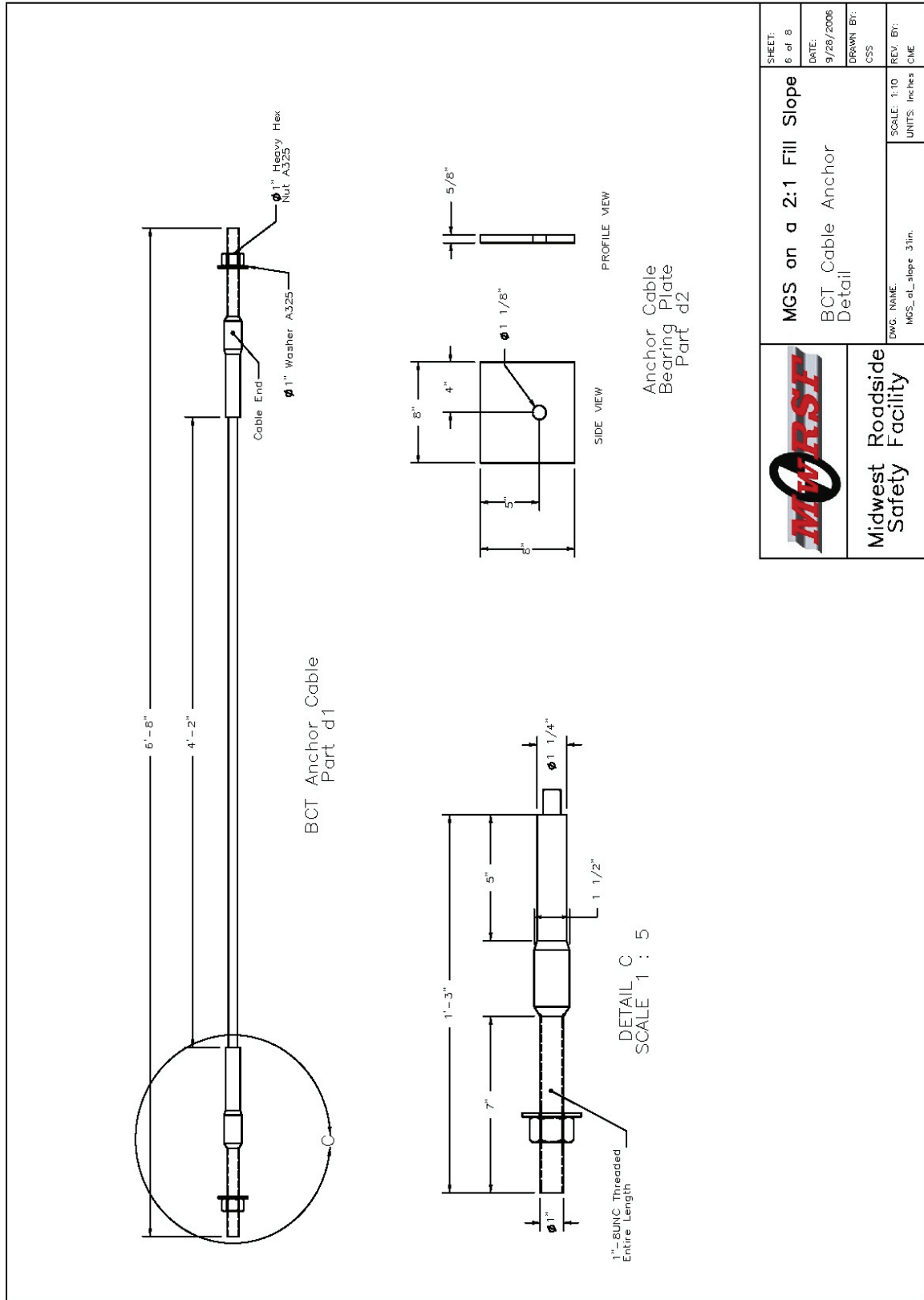
 Midwest Roadside Safety Facility	MGs on a 2:1 Fill Slope BCT Post and Foundation Tube Detail	SHEET: 5 of 8 DATE: 9/28/2006 DRAWN BY: CSS
	DWG. NAME: MGs_of_slope 3tin.	SCALE: 1:16 UNITS: Inches

Figure G-13. Post and Foundation Tube Details, Test No. MGS221-2 (English)




	MGs on a 2:1 Fill Slope BCT Cable Anchor Detail	SHEET: 6 of 8 DATE: 9/28/2006 DRAWN BY: CSS
	Midwest Roadside Safety Facility	DWG. NAME: MGS_sl_slope 31m. SCALE: 1:10 UNITS: Inches

Figure G-14. Anchor Cable Details, Test No. MGS221-2 (English)

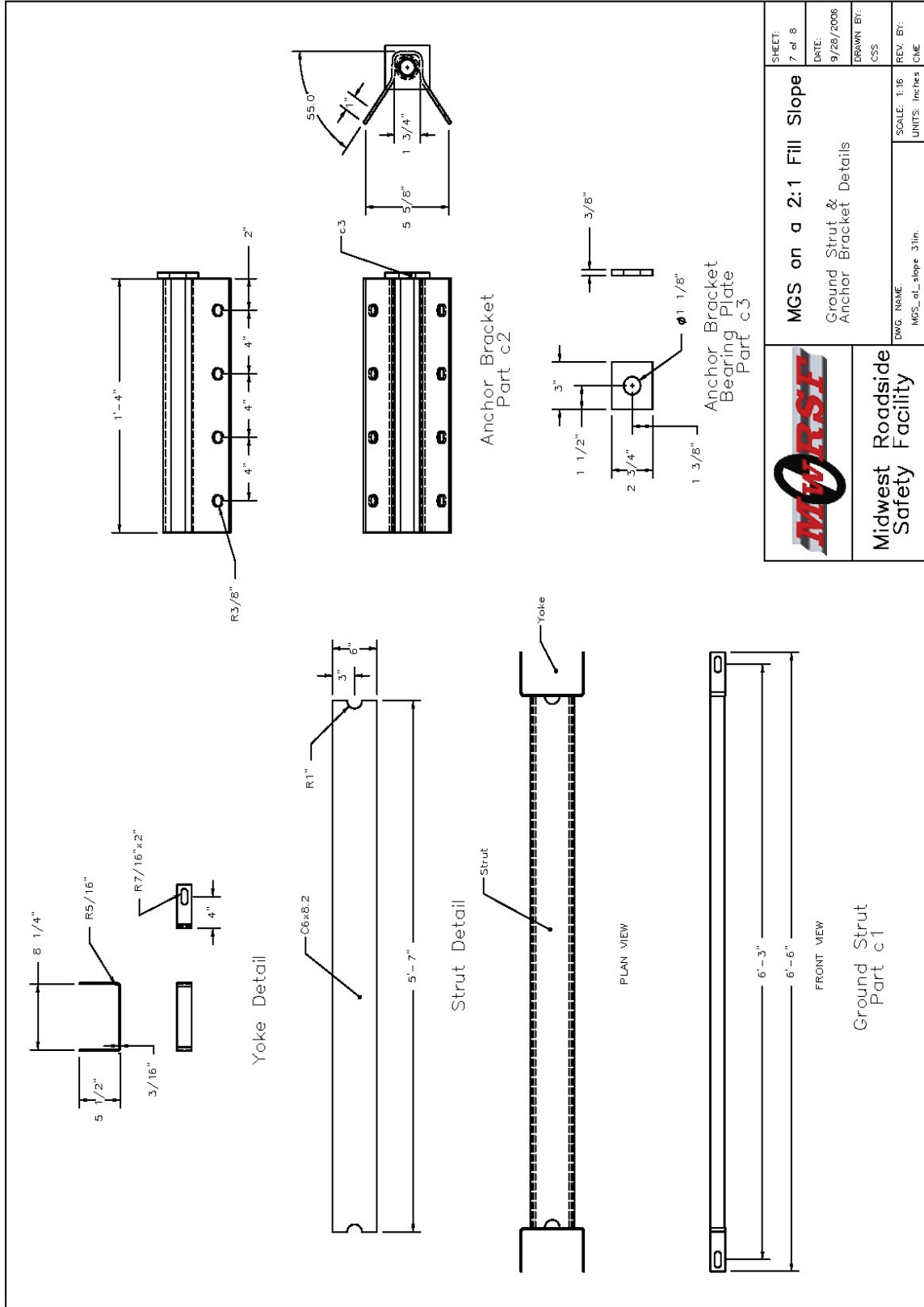


Figure G-15. Ground Strut and Anchor Bracket Details, Test No. MGS221-2 (English)

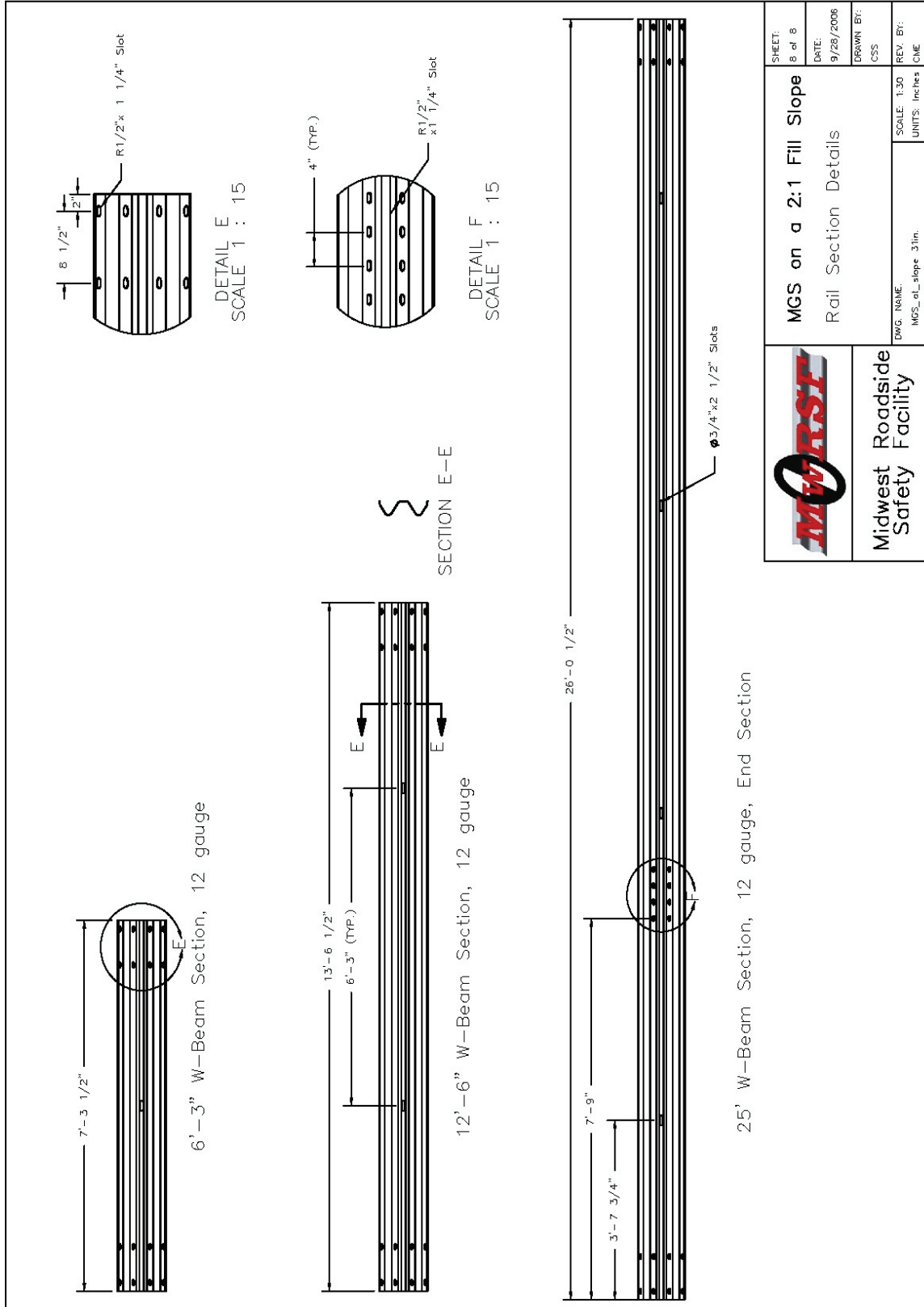


Figure G-16. Rail Details, Test No. MGS221-2 (English)

APPENDIX H
Occupant Compartment Deformation, Test No. MGS221-2

VEHICLE PRE/POST CRUSH INFO
Set-1

TEST: MGS221-2
VEHICLE: 2004 Dodge Ram 1500 QC

Note: If impact is on driver side need to enter negative number for Y

POINT	X	Y	Z	X'	Y'	Z'	DEL X	DEL Y	DEL Z
1	30	-25.25	0	30	-24.75	0	0	0.5	0
2	29	-19.5	-2.25	29	-19.75	-2	0	-0.25	0.25
3	28.75	-16.25	-2.5	28.75	-16	-2.25	0	0.25	0.25
4	25	-8.5	-1	25.25	-8.5	-0.75	0.25	0	0.25
5	25.25	-27.25	-4	25.25	-27.25	-3.75	0	0	0.25
6	25	-22.75	-4.5	24.75	-22.75	-4.25	-0.25	0	0.25
7	24.5	-16.5	-5	24.5	-16.75	-4.75	0	-0.25	0.25
8	24.5	-12	-5.25	24.75	-12	-5	0.25	0	0.25
9	21.75	-8.5	-1.25	21.75	-8	-1.25	0	0.5	0
10	22	-30.25	-5.75	22	-30.25	-5.5	0	0	0.25
11	21.75	-23.5	-6.25	21.5	-23.75	-6	-0.25	-0.25	0.25
12	21.5	-17	-6.75	21.5	-17	-6.5	0	0	0.25
13	21.25	-12.75	-6.75	21.25	-12.75	-6.75	0	0	0
14	19	-8.5	-2.25	19.25	-8.5	-2.25	0.25	0	0
15	17.5	-30.25	-7	17.5	-30.25	-7	0	0	0
16	17.5	-23.75	-7	17.5	-23.5	-6.75	0	0.25	0.25
17	17.5	-17.5	-7.25	17.5	-17.25	-7.25	0	0.25	0
18	16	-9	-3.75	16	-9.25	-3.75	0	-0.25	0
19	14	-30.5	-7	14	-30.5	-7	0	0	0
20	13.75	-24.25	-7	13.75	-24	-7	0	0.25	0
21	13.75	-17.5	-7.25	13.5	-17.25	-7.25	-0.25	0.25	0
22	13.25	-9.5	-5.25	13	-9.5	-5	-0.25	0	0.25
23	10	-30.5	-7.25	10.25	-30.75	-7.25	0.25	-0.25	0
24	9.75	-24.5	-7	9.75	-24.25	-7	0	0.25	0
25	9.5	-17.75	-7.5	9.75	-17.75	-7.5	0.25	0	0
26	9.25	-10.25	-6.75	9	-10	-6.5	-0.25	0.25	0.25
27	1	-24.25	-3.25	1	-24.5	-3.25	0	-0.25	0
28	0.75	-17.5	-3.75	0.75	-17.25	-3.75	0	0.25	0
29							0	0	0
30							0	0	0

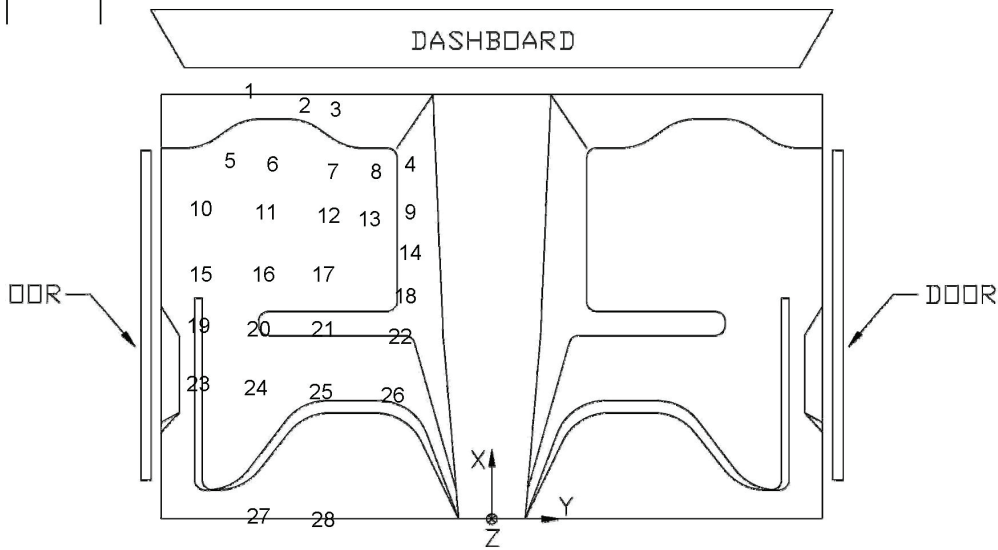


Figure H-1. Occupant Compartment Deformation Data - Set 1, Test MGS221-2

VEHICLE PRE/POST CRUSH INFO
Set-2

TEST: MGS221-2
VEHICLE: 2004 Dodge Ram 1500 QC

Note: If impact is on driver side need to enter negative number for Y

POINT	X	Y	Z	X'	Y'	Z'	DEL X	DEL Y	DEL Z
1	53	-19	-1.25	53	-18.5	-1.25	0	0.5	0
2	52	-13.25	-3	52	-13.5	-3	0	-0.25	0
3	51.75	-10	-3	51.75	-9.75	-3	0	0.25	0
4	48	-2.25	-1	48.25	-2.25	-0.75	0.25	0	0.25
5	48.25	-21	-5.25	48.25	-21	-5	0	0	0.25
6	48	-16.5	-5.5	47.75	-16.5	-5.25	-0.25	0	0.25
7	47.5	-10.25	-5.5	47.5	-10.5	-5.25	0	-0.25	0.25
8	47.5	-5.75	-5.25	47.75	-5.75	-5.25	0.25	0	0
9	44.75	-2.25	-1.25	44.75	-1.75	-1	0	0.5	0.25
10	45	-24	-7	45	-24	-7	0	0	0
11	44.75	-17.25	-7.25	44.5	-17.5	-7	-0.25	-0.25	0.25
12	44.5	-10.75	-7.25	44.5	-10.75	-7	0	0	0.25
13	44.25	-6.5	-7.25	44.25	-6.5	-7	0	0	0.25
14	42	-2.25	-2.5	42.25	-2.25	-2.25	0.25	0	0.25
15	40.5	-24	-8.5	40.5	-24	-8.25	0	0	0.25
16	40.5	-17.5	-8	40.5	-17.25	-7.75	0	0.25	0.25
17	40.5	-11.25	-8	40.5	-11	-7.75	0	0.25	0.25
18	39	-2.75	-4	39	-3	-3.75	0	-0.25	0.25
19	37	-24.25	-8.5	37	-24.25	-8.5	0	0	0
20	36.75	-18	-8	36.75	-17.75	-7.75	0	0.25	0.25
21	36.75	-11.25	-8	36.5	-11	-7.75	-0.25	0.25	0.25
22	36.25	-3.25	-5.25	36	-3.25	-5.25	-0.25	0	0
23	33	-24.25	-8.25	33.25	-24.5	-8.5	0.25	-0.25	-0.25
24	32.75	-18.25	-8	32.75	-18	-8	0	0.25	0
25	32.5	-11.5	-8	32.75	-11.5	-8	0.25	0	0
26	32.25	-4	-7	32	-3.75	-6.75	-0.25	0.25	0.25
27	24	-18	-4	24	-18.25	-4	0	-0.25	0
28	23.75	-11.25	-4.25	23.75	-11	-4	0	0.25	0.25
29							0	0	0
30							0	0	0

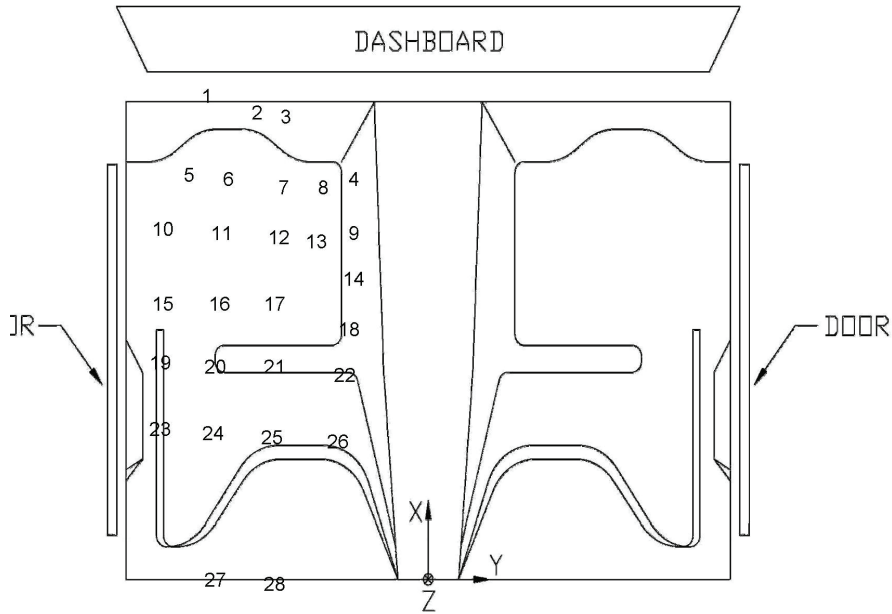


Figure H-2. Occupant Compartment Deformation Data - Set 2, Test MGS221-2

Occupant Compartment Deformation Index (OCDI)

Test No. MGS221-2
Vehicle Type: 2004 Dodge Ram 1500 QC

OCDI = XXABCDEFGHI

XX = location of occupant compartment deformation

A = distance between the dashboard and a reference point at the rear of the occupant compartment, such as the top of the rear seat or the rear of the cab on a pickup

B = distance between the roof and the floor panel

C = distance between a reference point at the rear of the occupant compartment and the motor panel

D = distance between the lower dashboard and the floor panel

E = interior width

F = distance between the lower edge of right window and the upper edge of left window

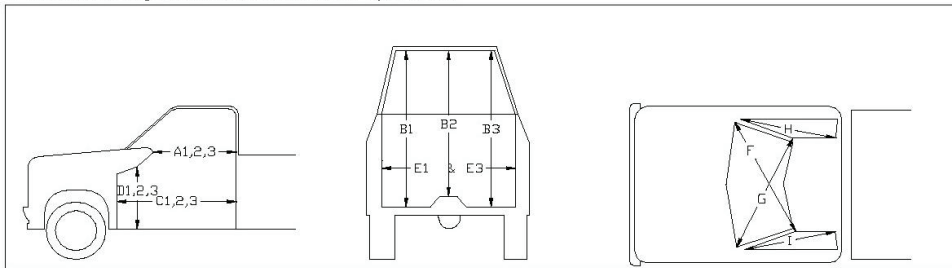
G = distance between the lower edge of left window and the upper edge of right window

H = distance between bottom front corner and top rear corner of the passenger side window

I = distance between bottom front corner and top rear corner of the driver side window

Severity Indices

- 0 - if the reduction is less than 3%
- 1 - if the reduction is greater than 3% and less than or equal to 10 %
- 2 - if the reduction is greater than 10% and less than or equal to 20 %
- 3 - if the reduction is greater than 20% and less than or equal to 30 %
- 4 - if the reduction is greater than 30% and less than or equal to 40 %



where,
1 = Passenger Side
2 = Middle
3 = Driver Side

Location: right front

Measurement	Pre-Test (in.)	Post-Test (in.)	Change (in.)	% Difference	Severity Index
A1	54.25	54.00	-0.25	-0.46	0
A2	50.00	50.00	0.00	0.00	0
A3	57.25	56.75	-0.50	-0.87	0
B1	47.75	47.75	0.00	0.00	0
B2	42.50	42.50	0.00	0.00	0
B3	43.50	43.50	0.00	0.00	0
C1	62.25	62.00	-0.25	-0.40	0
C2	47.00	47.00	0.00	0.00	0
C3	61.25	61.25	0.00	0.00	0
D1	22.50	22.50	0.00	0.00	0
D2	13.25	13.25	0.00	0.00	0
D3	25.50	25.50	0.00	0.00	0
E1	65.00	65.00	0.00	0.00	0
E3	64.75	64.50	-0.25	-0.39	0
F	56.75	56.75	0.00	0.00	0
G	55.75	55.75	0.00	0.00	0
H	37.75	37.75	0.00	0.00	0
I	37.75	37.75	0.00	0.00	0

Note: Maximum severity index for each variable (A-I) is used for determination of final OCDI value

Final OCDI: XXABCDEFGHI
RF 0 0 0 0 0 0 0 0 0

Figure H-3. Occupant Compartment Deformation Index (OCDI), Test MGS221-2

APPENDIX I
Accelerometer and Rate Transducer Data Analysis, Test No. MGS221-2

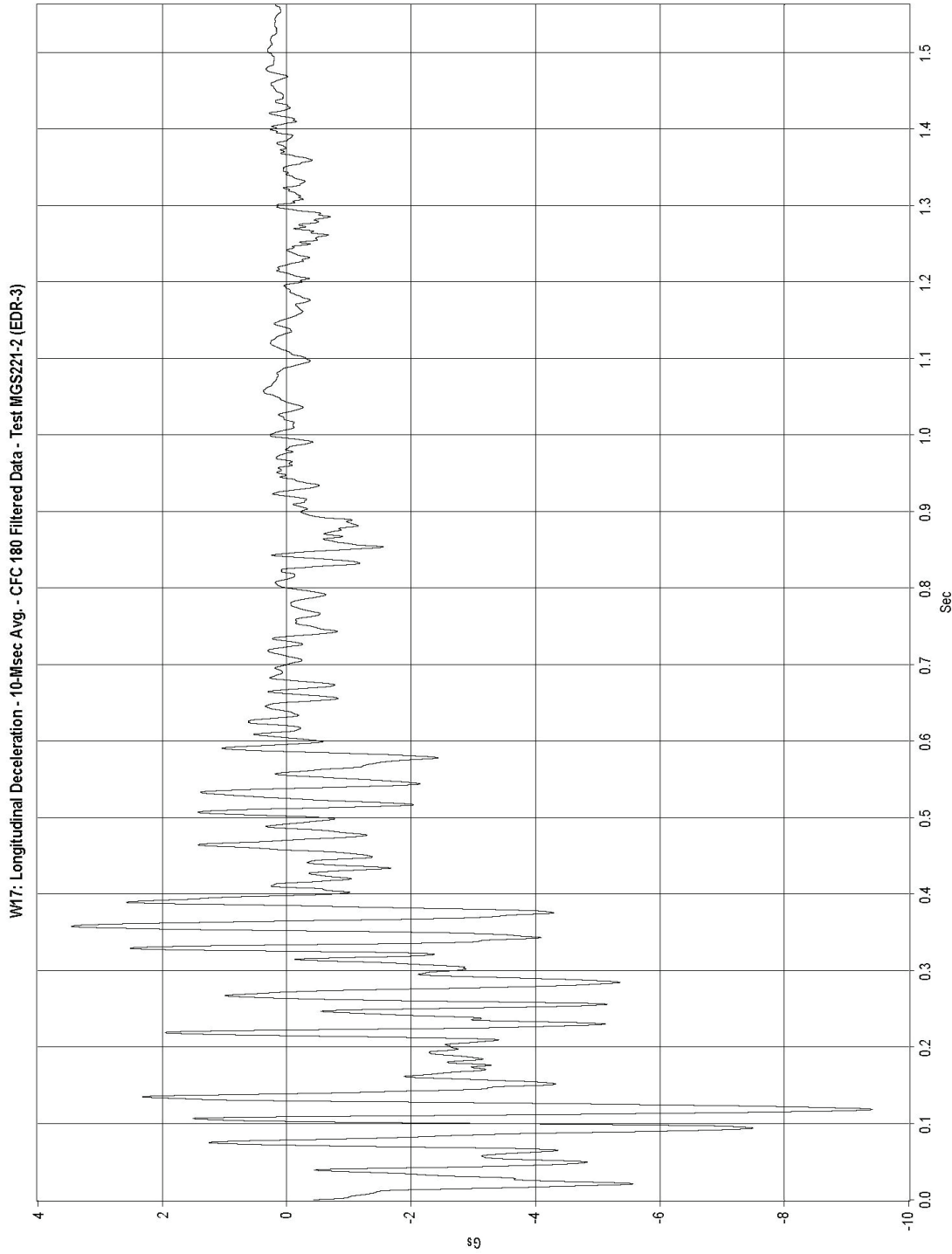


Figure I-1. Graph of Longitudinal Deceleration, Test MGS221-2

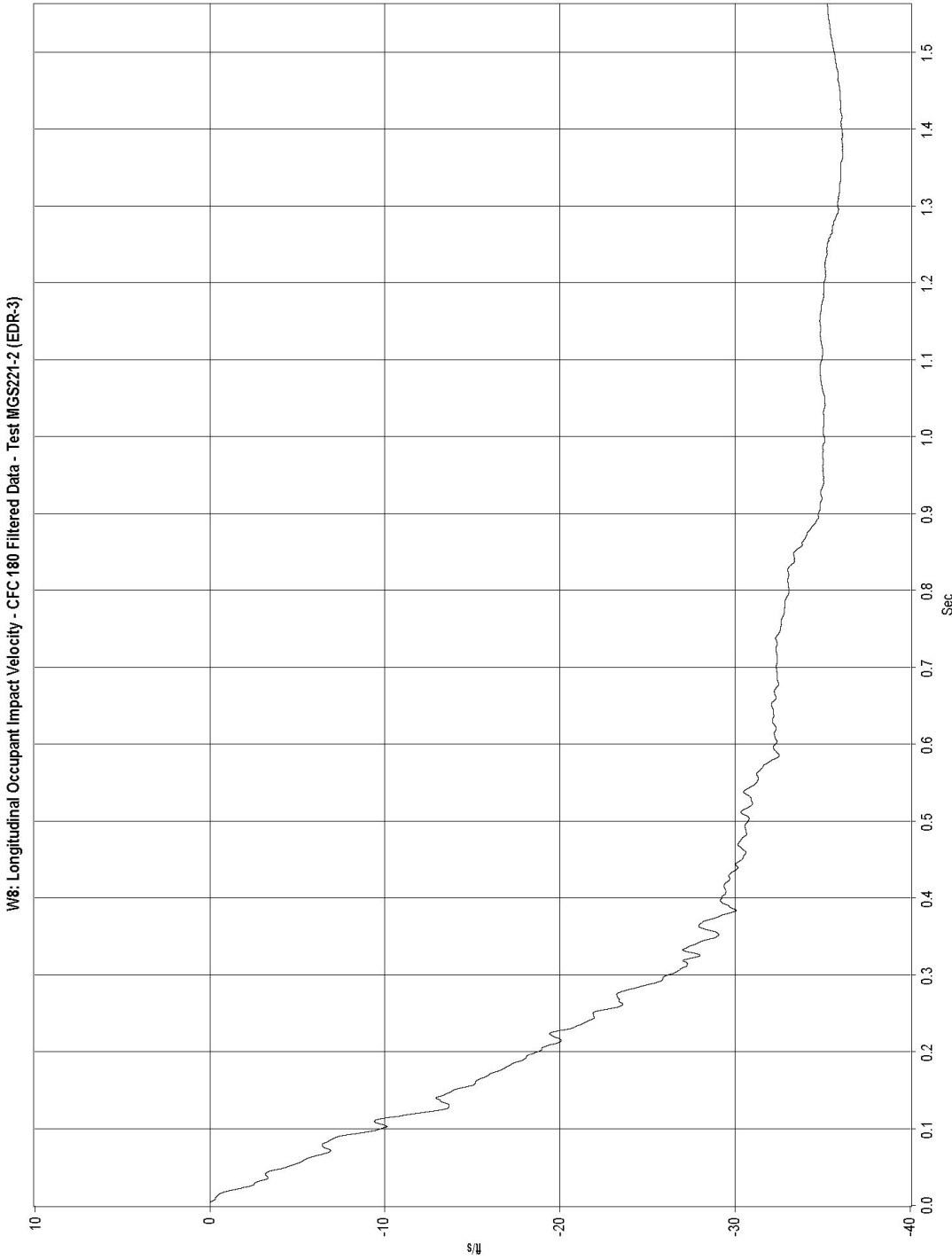


Figure I-2. Graph of Longitudinal Occupant Impact Velocity, Test MGS221-2

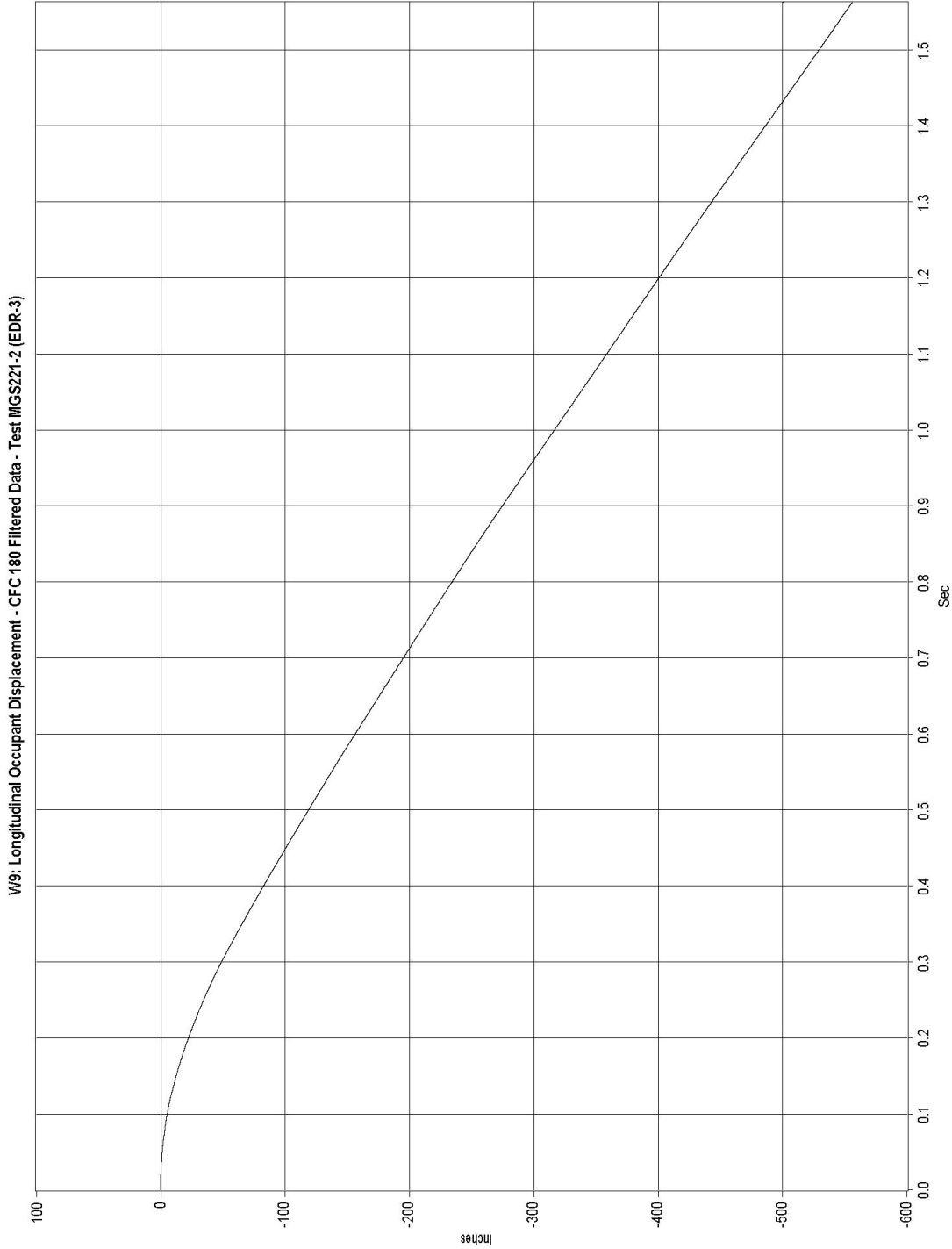


Figure I-3. Graph of Longitudinal Occupant Displacement, Test MGS221-2

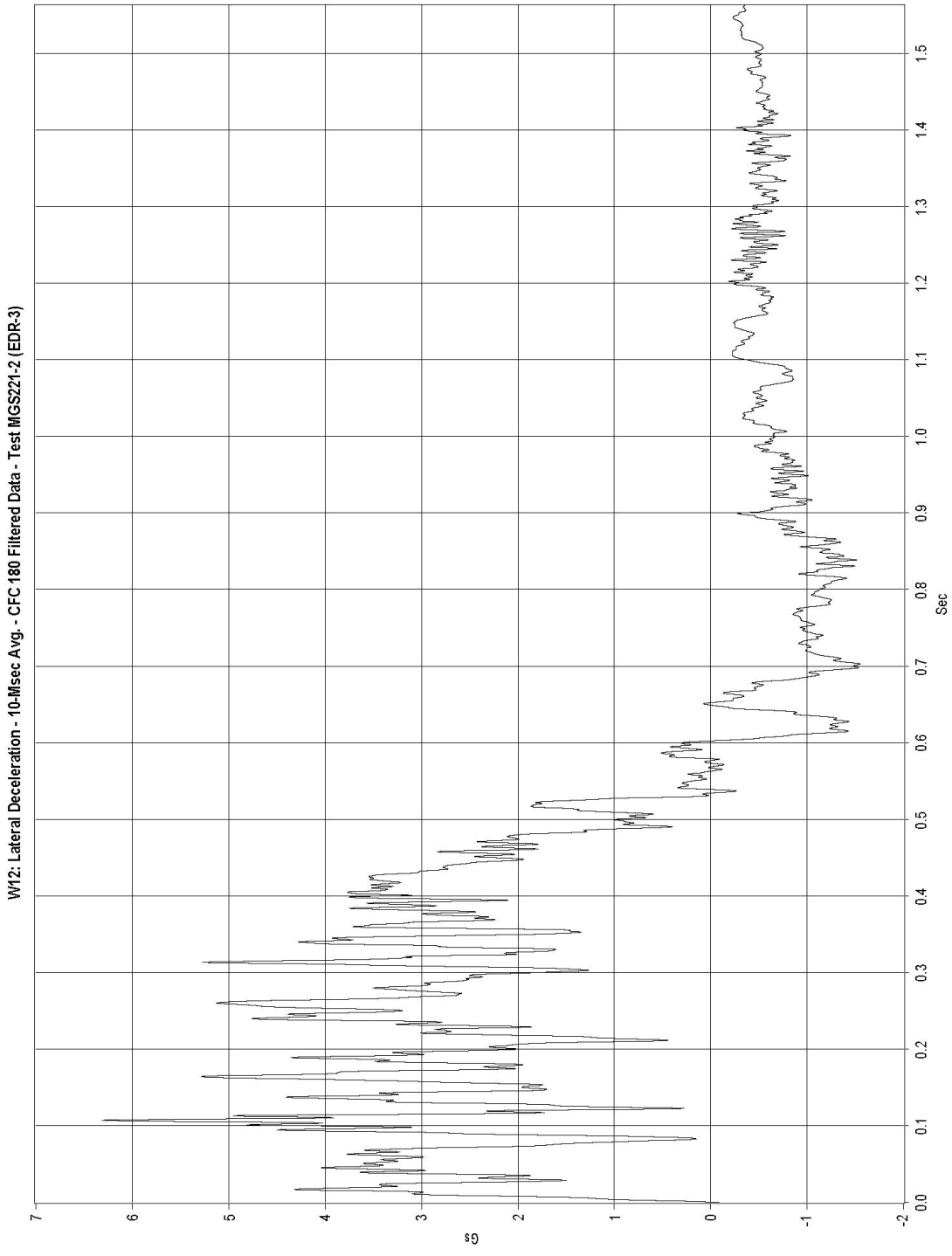


Figure I-4. Graph of Lateral Deceleration, Test MGS221-2

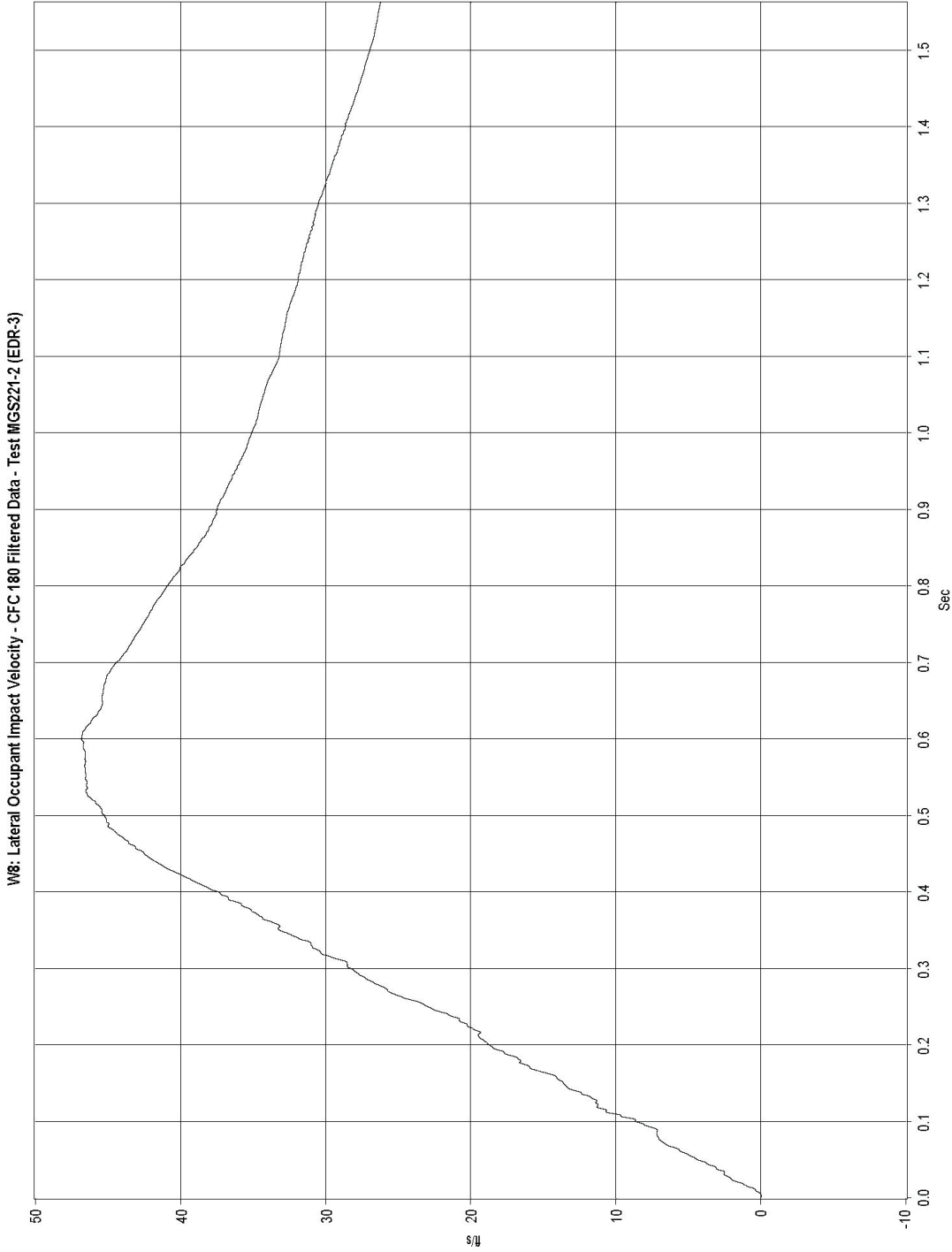


Figure I-5. Graph of Lateral Occupant Impact Velocity, Test MGS221-2

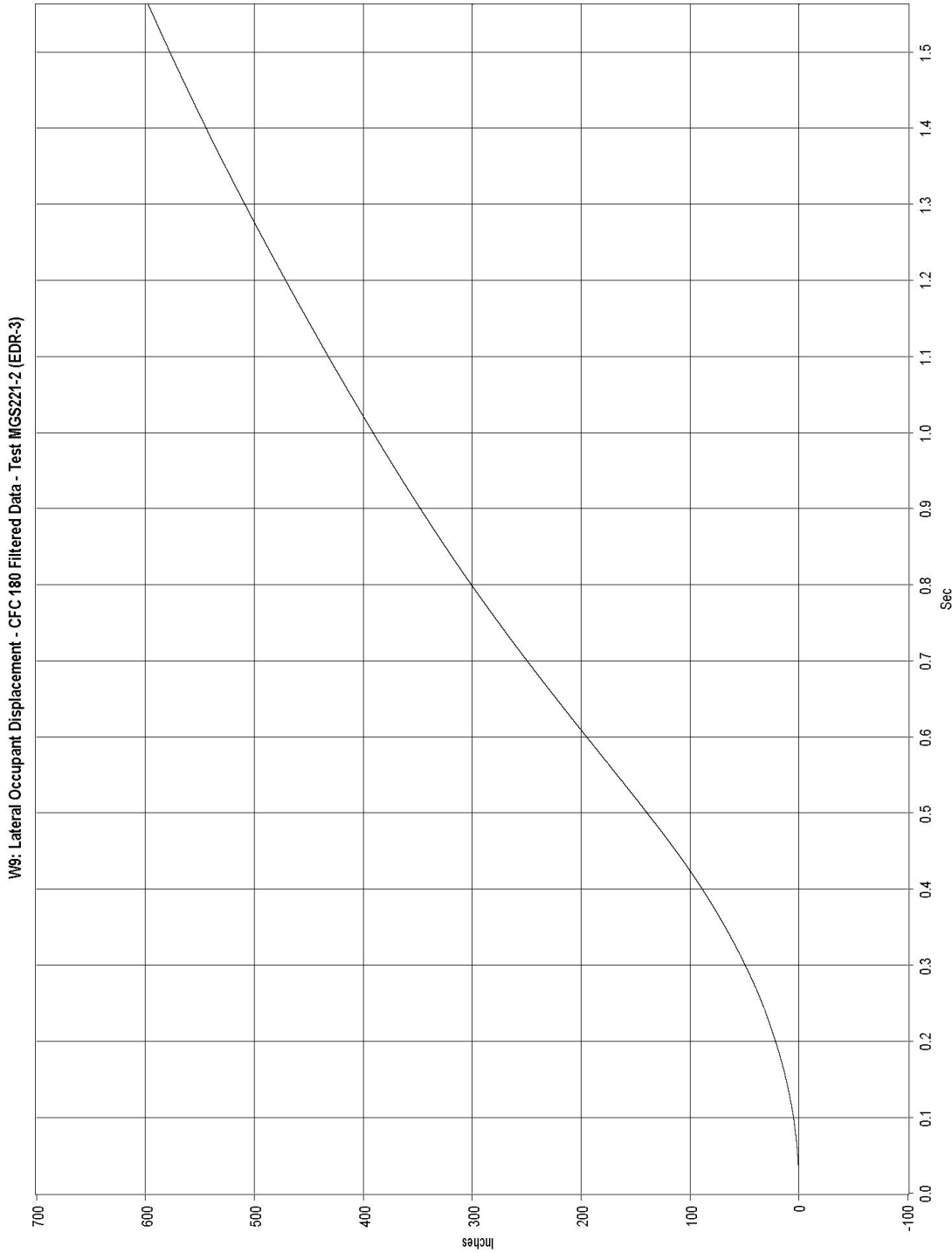


Figure I-6. Graph of Lateral Occupant Displacement, Test MGS221-2

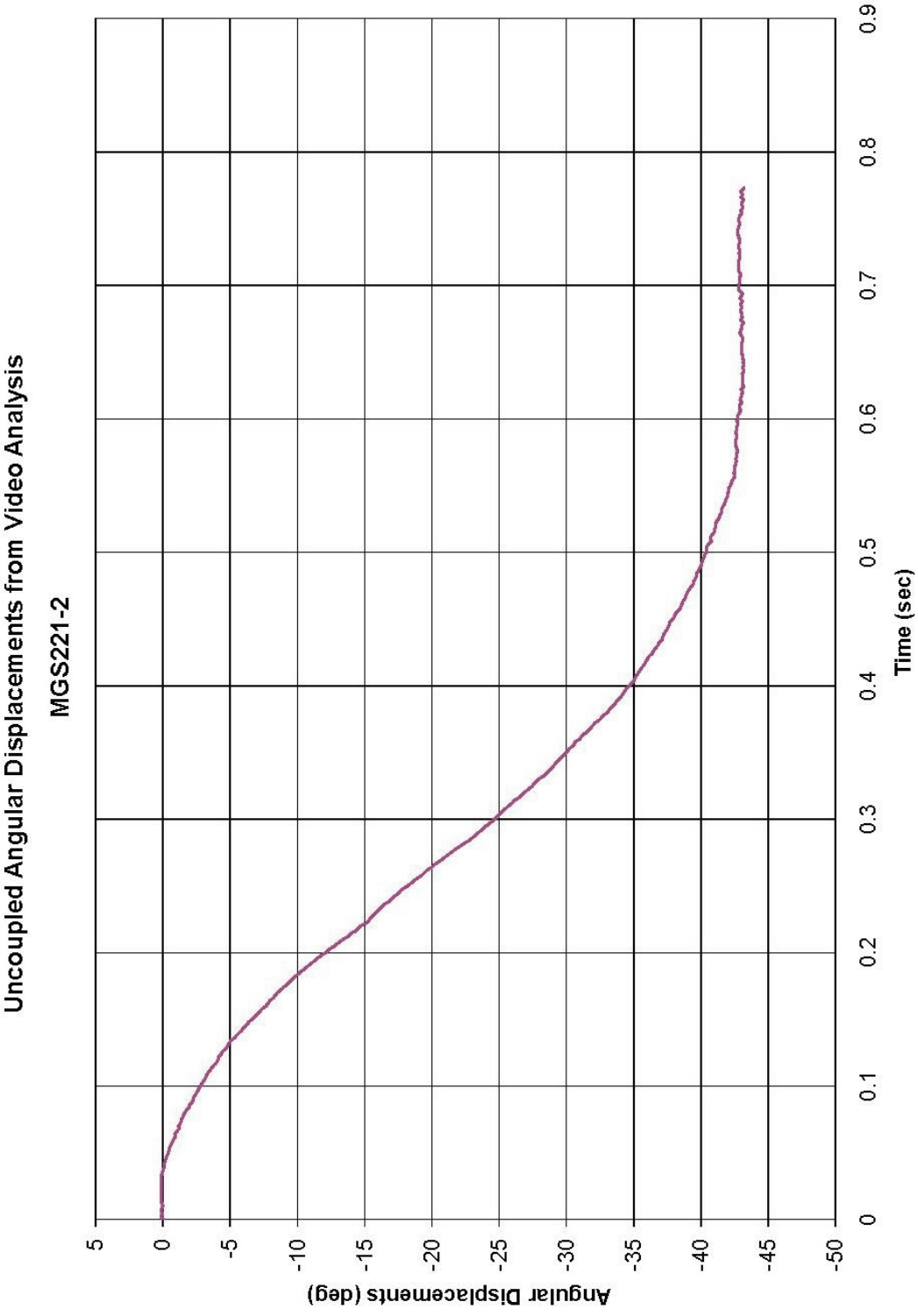


Figure I-7. Graph of Yaw Angular Displacement, Test MGS221-2

END OF DOCUMENT